Magnetic Resonance Imaging of Carotid Atherosclerosis: A Population-based Approach

Mariana Selwaness

Magnetic Resonance Imaging of Carotid Atherosclerosis: A Population-based Approach

Mariana Selwaness

The work in this thesis was conducted at the Departments of Radiology, Epidemiology and Cardiology (Biomedical Engineering) of the Erasmus MC, University Medical Center, Rotterdam, the Netherlands.

The research described in this thesis was performed within the framework of The Rotterdam Study. The contribution of all of the participants and staff of the Rotterdam Study, as well as the general practitioners and pharmacists of the Ommoord district for help with data collection and validation, is gratefully acknowledged.
The Rotterdam Study is supported by the Erasmus Medical Center and Erasmus University Rotterdam; The Netherlands Organization for Scientific Research (NWO); The Netherlands Organization for Health Research and Development (ZonMw); the Research Institute for Diseases in the Elderly (RIDE); The Netherlands Heart Foundation; the Ministry of Education, Culture and Science; the Ministry of Health Welfare and Sports; the European Commission (DG XII); and the Municipality of Rotterdam. The carotid MRI study was supported by the Dutch Heart Foundation (2009B044) and the Netherlands Organization for Scientific Research (NWO/ZonMwVici,918-76-619).

This work was carried out in the Netherlands Institute for Health Sciences (NIHES) and Cardiovascular Research school Erasmus MC Rotterdam (COEUR) graduate schools.

Financial support by the Dutch Heart Foundation for the publication of this thesis is gratefully acknowledged.

Additional financial support for printing of this thesis was kindly provided by the department of Radiology, Epidemiology and Biomedical Engineering, Erasmus MC.

Cover: Man lifting his eyes toward heaven. Cardiovascular system, including carotid arteries, is visualized. MRI image shows a carotid atherosclerotic plaque with intraplaque hemorrhage.

Printed by Ipskamp Drukkers

ISBN: 978-94-6259-332-9

Ontwerp: Mariana Selwaness/Ton Everaers - Erasmus MC department of radiology

Magnetic Resonance Imaging of Carotid Atherosclerosis: A Population-based Approach

Beeldvorming van Slagaderverkalkingen in de Halsslagaders Middels MRI Techniek: Een Onderzoek in de Algemene Bevolking

PROEFSCHRIFT

ter verkrijging van de graad van doctor aan de Erasmus Universiteit Rotterdam op gezag van de rector magnificus

prof. dr. H.A.P. Pols

en volgens het besluit van het College voor Promoties.

De openbare verdediging zal plaatsvinden op
dinsdag 21 oktober 2014 om **15.30 uur**
door

Mariana Selwaness
geboren te Rotterdam

ERASMUS UNIVERSITEIT ROTTERDAM

Promotiecommissie

Promotors: Prof. dr. A. van der Lugt
Prof. dr. O.H. Franco

Overige leden: Prof. dr. ir. E. Boersma
Prof. dr. P.J. Koudstaal
Prof. dr. M.L. Bots

Copromotors: Dr. J.J. Wentzel
Dr. M.W. Vernooij

The research described in this thesis was supported by a grant of the Dutch Heart Foundation, (2009B044 and 2012T008) and the Netherlands Organization for Scientific Research (NWO/ZonMwVici 918-76-619).

Financial support by the Dutch Heart Foundation for the publication of this thesis is gratefully acknowledged.

"Content in everything, but never complacent;
Always laboring to bring positive change in our world.
Not fazed by obstacles, but using them as opportunities;
Always filled with faith in God's power.
Joyful in God's blessing on us, but quick to dispense them unto others;
Always diligent in using our God given talents.
Burning with zeal for the Truth, yet sharing it with all gentleness and respect;
Always showing genuine humility to all people."

Core value of St. Paul Coptic Orthodox Church, Chicago, USA.

Contents

Manuscripts based on the studies described in this thesis

Chapter 2.1

Selwaness M, Van den Bouwhuijsen QJ, Verwoert GC, Dehghan A, Mattace-Raso FU, Vernooij MW, Franco, OH Hofman, A, Van der Lugt A, Wentzel JJ, Witteman JC. Blood pressure parameters and carotid intraplaque hemorrhage as measured by magnetic resonance imaging: The Rotterdam Study. Hypertension. 2013;61(1):76-81.

Chapter 2.2

Selwaness M, Van den Bouwhuijsen Q, Mattace-Raso FU, Verwoert GC, Hofman A, Franco OH, Witteman JC, Van der Lugt A, Vernooij MW, Wentzel JJ. Arterial stiffness is associated with carotid intraplaque hemorrhage in the general population: the rotterdam study. Arterioscler Thromb Vasc Biol. 2014;34(4):927-32.

Chapter 3

Selwaness M, van den Bouwhuijsen Q, Van Onkelen RS, Hofman A, Franco OH, van der Lugt A, Wentzel JJ, Vernooij MW. Atherosclerotic plaque in the left carotid artery is more vulnerable than on the right. [Stroke 2014. Epub ahead of print]

Chapter 4

Selwaness M, Van Den Bouwhuijsen Q, Portegies MLP, Ikram MA, Hofman A, Franco OH, Van der Lugt A, Wentzel JJ, Vernooij MW. The relation of carotid atherosclerotic plaque characteristics on MRI with a history of ischemic stroke and coronary heart disease: a population-based approach. [submitted]

Chapter 5.1

Hameeteman K, van 't Klooster R, Selwaness M, van der Lugt A, Witteman JC, Niessen WJ, Klein S. Carotid wall volume quantification from magnetic resonance images using deformable model fitting and learning-based correction of systematic errors. Physics in medicine and biology. 2013;58:1605-1623.

Chapter 5.2

Selwaness M, Hameeteman K, Van 't Klooster R, Van den Bouwhuijsen Q, Hofman A, Franco OH, Niessen WJ, Klein S, Vernooij MW, Wentzel JJ, Van der Lugt A. Determinants of carotid atherosclerotic plaque burden in a stroke-free population. [Submitted]

Chapter 6.1

Tang H, Selwaness M, Hameeteman K, Van Dijk AC, Van der Lugt A, Witteman JC, Niessen WJ, Van Vliet LJ, Van Walsum T. Semi-automatic MRI segmentation and volume quantification of intra-plaque hemorrhage. International journal of computer assisted radiology and surgery. 2014 May 12. [Int J Comput Assist Radiol Surg. 2014 May 12. Epub ahead of print]

Chapter 6.2

Selwaness M, Van den Bouwhuijsen Q, Tang H, Van Dijk AC, Hameeteman K, Van Walsum T, Niessen WJ, Hofman A, Krestin GB, Franco OH, Van der Lugt A, Vernooij MW. Change of carotid intraplaque hemorrhage in the general population: a 1-year follow up study. [submitted]

Chapter 1

General Introduction

He who cures a disease may be the skill-fullest, but he who prevents it is the safest physician.

— Thomas Fuller

Worldwide, about 17 million people die from cardiovascular disease (CVD) each year, chiefly from ischemic heart disease and stroke.(1) Amongst those, stroke, the most common manifestation of cerebrovascular disease, has been the leading cause of serious, long-term disability in adults worldwide (1990-2010) (2) There are two main types of stroke — ischemic and hemorrhagic. Ischemic stroke is more common and caused by an obstruction in the cerebral vasculature. The causes of ischemic strokes are heterogeneous, including atherosclerosis in the large arteries such as the carotid arteries (see fig 1.), lacunar infarctions and cardiogenic embolism. In this thesis, I will focus on carotid atherosclerosis as it is the most prominent to identify patients with a high risk of ischemic stroke. Atherosclerotic plaques can rupture which will lead to thrombo-embolization into the intracranial circulation or to acute occlusion of the carotid artery. Despite major advances in treatment strategies,

Fig 1. Ischemic stroke may occur as a result of atherosclerotic plaques located in the carotid artery, that is the blood vessel that carries blood from the heart to the brains.

ischemic stroke due to carotid atherosclerotic remains a serious public health problem. Current screening and diagnostic methods are insufficient to identify the plaques that have a high rupture risk and thus to select the individual before he is confronted with an ischemic stroke. One of the strategies to better face the challenges of cerebrovascular disease and improve well being of the population and of the individual includes early recognition of the vulnerable high-risk atherosclerotic plaque.

Atherosclerosis

Atherosclerosis is an inflammatory condition of the vessel wall, which is affected by systemic risk factors including hypercholesteremia, hypertension, diabetes and overweight. It can affect the entire arterial tree, but is most relevant for cerebrovascular disease and events, if present in the carotid arteries. Atherosclerosis has affected humans for at least several thousand years and probably much longer. Although it is believed to be a disease of modern human beings and related to contemporary lifestyles, the ancient Egyptians were already found to suffer from the disease.(3)

Atherosclerotic plaques are characterized by fatty material, cholesterol deposits within the inner wall of artery, which cause wall thickening and eventually narrow the arterial lumen, the inside diameter of the artery, reducing blood flow or finally leading to a total obstruction.(4, 5) The traditional view was that arterial narrowing, i.e. stenosis, was the main causative factor in vascular diseases such as ischemic stroke. Accumulation of atherosclerotic plaque in the carotid artery may lead to positive remodeling in which the artery enlarges to preserve the luminal area, in particular in early stages. So the degree of luminal narrowing, however, is not the only determining factor for ischemic stroke and plaque composition and morphology, independent of their hemodynamic effect on the lumen, are related to plaque rupture and future cerebrovascular events. Plaque composition and plaque burden may therefore be additional parameters in the assessment of ischemic stroke risk.

Vulnerable plaques and intraplaque hemorrhage

Vulnerable plaques are atherosclerotic plaques that have a high-risk to rupture and, in the carotid arteries, they may lead to thromboembolism and complicate to ischemic stroke. (6-10) Vulnerable plaques are characterized by a large lipid-rich necrotic core (LRNC), intraplaque hemorrhage (IPH) or thin or ruptured fibrous cap (11-14). In previous studies, a number of vulnerable plaques have been found in arteries with lower grade stenosis. (15, 16) Although treatment decisions are still based predominantly on degree of stenosis, detection and management of the vulnerable plaque may improve risk reduction.(17, 18)

The studies described in this thesis will mainly evaluate the role of carotid IPH. The mechanism leading to IPH has not been unraveled yet. Some researchers suggested that rupture of the vasa vasorum or the immature neovessels with "leaky" immature linings may lead to the IPH.(19) (see fig 2 and 3) Others postulated that hemorrhage into a plaque is merely a complication of the rupture of the fibrous cap.(20) Nevertheless, evidence is accumulating that carotid IPH is significantly associated with ischemic stroke, possibly by stimulating the progression and destabilization of the plaque.(21-29) IPH that follows from immature neovessels formation seems to be the main mechanism of necrotic core expansion, oxidation, and inflammation in complex atherosclerosis.(30-32) These processes are considered

to cause carotid plaque destabilization.(8, 32) Carotid IPH is present in both symptomatic individuals as well as asymptomatic individuals from the general population.(33) In a recent meta-analysis amongst 689 individuals, it was shown that the pooled relative risk estimate (hazard ratio) for IPH in symptomatic individuals was 5.9 and in asymptomatic individuals was 3.5.(29) Prospective studies relating risk factors to IPH are lacking. Within the Rotterdam Study, we found in a previous study that age, male sex, smoking and hypertension are determinants of IPH in general population.(33) Identifying additional risk factors of IPH may contribute in early detection of the vulnerable plaque. The finding that hypertension is strongly related with IPH suggests a role for hemodynamic parameters as potential risk factors for plaque composition.

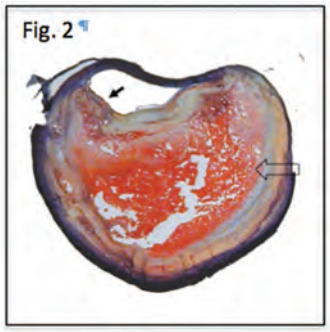

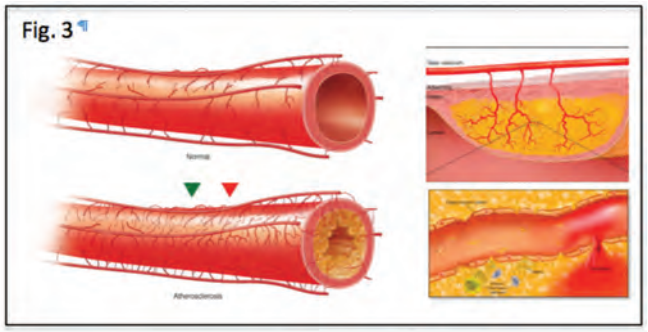

Fig 2 Cross-section of a carotid plaque with a large necrotic core (block arrow) containing hemorrhage (red staining) and thin fibrous cap near the shoulder of the core (arrow in the lumen). (Movat's Pentachrome stain, magnification 10×).(34)
IPH **fig 3:** Increased proangiogenic activity results in vasa vasorum proliferation and intimal neovascularization. Neovessels are fragile and may rupture or leak resulting in intraplaque hemorrhage.(35)

Hemodynamic parameters; potential risk factors for plaque composition

Blood pressure (BP) is a strong risk factor for cerebrovascular disease. The pulsatile component of blood pressure, pulse pressure (PP), is the consequence of intermittent ventricular ejection from the heart. In addition, PP is determined by the cushioning capacity of arteries and the timing and intensity of wave reflections.(36) (fig 4) The former is influenced by arterial stiffness.

BP is involved in two distinct functions of large arteries: the conduit function, which, on the basis of a pressure gradient, consists of supplying blood flow to peripheral tissues and organs; and a cushioning function, which is able to dampen the pressure oscillations that result from intermittent ventricular ejection ("Windkessel effect").(37)

Arterial stiffness describes the reduced capability of an artery to expand and contract in response to pressure changes. Parameters that describe vessel stiffness include compliance and distensibility. In a stiff vessel compliance is reduced. The consequence of reduced compliance/distensibility is increased pulse wave velocity (PWV), which is the velocity of the pressure pulse along the arterial tree. PWV is calculated by measuring time taken for a pressure pulse to travel between the carotid and femoral artery. Arterial stiffness, as measured by carotid-femoral PWV, is an independent predictor of cardiovascular morbidity and mortality in hypertensive patients, type 2 diabetes, end-stage renal disease and in elderly populations.(38) Given the common risk factors for arterial stiffness and atherosclerosis, studies that unravel mechanisms that link both conditions may be important in the prevention of cardiovascular events.(39)

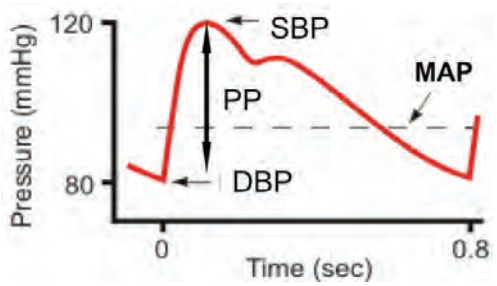

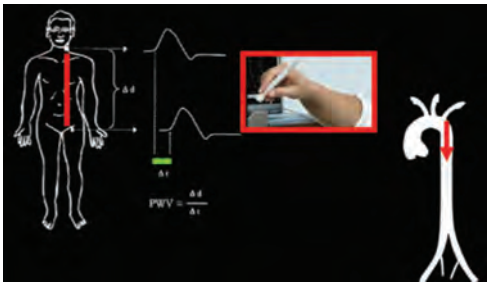

Fig 4. Blood pressure parameters: pulse pressure is the difference between the systolic and diastolic blood pressure. **Fig 5.** Measuring arterial stiffness: pulse wave velocity is calculated as the ratio between two pulse waves divided by the travel time.

MR Imaging of atherosclerosis

Several imaging modalities are available for imaging of carotid atherosclerosis. Currently, carotid ultrasonography is the most widely performed noninvasive test in the evaluation of a patient suspected of having carotid arterial disease.(40) However, the modality is highly operator dependent and not capable of consistent demonstration of plaque morphology.(40-42) Another noninvasive imaging technique is magnetic resonance imaging (MRI). MRI of the carotid wall has shown to be highly feasible to discriminate between the different atherosclerotic plaque features. For instance IPH, was detected with a good sensitivity and moderate to good specificity with histology as the gold standard.(22, 43-46) In this thesis, we used a 1.5 Tesla MRI scanner, with a bilateral 4 channel surface coil and a standard scanning protocol to visualize carotid atherosclerosis in the general population. Fig 6 shows three different plaque components, these are lipid, calcification and intraplaque haemorrhage, as can be detected on MRI scanning of the carotid arteries.

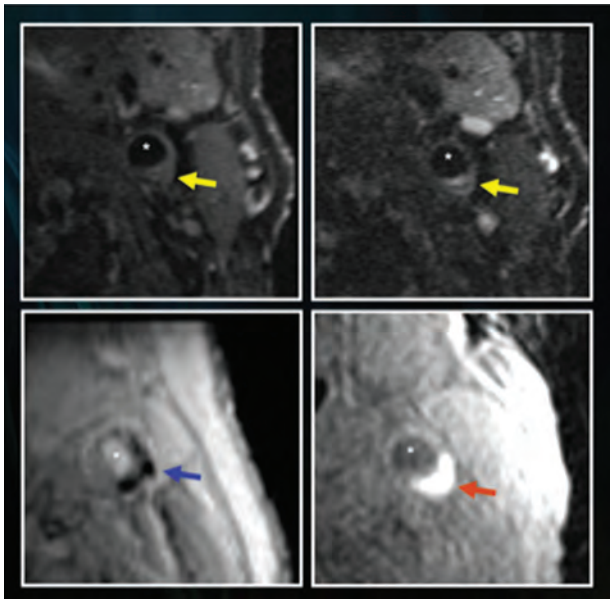

Fig 6. Carotid MRI scan, axial plan. A+B: Lipid core on PDw-EPI and T2w-EPI sequences, respectively (yellow arrow). C: Calcification on Phase-contrast MRA (blue arrow). D: Intraplaque haemorrhage on T1w-GRE sequence (red arrow). (*) Lumen carotid artery

Study population

All research is embedded in the Rotterdam Study (RS), a large prospective population-based cohort study among people of 55 years and older in Ommoord, a district of Rotterdam, The Netherlands. The study started in 1990 and participants have been followed for occurrence of cardiovascular diseases and other diseases since (RS-1). The cohort was extended in 2000 with persons who had become 55 years of age or moved into the study district since the start of the study (RS-2), and again in 2006 with persons aged 45 years and older (RS-3). The studies described in this thesis are based on participants that took part in all three cohorts (RS-1, RS-2 and RS-3). The carotid MRI scanning study was from October 2007 – November 2012.

Thesis objective

Rationale of this thesis

Knowledge about factors that influence carotid atherosclerotic plaque composition may eventually contribute to stroke prevention. From public health perspective, it is therefore important to investigate subclinical atherosclerosis in the general population. However, the majority of the investigations on carotid atherosclerotic plaque composition are in selected populations, such as symptomatic patients or patients with severe stenosis, while studies with unselected populations or that include subjects with less severe stenosis are scarce.

Therefore, we aimed to study risk factors for carotid atherosclerotic plaque composition as detected on MRI using a population-based approach. New parameters found in the general population might be used to improve prevention strategies.

Thesis outline

short description of every chapter

Chapter 2 focuses on the influence of hemodynamic parameters on plaque composition. Recently, hypertension was reported to be associated with presence of IPH.(33) However, of the different components of blood pressure, it is unclear which blood pressure parameter, systolic blood pressure, diastolic blood pressure, mean arterial pressure, or pulse pressure, contributes most to the development of IPH. The objective of the study described in **Chapter 2.1** is to investigate which hemodynamic parameter is most associated with presence of IPH as detected by MRI in asymptomatic subjects.

Arterial stiffness and atherosclerosis are both determinants of cerebral vascular disease. Arterial pulse wave velocity (PWV), an established measure of arterial stiffness, was previously shown as an independent risk factor for stroke and cardiovascular mortality.(47-50) The relation between PWV and presence of carotid atherosclerotic plaques and in specific the influence of arterial stiffness on atherosclerotic plaque composition is largely unknown. By examining the roll of arterial wall stiffening in relation to carotid atherosclerosis, we aim to gain more insight in the etiology of the vulnerable plaque. In **Chapter 2.2** we investigated the association between arterial stiffness, as assessed by PWV, and the presence of carotid atherosclerotic plaque and its various components in a large population-based cohort, using both ultrasound and MRI assessment of plaques.

Chapter 3 Ischemic strokes are more often diagnosed in the left hemisphere than in the right. It is unknown whether this asymmetrical prevalence relates to differences in carotid atherosclerosis. Although atherosclerosis is considered a systemic disease, its distribution across the vascular system is known to be not uniform, and it is thought to depend on several factors, including vessel geometry.(51, 52) Asymmetry in plaque characteristics between the left and right carotid artery has been poorly investigated, in particular with respect to vulnerable plaque components. In this chapter, we assessed the prevalence, severity and composition of atherosclerotic carotid plaque and investigated whether these characteristics differed between the left and right carotid artery.

Chapter 4 focuses on the association of carotid plaque characteristics and cardiovascular diseases. Atherosclerosis is the primary cause of cardiovascular disease, with stroke and ischemic heart disease as its most important manifestations. A systemic predisposition to plaque instability, attributable to systemic risk factors, suggests that plaque instability in the carotid arteries may be related with both stroke and ischemic heart disease. Until now, in

examining carotid plaque composition, the focus has primarily been directed to the risk of ischemic diseases in the brains, whilst the risk of ischemic disease in other end organs, such as the heart, remains to be elucidated. Carotid plaque characteristics related to ischemic stroke may differ from those related to ischemic heart disease. Hence, we examined the association between carotid atherosclerotic plaque characteristics, including vulnerable components, and history of ischemic stroke and coronary heart disease in a population-based cohort study.

Chapter 5 Atherosclerotic plaque burden is related to stroke and coronary heart disease.(53-55) Direct non-invasive measurements of the burden and composition of subclinical atherosclerosis have been proposed as a way to improve cardiovascular disease prevention and management. It has been suggested that plaque burden may provide more information on the extent of atherosclerosis beyond luminal stenosis.(56, 57) Accurate and reliable techniques are being actively pursued, as quantifying carotid plaque burden remains a challenging assignment. In a recent study, Van 't Klooster et al. presented a MRI-based method for carotid lumen and wall volume quantification.(58) In **Chapter 5.1** we present our initial experience using an MRI-based automated segmentation method for the inner and outer wall segmentation of the carotid arteries. In **chapter 5.2** we used post-processing software to quantify the sex-specific lumen volume and plaque burden of the carotid artery in a region around the bifurcation. The method was evaluated using a population-based approach.

IPH is an important marker of plaque destabilization through enhancement of inflammation and lipid accumulation.(8, 32) How IPH evolves over time remains to be elaborated. So far, few studies investigated IPH progression. These studies were predominantly conducted in symptomatic patients. Serial imaging of IPH in both carotid arteries is important for understanding the evolvement of subclinical atherosclerotic plaques into rupture-prone lesions. Evaluation of changes in IPH in asymptomatic individuals can identify novel risk factors for IPH growth and may provide further clues for prevention strategies. Quantifying IPH volumes using manual segmentations is a time-invasive process. Automated post-processing software is preferred in order to quantify the change of IPH volumes in large data sets. Furthermore, automated tools are preferred as they are more robust and reproducible. In **Chapter 6.1**, we introduce a validated semi-automated segmentation approach with minimal user interaction to quantify IPH volumes. The aim of **Chapter 6.2** is to evaluate the visual and quantitative change of IPH after one year follow up in asymptomatic subjects and to identify risk factors of IPH growth. For this purpose, we used automated segmentation to assess IPH volumes as detected on MRI in a nested-case-control approach.

References

1. Go AS, Mozaffarian D, Roger VL, Benjamin EJ, Berry JD, Blaha MJ, et al. Heart disease and stroke statistics--2014 update: a report from the American Heart Association. Circulation. 2014;129(3):e28-e292.
2. Feigin VL, Forouzanfar MH, Krishnamurthi R, Mensah GA, Connor M, Bennett DA, et al. Global and regional burden of stroke during 1990-2010: findings from the Global Burden of Disease Study 2010. Lancet. 2014;383(9913):245-54.
3. Thompson RC, Allam AH, Lombardi GP, Wann LS, Sutherland ML, Sutherland JD, et al. Atherosclerosis across 4000 years of human history: the Horus study of four ancient populations. Lancet. 2013;381(9873):1211-22.
4. Thiele BL, Young JV, Chikos PM, Hirsch JH, Strandness DE, Jr. Correlation of arteriographic findings and symptoms in cerebrovascular disease. Neurology. 1980;30(10):1041-6.
5. Harrison MJ, Marshall J. Angiographic appearance of carotid bifurcation in pateints with completed stroke, transient ischaemic attacks, and cerebral tumour. British medical journal. 1976;1(6003):205-7.
6. Little WC. Angiographic assessment of the culprit coronary artery lesion before acute myocardial infarction. Am J Cardiol. 1990;66(16):44G-7G.
7. Muller JE, Tofler GH, Stone PH. Circadian variation and triggers of onset of acute cardiovascular disease. Circulation. 1989;79(4):733-43.
8. Naghavi M, Libby P, Falk E, Casscells SW, Litovsky S, Rumberger J, et al. From vulnerable plaque to vulnerable patient: a call for new definitions and risk assessment strategies: Part I. Circulation. 2003;108(14):1664-72.
9. Millon A, Mathevet JL, Boussel L, Faries PL, Fayad ZA, Douek PC, et al. High-resolution magnetic resonance imaging of carotid atherosclerosis identifies vulnerable carotid plaques. J Vasc Surg. 2013;57(4):1046-51 e2.
10. Zavodni AE, Wasserman BA, McClelland RL, Gomes AS, Folsom AR, Polak JF, et al. Carotid Artery Plaque Morphology and Composition in Relation to Incident Cardiovascular Events: The Multi-Ethnic Study of Atherosclerosis (MESA). Radiology. 2014:131020.
11. Hatsukami TS, Ross R, Polissar NL, Yuan C. Visualization of fibrous cap thickness and rupture in human atherosclerotic carotid plaque in vivo with high-resolution magnetic resonance imaging. Circulation. 2000;102(9):959-64.
12. Kampschulte A, Ferguson MS, Kerwin WS, Polissar NL, Chu B, Saam T, et al. Differentiation of intraplaque versus juxtaluminal hemorrhage/thrombus in advanced human carotid atherosclerotic lesions by in vivo magnetic resonance imaging. Circulation. 2004;110(20):3239-44.
13. Teng Z, He J, Degnan AJ, Chen S, Sadat U, Bahaei NS, et al. Critical mechanical conditions around neovessels in carotid atherosclerotic plaque may promote intraplaque hemorrhage. Atherosclerosis. 2012;223(2):321-6.
14. Virmani R, Burke AP, Kolodgie FD, Farb A. Pathology of the thin-cap fibroatheroma: a type of vulnerable plaque. J Interv Cardiol. 2003;16(3):267-72.

15. Barnett HJ, Taylor DW, Eliasziw M, Fox AJ, Ferguson GG, Haynes RB, et al. Benefit of carotid endarterectomy in patients with symptomatic moderate or severe stenosis. North American Symptomatic Carotid Endarterectomy Trial Collaborators. N Engl J Med. 1998;339(20):1415-25.
16. Cai J, Hatsukami TS, Ferguson MS, Kerwin WS, Saam T, Chu B, et al. In vivo quantitative measurement of intact fibrous cap and lipid-rich necrotic core size in atherosclerotic carotid plaque: comparison of high-resolution, contrast-enhanced magnetic resonance imaging and histology. Circulation. 2005;112(22):3437-44.
17. DeMarco JK, Huston J, 3rd. Imaging of high-risk carotid artery plaques: current status and future directions. Neurosurgical focus. 2014;36(1):E1.
18. Yuan C, Mitsumori LM, Beach KW, Maravilla KR. Carotid atherosclerotic plaque: noninvasive MR characterization and identification of vulnerable lesions. Radiology. 2001;221(2):285-99.
19. Takaya N, Yuan C, Chu B, Saam T, Polissar NL, Jarvik GP, et al. Presence of intraplaque hemorrhage stimulates progression of carotid atherosclerotic plaques: a high-resolution magnetic resonance imaging study. Circulation. 2005;111(21):2768-75.
20. Davies MJ, Thomas AC. Plaque fissuring--the cause of acute myocardial infarction, sudden ischaemic death, and crescendo angina. British heart journal. 1985;53(4):363-73.
21. Singh N, Moody AR, Rochon-Terry G, Kiss A, Zavodni A. Identifying a high risk cardiovascular phenotype by carotid MRI-depicted intraplaque hemorrhage. Int J Cardiovasc Imaging. 2013.
22. Pasterkamp G, van der Steen AF. Intraplaque hemorrhage: an imaging marker for atherosclerotic plaque destabilization? Arterioscler Thromb Vasc Biol. 2012;32(2):167-8.
23. Altaf N, Daniels L, Morgan PS, Auer D, MacSweeney ST, Moody AR, et al. Detection of intraplaque hemorrhage by magnetic resonance imaging in symptomatic patients with mild to moderate carotid stenosis predicts recurrent neurological events. J Vasc Surg. 2008;47(2):337-42.
24. Albuquerque LC, Rohde LE. Correlation between carotid intraplaque hemorrhage and clinical symptoms. Stroke. 2008;39(5):e84.
25. Gao P, Chen ZQ, Bao YH, Jiao LQ, Ling F. Correlation between carotid intraplaque hemorrhage and clinical symptoms: systematic review of observational studies. Stroke. 2007;38(8):2382-90.
26. Altaf N, MacSweeney ST, Gladman J, Auer DP. Carotid intraplaque hemorrhage predicts recurrent symptoms in patients with high-grade carotid stenosis. Stroke. 2007;38(5):1633-5.
27. Hellings WE, Peeters W, Moll FL, Piers SR, van Setten J, Van der Spek PJ, et al. Composition of carotid atherosclerotic plaque is associated with cardiovascular outcome: a prognostic study. Circulation. 2010;121(17):1941-50.
28. Zhao H, Zhao X, Liu X, Cao Y, Hippe DS, Sun J, et al. Association of carotid atherosclerotic plaque features with acute ischemic stroke: A magnetic resonance imaging study. Eur J Radiol. 2013;82(9):e465-70.
29. Saam T, Hetterich H, Hoffmann V, Yuan C, Dichgans M, Poppert H, et al. Meta-analysis and systematic review of the predictive value of carotid plaque hemorrhage on cerebrovascular events by magnetic resonance imaging. J Am Coll Cardiol. 2013;62(12):1081-91.
30. Finn AV, Narula J. Intraplaque hemorrhage: most dangerous is the wound that bleedeth inwardly. JACC Cardiovasc Imaging. 2012;5(8):856-8.

31. Moreno PR, Purushothaman M, Purushothaman KR. Plaque neovascularization: defense mechanisms, betrayal, or a war in progress. Annals of the New York Academy of Sciences. 2012;1254:7-17.
32. Kolodgie FD, Gold HK, Burke AP, Fowler DR, Kruth HS, Weber DK, et al. Intraplaque hemorrhage and progression of coronary atheroma. N Engl J Med. 2003;349(24):2316-25.
33. van den Bouwhuijsen QJ, Vernooij MW, Hofman A, Krestin GP, van der Lugt A, Witteman JC. Determinants of magnetic resonance imaging detected carotid plaque components: the Rotterdam Study. Eur Heart J. 2012;33(2):221-9.
34. Dong L, Kerwin WS, Ferguson MS, Li R, Wang J, Chen H, et al. Cardiovascular magnetic resonance in carotid atherosclerotic disease. J Cardiovasc Magn Reson. 2009;11:53.
35. Doyle B, Caplice N. Plaque neovascularization and antiangiogenic therapy for atherosclerosis. J Am Coll Cardiol. 2007;49(21):2073-80.
36. O'Rourke MF, Hayward CS. The pulse of cardiology: quo vadis? J Am Coll Cardiol. 2009;54(8):714-7.
37. Safar ME, Levy BI, Struijker-Boudier H. Current perspectives on arterial stiffness and pulse pressure in hypertension and cardiovascular diseases. Circulation. 2003;107(22):2864-9.
38. Laurent S, Cockcroft J, Van Bortel L, Boutouyrie P, Giannattasio C, Hayoz D, et al. Expert consensus document on arterial stiffness: methodological issues and clinical applications. Eur Heart J. 2006;27(21):2588-605.
39. Cecelja M, Chowienczyk P. Role of arterial stiffness in cardiovascular disease. JRSM cardiovascular disease. 2012;1(4).
40. Gronholdt ML. Ultrasound and lipoproteins as predictors of lipid-rich, rupture-prone plaques in the carotid artery. Arterioscler Thromb Vasc Biol. 1999;19(1):2-13.
41. Kimura BJ, Bhargava V, DeMaria AN. Value and limitations of intravascular ultrasound imaging in characterizing coronary atherosclerotic plaque. Am Heart J. 1995;130(2):386-96.
42. Dogan A, Dempsey RJ. Diagnostic modalities for carotid artery disease. Neurosurgery clinics of North America. 2000;11(2):205-20.
43. Yuan C, Mitsumori LM, Ferguson MS, Polissar NL, Echelard D, Ortiz G, et al. In vivo accuracy of multispectral magnetic resonance imaging for identifying lipid-rich necrotic cores and intraplaque hemorrhage in advanced human carotid plaques. Circulation. 2001;104(17):2051-6.
44. Bitar R, Moody AR, Leung G, Symons S, Crisp S, Butany J, et al. In vivo 3D high-spatial-resolution MR imaging of intraplaque hemorrhage. Radiology. 2008;249(1):259-67.
45. Cappendijk VC, Cleutjens KB, Kessels AG, Heeneman S, Schurink GW, Welten RJ, et al. Assessment of human atherosclerotic carotid plaque components with multisequence MR imaging: initial experience. Radiology. 2005;234(2):487-92.
46. Saam T, Ferguson MS, Yarnykh VL, Takaya N, Xu D, Polissar NL, et al. Quantitative evaluation of carotid plaque composition by in vivo MRI. Arterioscler Thromb Vasc Biol. 2005;25(1):234-9.
47. Laurent S, Boutouyrie P, Asmar R, Gautier I, Laloux B, Guize L, et al. Aortic stiffness is an independent predictor of all-cause and cardiovascular mortality in hypertensive patients. Hypertension. 2001;37(5):1236-41.
48. Lehmann ED, Hopkins KD, Jones RL, Rudd AG, Gosling RG. Aortic distensibility in patients with cerebrovascular disease. Clin Sci (Lond). 1995;89(3):247-53.

49. Mattace-Raso FU, van der Cammen TJ, Hofman A, van Popele NM, Bos ML, Schalekamp MA, et al. Arterial stiffness and risk of coronary heart disease and stroke: the Rotterdam Study. Circulation. 2006;113(5):657-63.
50. Sutton-Tyrrell K, Najjar SS, Boudreau RM, Venkitachalam L, Kupelian V, Simonsick EM, et al. Elevated aortic pulse wave velocity, a marker of arterial stiffness, predicts cardiovascular events in well-functioning older adults. Circulation. 2005;111(25):3384-90.
51. Odink AE, van der Lugt A, Hofman A, Hunink MG, Breteler MM, Krestin GP, et al. Association between calcification in the coronary arteries, aortic arch and carotid arteries: the Rotterdam study. Atherosclerosis. 2007;193(2):408-13.
52. Phan TG, Beare RJ, Jolley D, Das G, Ren M, Wong K, et al. Carotid artery anatomy and geometry as risk factors for carotid atherosclerotic disease. Stroke. 2012;43(6):1596-601.
53. Stone GW, Maehara A, Lansky AJ, de Bruyne B, Cristea E, Mintz GS, et al. A prospective natural-history study of coronary atherosclerosis. N Engl J Med. 2011;364(3):226-35.
54. Mathiesen EB, Johnsen SH, Wilsgaard T, Bonaa KH, Lochen ML, Njolstad I. Carotid plaque area and intima-media thickness in prediction of first-ever ischemic stroke: a 10-year follow-up of 6584 men and women: the Tromso Study. Stroke. 2011;42(4):972-8.
55. Inaba Y, Chen JA, Bergmann SR. Carotid plaque, compared with carotid intima-media thickness, more accurately predicts coronary artery disease events: a meta-analysis. Atherosclerosis. 2012;220(1):128-33.
56. Rozie S, de Weert TT, de Monye C, Homburg PJ, Tanghe HL, Dippel DW, et al. Atherosclerotic plaque volume and composition in symptomatic carotid arteries assessed with multidetector CT angiography; relationship with severity of stenosis and cardiovascular risk factors. European radiology. 2009;19(9):2294-301.
57. de Labriolle A, Mohty D, Pacouret G, Giraudeau B, Fichet J, Fremont B, et al. Comparison of degree of stenosis and plaque volume for the assessment of carotid atherosclerosis using 2-D ultrasound. Ultrasound Med Biol. 2009;35(9):1436-42.
58. van 't Klooster R, de Koning PJ, Dehnavi RA, Tamsma JT, de Roos A, Reiber JH, et al. Automatic lumen and outer wall segmentation of the carotid artery using deformable three-dimensional models in MR angiography and vessel wall images. J Magn Reson Imaging. 2012;35(1):156-65.

Chapter 2

Hemodynamic parameters and intraplaque hemorrhage

Chapter 2.1

Blood pressure parameters and carotid intraplaque hemorrhage as measured by MRI: The Rotterdam Study

Mariana Selwaness
Quirijn van den Bouwhuijsen
Germaine C Verwoert
Abbas Dehghan
Francesco Mattace-Raso
Meike W. Vernooij
Oscar H Franco
Albert Hofman
Aad van der Lugt
Jolanda J Wentzel
Jacqueline CM Witteman

Abstract

Background: Intraplaque hemorrhage (IPH) is a characteristic of the vulnerable atherosclerotic plaque that has been associated with ischemic stroke. Not much is known about determinants of IPH. We studied whether blood pressure parameters are associated with presence of IPH.

Materials and methods: Within the framework of a prospective population-based cohort study, The Rotterdam Study, the carotid arteries of 1,006 healthy participants ≥45 years and with intima-media thickening (≥2.5mm) on ultrasound were imaged with a 1.5-T MRI scanner. IPH was defined as a hyperintense signal on a 3D-T1w-GRE MR sequence. Generalized estimation equation analysis, adjusted for age, sex, carotid wall thickness and cardiovascular risk factors, was used to assess the association between blood pressure parameters and IPH.

Results: MR imaging of the carotid arteries revealed presence of IPH in 444 of 1,860 (24%) plaques. Systolic blood pressure (SBP) and pulse pressure (PP) were significantly associated with IPH after adjustment for age and sex. In multivariate analysis, PP yielded the strongest association, with an odds ratio (OR) per SD increase in PP of 1.22 (95% CI 1.07-1.40). The OR per SD for SBP was 1.13 (0.99-1.28). Only PP remained significant after additional adjustment for other blood pressure components. The combination of smoking and isolated systolic hypertension was associated with a 2.5 times increased risk of IPH (1.2-5.2).

Conclusion: In conclusion, pulse pressure was the strongest determinant of IPH independent of cardiovascular risk factors and other blood pressure components. The association between pulsatile flow and IPH may provide novel insights in the development of the vulnerable plaque.

Introduction

Atherosclerotic plaques in the carotid arteries represent an important cause of cerebral ischemia. The composition of an atherosclerotic plaque is an important predictor for plaque rupture and subsequent thromboembolic events. Intraplaque hemorrhage (IPH) is considered a high-risk component of the vulnerable plaque through contribution of cholesterol to the necrotic core of the plaque and by increasing macrophage infiltration, making the plaque more unstable.[1-3] Several studies have indicated a strong association of IPH with cerebrovascular events.[3-5] Furthermore, even in atherosclerotic lesions of asymptomatic subjects, IPH was shown to contribute to plaque progression and destabilization.[6,7] Magnetic Resonance Imaging (MRI) has emerged as a reliable and accurate tool for discriminating plaque components *in vivo* and for detecting IPH.[7, 8] However, only few studies have investigated determinants of plaque composition in the carotid artery[9, 10] and, specifically, studies relating risk factors to IPH are scarce. We recently reported that sex, age, smoking and hypertension are associated with IPH in the general population.[11] Hypertension is a highly prevalent condition and a major contributor to atherosclerotic cardiovascular disease. However, the pathophysiology of the contribution of high blood pressure to atherosclerotic plaques is still not fully elucidated.

For a long time, hemodynamic forces have been linked to atherosclerosis formation and plaque destabilization.[12] Plaque instability is in part determined by local factors, but it has been suggested that systemic factors are also important.[13] Atherosclerotic plaques form at positions of disturbed blood flow and concomitant low and oscillating wall shear stress,[14] whereas all structures of the arterial wall are influenced by blood pressure fluctuations.

As a continuation of our previous study,[11] the current study was designed to determine the association of various blood pressure parameters with the presence of carotid intraplaque hemorrhage in a large population-based study.

Materials and methods

Study population

The study was performed within the framework of the Rotterdam Study, a population-based cohort study in The Netherlands, aimed at investigating determinants of various chronic diseases among the elderly. The study design and objectives of the Rotterdam Study were described elsewhere.[15] Briefly, the baseline visit started between 1990 and 1993. All inhabitants of Ommoord, a suburb of Rotterdam, aged 45 years and older were invited to participate. All participants were subsequently invited every three to four years to the research center for follow-up examinations, including carotid ultrasonography. The ultrasonography

protocol and reading has been described in detail previously.[16] For each individual, carotid wall thickening was determined as the maximum near and far wall measurements.

From October 2007 onwards, carotid MRI scanning was performed in all subjects with a maximum intima-media thickness ≥2.5mm on carotid ultrasound. Until October 2009, ultrasonography in 1,417 participants of the Rotterdam Study revealed intima-media thickness ≥2.5mm in left, right or both carotid arteries. These subjects were selected for MRI. Participants with contra-indications for MRI, prior carotid endarterectomy or poor image quality by MRI scan were excluded. As described previously, a total of 1,006 complete MRI examinations were performed. This resulted in 1,866 carotid arteries with plaque that were available for further analyses.[11] Information on blood pressure levels, cardiovascular risk factors and history of cardiovascular disease was obtained from the visit previous to MRI scanning. The Medical Ethics Committee of Erasmus Medical Center approved the study protocol and written informed consent was obtained from all participants. The study procedures were in accordance with institutional guidelines.

Blood pressure parameters

Two blood pressure measurements were taken with a random-zero sphygmomanometer after 5 minutes of rest with the subject in a sitting position. The mean of the two blood pressure values was used in the analyses. Pulse pressure (PP) was calculated as PP = SBP-DBP; mean arterial pressure (MAP) was calculated as MAP = DBP + 1/3 PP.[17] To quantify the relative magnitude of pulse pressure to mean artery pressure, we normalized the pulse pressure to the mean arterial pressure and referred to this value as the fractional pulse pressure (FPP) with FPP=PP/MAP.[18]

Hypertension at baseline was defined as a minimal level of 140/100mmHg (according to European Society of Cardiology criteria)[19] and/or the use of antihypertensive medication. The latter was assessed through automated linkage to pharmacies with computerized records. Assessment of antihypertensive drug usage included usage of diuretics, beta blockers, calcium channel blockers or ACE inhibitors at date of MRI scanning.

Covariates

Information on medical history and smoking behavior was collected through home interviews and covariates were measured at a study center visit as described previously.[11] Smoking status was classified as current, past and never. Body mass index (BMI) [weight (kg)/ height2 (m)] was calculated. Serum total cholesterol and high-density lipoprotein (HDL) cholesterol values were measured using standard laboratory techniques. Diabetes mellitus was considered to be present when fasting blood glucose exceeded 7.0 mmol/L, when

non-fasting glucose exceeded 11.1 mmol/L, or when antidiabetic medication was used. A history of cardiovascular disease was defined as a history of coronary heart disease or stroke at baseline.

MRI acquisition and image analysis

All scans were obtained with a 1.5 Tesla scanner with a bilateral phased-array surface coil. A standard scanning protocol was used with a total scanning time of about 30 minutes. Sequence parameters have been described in detail elsewhere.[11] Two-dimensional (2D) time-of-flight MR angiography was performed to cover the carotid bifurcation at both sides ranging from 15 mm caudal to 30 mm cranial from the point of bifurcation. Presence of IPH was determined using the 3D-T1w-GRE MRI sequence. Prior to the evaluation of plaque composition, the quality of all sequences in each MRI scan was rated on a five-point scale (1 = worst; 5 = best).[20] Scans were included in the analyses if the image quality was scored ≥3 on all MRI sequences. We assessed plaque characteristics in all plaques with a minimum carotid wall thickness of ≥ 2.0 mm on MRI.

Data analysis

Data are expressed as mean ± standard deviation for quantitative variables and percentages for discrete variables. All analyses were carried out using SAS version 9.2 (Cary, NC, USA). In primary analyses, we assessed the association of single blood pressure parameters, as continuous variables, with IPH. To adjust for the correlation between plaques in the two carotid arteries of the same participant, we performed Generalized Estimation Equation (GEE), with an independent or unstructured working correlation matrix including two levels per participant, namely the left and right carotid artery. To compare the associations between different blood pressure parameters and presence of IPH, odds ratios (ORs) with corresponding 95% confidence intervals (CIs) were estimated for a 1-standard deviation (SD) difference in each component. Adjustments were made for age, sex, carotid wall thickness on MRI, smoking status (current, past and never), BMI, total cholesterol and diabetes. Missing values in the covariates (6.1%) were imputed using the Expectation Maximization method.[21] P-values less than 0.05 were considered statistically significant.

The close correlation between SBP and PP hinders efforts to distinguish between these two components. Therefore, secondary analyses were performed in which the SBP and PP were additionally adjusted for the other blood pressure parameters. Probabilities of joint influences of SBP and DBP were estimated using the beta-coefficients obtained from the GEE model, for 55 year old males. We previously found an interaction between smoking and hypertension in relation to risk of IPH. We here evaluate the interaction of smoking with types of hypertension reflecting different levels of blood pressure components. The follow-

ing clinical classification was used: combined systolic/diastolic hypertension (SDH, SBP≥140 & DBP≥90 mmHg), isolated systolic hypertension (ISH, SBP≥140 & DBP<90 mmHg), and isolated diastolic hypertension (IDH, SBP<140 & DBP≥90 mmHg).[22] Normal blood pressure was defined as SBP<140 and DBP<90 mmHg. The combinations of types of hypertension and smoking status were evaluated by adding a product term to the multivariate model, using never smoking and normal blood pressure as reference. Finally, to examine whether blood pressure components are associated with severity of the outcome, i.e. bilateral IPH, we made categorical variables of blood pressure components based on quartiles. Hereby, the unilateral and bilateral IPH frequency was counted. Unadjusted analysis was conducted using Pearson's Chi-square test.

Table 1. Baseline characteristics of the study population

Variable	**MRI population (n=1,006)**
Sex (male) , n	524 (52.1%)
Age (years)	70.4 ± 10.2
Smoking **-** never, n	248 (24.7%)
- past, n	440 (43.7%)
- current, n	318 (31.6%)
BMI unit	27.4 ± 3.8
Total cholesterol (mmol/l)	5.6 ± 1.1
HDL (mmol/L)	1.4 ± 0.4
Diabetes, n	162 (16.1%)
Medical history - stroke, n	42 (4.2%)
- CHD, n	155 (15.4%)
Hypertension, n	726 (72.2%)
Systolic blood pressure (mmHg)	143 ± 20
Diastolic blood pressure (mmHg)	80 ± 11
Mean arterial pressure (mmHg)	101.2 ± 12.6
Pulse pressure (mmHg)	63.3 ± 17.3
Fractional pulse pressure	0.6 ± 0.2
Heart rate (beats/min)	70.4 ±13.7
Antihypertensive drug use, n (%)	478 (54.4%)
Carotid plaque on MRI scan	
Unilateral plaque, n	146 (14.5%)
Bilateral plaque, n	860 (85.5%)

Categorical variables are presented as numbers (%). Continuous values are expressed as mean±sd.

Results

Of the 2,012 carotid arteries scanned (n=1,006 subjects), 1,866 contained an atherosclerotic plaque >2.0 mm on MRI. 3 participants were excluded as information of blood pressure level was unavailable. This resulted in 1,860 carotid arteries for further analyses. Table 1 describes baseline characteristics of the study population.[11] The mean age was 70.4±10.2 years and 52.1% was male. In 444 (24%) carotid arteries, IPH was revealed on MRI while 1422 (76%) carotid arteries did not have IPH. In comparison with carotid arteries without IPH, plaques with IPH had a thicker carotid wall (3.9±1.2 vs. 3.1±0.8 mm) and 5.9% of the plaques caused moderate or severe stenosis (>30% stenosis) compared to 0.8% for plaques without IPH. Figure 1 shows magnetic resonance images of 3 carotid atherosclerotic plaques with intraplaque hemorrhage of subjects with high pulse pressure and low systolic blood pressure.

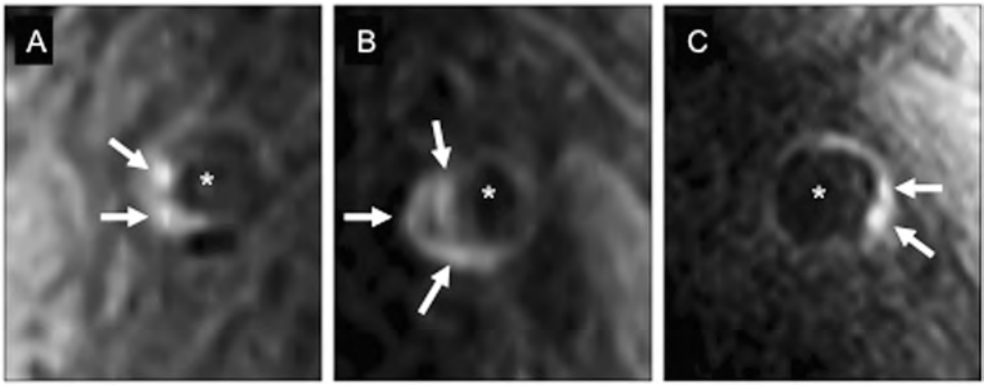

Figure 1. MRI images of carotid atherosclerotic plaques with IPH; Three subjects with a high pulse pressure and a low systolic blood pressure. A. Male (73y) RR 137/61 mmHg, B. Female (83y) RR 137/57 mmHg, C. Female (64y) RR 139/61 mmHg.
Asterisk: lumen of internal carotid artery. Arrow: intraplaque hemorrhage (high signal intensity on the T1w-GRE image).

Table 2 presents ORs per SD increase for each blood pressure parameter adjusted for age and sex (model 1) and adjusted for age, sex, carotid wall thickness and cardiovascular risk factors (model 2). SBP, PP and FPP were significantly associated with IPH after adjustment for age and sex. In multivariable analysis, PP yielded the strongest association with an OR per 1 SD in PP of 1.22 (1.07-1.40). Although the risk estimate of SBP changed only marginally in multivariable analysis, the association lost significance (model 2). No association was found of DBP and MAP with IPH. Additional adjustments for antihypertensive drug use, as well as exclusion of participants with prevalent coronary heart disease or stroke, did not affect the estimates (data not shown).

Table 2. Odds ratio's of intraplaque hemorrhage associated with blood pressure parameters in 1,860 carotid atherosclerotic plaques.

Variable	Model 1 OR (95%CI) p-value	Model 2 OR (95%CI) p-value
Systolic blood pressure (per sd)	1.14 (1.01-1.29) 0.04	1.13 (0.99-1.28) 0.07
Diastolic blood pressure (per sd)	0.96 (0.85-1.09) 0.55	0.94 (0.82-1.07) 0.33
Mean arterial pressure (per sd)	1.05 (0.93-1.18) 0.45	1.03 (0.91-1.16) 0.68
Pulse pressure (per sd)	1.23 (1.08-1.40) 0.002	1.22 (1.07-1.40) 0.004
Fractional pulse pressure (per sd)	1.22 (1.06-1.39) 0.004	1.23 (1.07-1.41) 0.003

Model 1: adjusted for age and sex.
Model 2: adjusted for age, sex, carotid wall thickness, smoking, diabetes, total cholesterol, BMI.
OR=Odds ratio. CI=confidence interval. sd=standard deviation.

Table 3 presents associations of SBP and PP with IHP, where these main variables were successively adjusted for each other as well as for the other blood pressure components. Adding any of the other blood pressure components to the model did not affect the association of PP with IPH, whereas the association of SBP with IPH was attenuated after adjustment for PP. Furthermore, risk estimates for SBP were increased after adjustment for DBP and MAP.

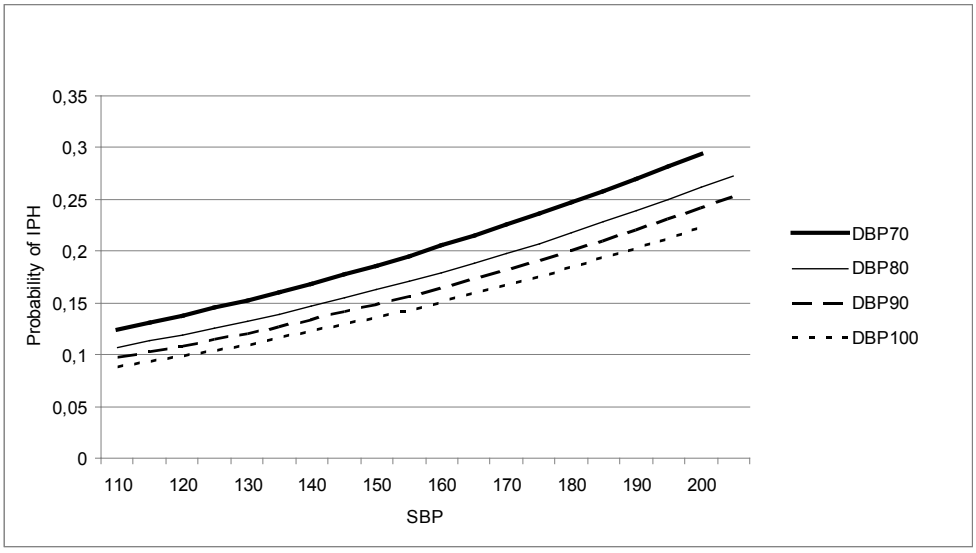

Figure 2. Joint influences of systolic blood pressure and diastolic blood pressure on intraplaque hemorrhage risk.
Probabilities were determined from GEE analysis for male gender with age 55 years. The probability of having an IPH increases with each level of SBP; However, at any given value of SBP, the risk is higher with lower DBP and thus, wider pulse pressure.
IPH=intraplaque hemorrhage. SBP=systolic blood pressure. DBP=Diastolic blood pressure.

Table 3. Odds ratio's of intraplaque hemorrhage associated with systolic blood pressure and pulse pressure with adjustment for other blood pressure components in 1,860 carotid atherosclerotic plaques.

Variable	Model 1 OR (95%CI) p-value	Model 2 OR (95%CI) p-value
Systolic blood pressure additionally adjusted for		
DBP	1.28 (1.09-1.50) 0.002	1.28 (1.09-1.50) 0.003
PP	0.91 (0.72-1.15) 0.43	0.87 (0.69-1.10) 0.26
MAP	1.51 (1.16-1.99) 0.003	1.54 (1.17-2.03) 0.002
Pulse pressure additionally adjusted for		
SBP	1.33 (1.04-1.69) 0.02	1.38 (1.07-1.76) 0.01
DBP	1.23 (1.08-1.41) 0.002	1.23 (1.07-1.41) 0.003
MAP	1.26 (1.09-1.47) 0.003	1.28 (1.09-1.49) 0.002

Model 1: adjusted for age and sex and other blood pressure parameter.
Model 2: adjusted for age, sex, carotid wall thickness, smoking, diabetes, total cholesterol, BMI and other blood pressure parameter.
OR=Odds ratio. CI=confidence interval. DBP=diastolic blood pressure. PP=pulse pressure. MAP=mean arterial pressure. SBP=systolic blood pressure.

Next, we evaluated the interaction between types of hypertension and smoking status. In subjects with SDH, ISH and IDH, mean±SD MAP and PP were 120.4±8.2 and 66.8±14.6, 104.2±7.1 and 76.8±13.9, 106.8±2.5 and 41.6±3.1 mmHg, respectively. The odds ratio of IPH was 1.9 (0.6-5.4) for the combination of current smoking and SDH, whereas for current smoking and ISH the risk of IPH was two and half times increased (OR 2.5, 1.2-5.2) compared to the reference category (normal blood pressure, never smoking). Due to low numbers of subjects with IDH (n=24), we were not able to evaluate the modifying effect of smoking for this type.

Figure 2 shows the joint influence of SBP and DBP on IPH. Probabilities were determined from GEE analysis for a male aged 55 years. The probability of IPH increased with increasing SBP level. However, at any given value of SBP, the probability of IPH is higher with lower DBP and thus, higher pulse pressure.

Finally, we examined the relation between PP and unilateral and bilateral presence of IPH. Figure 3 shows that the frequencies of unilateral and bilateral IPH increased with increasing quartile of PP (Pearson's Chi-square test $p<0.001$). The forth quartile of PP harbors the highest percentage of bilateral IPH (16.7%).

Discussion

In a large population-based study, we evaluated the association between various blood pressure parameters and the presence of IPH in carotid atherosclerotic plaques of subjects from the general population. The pulsatile component of blood pressure, as indicated by PP and FPP, was the strongest determinant of IPH independent of carotid wall thickness and cardiovascular risk factors. Furthermore, the association of PP with IPH was independent of the other blood pressure parameters. These findings add to our previous work showing that hypertension is an important risk factor for IPH.[11]

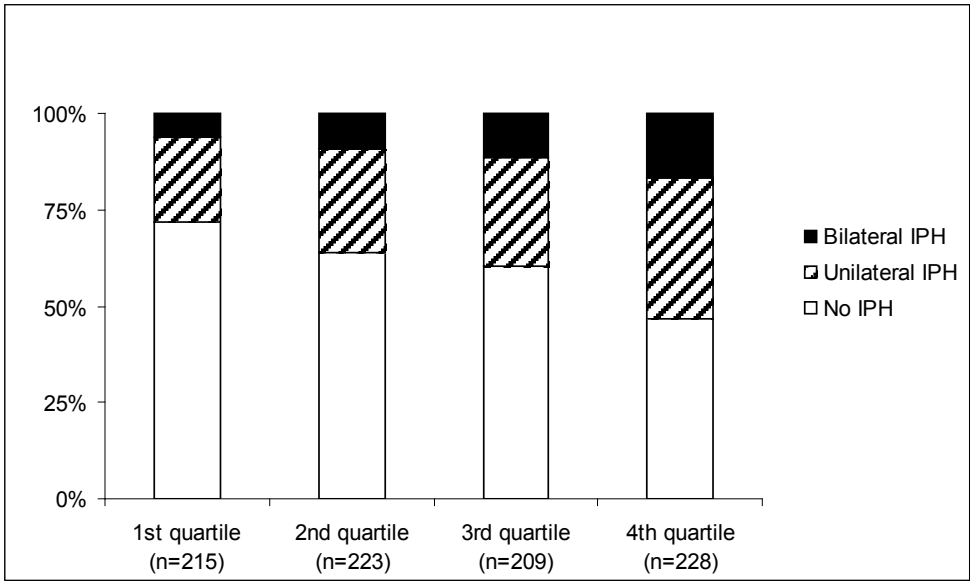

Figure 3. Prevalence of uni- and bilateral intraplaque hemorrhage per pulse pressure quartile. Pearson's Chi square test p=<0.0001.

PP and SBP are highly correlated, because both parameters rise with increases in vascular resistance and large-artery stiffness. Our results show that not all subjects with the same level of SBP have the same IPH risk. Subjects with lower DBP, and therefore higher PP, have a higher probability of IPH. In middle-aged and elderly subjects, an increase in PP with fixed SBP occurs solely as a function of declining DBP; and is a consequence of a rise in large-artery stiffness.[23] Statistical models in which PP and SBP parameters were additionally adjusted for each other as well as for the other blood pressure parameters enabled us to compare the contribution of both parameters individually. PP remained significantly associated with IPH after adjusting for all other blood pressure components, confirming the independent association of pulsatile pressure with IPH. Further support favoring PP over SBP in determining IPH was provided by the increase in association of SBP with IPH after adjustment for DBP and MAP, hereby reflecting the remaining influence of pulsatility. On the other hand,

SBP adjusted for PP was not significant. Our findings support the view that in particular the pulsatile component of blood pressure plays an important role in the development of IPH.

In a previous study, we found that current smoking and hypertension combined increased the risk of IPH almost three-fold.[11] In the current study, we extended the analysis by using different subtypes of hypertension, each type characterized by different values of MAP and PP. The combination of current smoking and ISH was associated with a 2.5 times increased risk of IPH. The strong and significant interaction between smoking and ISH compared to the non-significant interaction between smoking and SDH reflects the somewhat stronger effect of PP compared to SBP on IPH. However, our findings do not exclude an interaction of smoking and SDH in relation to risk of IPH. The smaller risk estimate for the combination of smoking and SDH in the current study as compared to the combination of smoking and hypertension, as reported by us previously[11], may be explained by the fact that SDH was based on blood pressure measurements only, we used lower threshold values (140/90 mmHg vs. 160/100mmHg) and subjects with ISH and IDH where naturally excluded from this subgroup.

Our findings are in agreement with previous studies in which PP has been reported as a predictor of acute coronary events and as an independent risk factor for stroke. [23-26] The randomized multicenter clinical trial Systolic Hypertension in the Elderly Program (SHEP) found that in patients with isolated systolic hypertension a decrease of the DBP, and concomitant increase in PP, increased the risk for stroke, coronary heart disease and cardiovascular disease.[26] This study also showed that the occurrence of both stroke and total mortality was related to PP level at baseline independent of mean pressure.[25]

Plaque components, such as IPH and lipid with or without a necrotic core are presumed to be important determinants of progression and destabilization of the plaque.[2, 7] That cyclic hemodynamic factors affect atherosclerosis progression and plaque instability is supported by several experimental models in which pulsatile strain was shown to affect the endothelium, vascular smooth muscle cells, and the production of elastin, collagen and glycosaminoglycans, resulting in increased atherosclerotic plaque volume.[27-30] However, rupture of a plaque occurs when the stresses within the plaque exceed the strength of the plaque. Accordingly one would expect a greater contribution of SBP than PP causing rupture of the neovessels. However, our findings suggest that the pulsatile mechanical load that acts on the arterial wall, irrespectively of the absolute value of blood pressure, is at least as important in the development of IPH.

IPH is believed to develop from the disruption of thin-walled microvessels that are lined by discontinuous endothelium without supporting–muscle cells.[31] An underlying pathophysiological mechanism linking PP to IPH could include the involvement of arterial stiffness. Large elastic arteries, such as the aorta and the carotid arteries, work predominantly as cushions, but with progressive arterial stiffening, the pulsations are not completely ab-

sorbed and may extend to the microcirculation[32], as was already shown in the brains[33] and the kidneys[34]. Likewise, enhanced pulsatile flow in the vasa vasorum of the carotid arteries may occur and cause hemorrhage of the neovessels in the plaque. Another possible explanation includes the involvement of enhanced microvessel formation, and hereby increasing the risk of IPH. IPH as well as rupture of the fibrous cap are associated with an increased density of microvessels in the plaque.[35] When subjecting the vessel wall, and in specific vascular smooth muscle cells *in vitro* to cyclic strain, it was shown that vascular endothelial growth factor (VEGF), which is an indicator of angiogenesis, is upregulated.[36] Also nicotine has been found to accelerate plaque growth and vascularization, and it has been suggested that VEGF has a role in this process.[37, 38] That both cyclic strain and nicotine are associated with enhanced angiogenesis may explain the interaction we found between smoking and ISH. Another theory involves the observations of Takaya et al[7] who reported that IPH remained detectable in the same plaque even after18 months, and therefore he suggested that either IPH does not resolve very rapidly or that IPH recurs in the same plaque repetitively. Recurrent rupture of the neovessel wall represents structural failure of a component of the diseased vessel.[39] The wall continuously interacts with hemodynamic forces,[40] and pulsatile pressure could possibly be the main mechanical trigger for such failure.

A major strength of this study is the large sample size and the high response rate. All 1,860 carotid arteries were from 1,006 individuals from the general population who had early signs of atherosclerosis on ultrasound. A limitation of this study is the cross-sectional design, which restricts our interpretation of the data with respect to cause and consequence. Although it is theoretically possible that IPH, or more in general presence of atherosclerosis, lead to an elevation in PP, a causal link is more likely to be in the opposite direction. In addition, blood pressure measurements can be variable, therefore, we tried to minimize this phenomenon by using the mean of two blood pressure measurements. Furthermore, effect modification by smoking was examined using types of hypertension based on single blood pressure measurements, irrespectively of the clinical diagnosis and usage of antihypertensive medication of the subjects. Also, plaques with wall thickness <2.0 mm were excluded because MRI differentiation between plaque components was not feasible in these small plaques.

Perspectives

The present study is the first that investigated the association between different blood pressure parameters and IPH in a large population-based study. We found that the pulsatile component, as indicated by PP, had the strongest association with IPH. The association was independent of traditional cardiovascular risk factors and other blood pressure components. We found that the combination of current smoking and ISH strongly increased the risk of IPH. Repetitive deformations in the carotid artery induced by pulsatile flow may play an important role in atherosclerosis progression and plaque destabilization. The observed

association between pulsatile flow and IPH, and additionally the effect modifying effect of smoking, provide novel insights in the pathology of the vulnerable plaque. However, further investigations are necessary to elucidate the pathophysiological mechanism.

Sources of Funding

This study was supported by the Netherlands Heart Foundation, (grant no. 2009B044) and the Netherlands Organization for Scientific Research (NWO/ZonMw) (Vici, grant no. 918-76-619).

Disclosure

None.

References

1. Kolodgie FD, Gold HK, Burke AP, Fowler DR, Kruth HS, Weber DK, Farb A, Guerrero LJ, Hayase M, Kutys R, Narula J, Finn AV, Virmani R. Intraplaque hemorrhage and progression of coronary atheroma. *N Engl J Med*. 2003;349:2316-2325.
2. Underhill HR, Yuan C, Yarnykh VL, Chu B, Oikawa M, Dong L, Polissar NL, Garden GA, Cramer SC, Hatsukami TS. Predictors of surface disruption with mr imaging in asymptomatic carotid artery stenosis. *AJNR Am J Neuroradiol*. 2010;31:487-493.
3. Altaf N, Daniels L, Morgan PS, Auer D, MacSweeney ST, Moody AR, Gladman JR. Detection of intraplaque hemorrhage by magnetic resonance imaging in symptomatic patients with mild to moderate carotid stenosis predicts recurrent neurological events. *J Vasc Surg*. 2008;47:337-342.
4. Gao P, Chen ZQ, Bao YH, Jiao LQ, Ling F. Correlation between carotid intraplaque hemorrhage and clinical symptoms: Systematic review of observational studies. *Stroke*. 2007;38:2382-2390.
5. Takaya N, Yuan C, Chu B, Saam T, Underhill H, Cai J, Tran N, Polissar NL, Isaac C, Ferguson MS, Garden GA, Cramer SC, Maravilla KR, Hashimoto B, Hatsukami TS. Association between carotid plaque characteristics and subsequent ischemic cerebrovascular events: A prospective assessment with mri--initial results. *Stroke*. 2006;37:818-823.
6. Underhill HR, Yuan C, Yarnykh VL, Chu B, Oikawa M, Polissar NL, Schwartz SM, Jarvik GP, Hatsukami TS. Arterial remodeling in [corrected] subclinical carotid artery disease. *JACC Cardiovasc Imaging*. 2009;2:1381-1389.
7. Takaya N, Yuan C, Chu B, Saam T, Polissar NL, Jarvik GP, Isaac C, McDonough J, Natiello C, Small R, Ferguson MS, Hatsukami TS. Presence of intraplaque hemorrhage stimulates progression of carotid atherosclerotic plaques: A high-resolution magnetic resonance imaging study. *Circulation*. 2005;111:2768-2775.
8. Bitar R, Moody AR, Leung G, Symons S, Crisp S, Butany J, Rowsell C, Kiss A, Nelson A, Maggisano R. In vivo 3d high-spatial-resolution mr imaging of intraplaque hemorrhage. *Radiology*. 2008;249:259-267.
9. Wagenknecht L, Wasserman B, Chambless L, Coresh J, Folsom A, Mosley T, Ballantyne C, Sharrett R, Boerwinkle E. Correlates of carotid plaque presence and composition as measured by mri: The atherosclerosis risk in communities study. *Circ Cardiovasc Imaging*. 2009;2:314-322.
10. Wasserman BA, Sharrett AR, Lai S, Gomes AS, Cushman M, Folsom AR, Bild DE, Kronmal RA, Sinha S, Bluemke DA. Risk factor associations with the presence of a lipid core in carotid plaque of asymptomatic individuals using high-resolution mri: The multi-ethnic study of atherosclerosis (mesa). *Stroke*. 2008;39:329-335.
11. Van den Bouwhuijsen QJ, Vernooij MW, Hofman A, Krestin GP, van der Lugt A, Witteman JC. Determinants of magnetic resonance imaging detected carotid plaque components: The rotterdam study. *Eur Heart J*. 2012;33:221-229.
12. Glagov S, Zarins C, Giddens DP, Ku DN. Hemodynamics and atherosclerosis. Insights and perspectives gained from studies of human arteries. *Arch Pathol Lab Med*. 1988;112:1018-1031.
13. Rothwell PM, Villagra R, Gibson R, Donders RC, Warlow CP. Evidence of a chronic systemic cause of instability of atherosclerotic plaques. *Lancet*. 2000;355:19-24.

14. Sadat U, Teng Z, Gillard JH. Biomechanical structural stresses of atherosclerotic plaques. *Expert Rev Cardiovasc Ther*. 2010;8:1469-1481.
15. Hofman A, van Duijn CM, Franco OH, Ikram MA, Janssen HL, Klaver CC, Kuipers EJ, Nijsten TE, Stricker BH, Tiemeier H, Uitterlinden AG, Vernooij MW, Witteman JC. The rotterdam study: 2012 objectives and design update. *Eur J Epidemiol*. 2011;26:657-686.
16. Iglesias del Sol A, Bots ML, Grobbee DE, Hofman A, Witteman JC. Carotid intima-media thickness at different sites: Relation to incident myocardial infarction; the rotterdam study. *Eur Heart J*. 2002;23:934-940.
17. Mattace-Raso FU, van der Cammen TJ, van Popele NM, van der Kuip DA, Schalekamp MA, Hofman A, Breteler MM, Witteman JC. Blood pressure components and cardiovascular events in older adults: The rotterdam study. *J Am Geriatr Soc*. 2004;52:1538-1542.
18. Jankowski P, Kawecka-Jaszcz K, Czarnecka D, Brzozowska-Kiszka M, Styczkiewicz K, Styczkiewicz M, Posnik-Urbanska A, Bryniarski L, Dudek D. Ascending aortic, but not brachial blood pressure-derived indices are related to coronary atherosclerosis. *Atherosclerosis*. 2004;176:151-155.
19. European Society of Hypertension-European Society of Cardiology Guidelines C. 2003 european society of hypertension-european society of cardiology guidelines for the management of arterial hypertension. *J Hypertens*. 2003;21:1011-1053.
20. Yuan C, Mitsumori LM, Ferguson MS, Polissar NL, Echelard D, Ortiz G, Small R, Davies JW, Kerwin WS, Hatsukami TS. In vivo accuracy of multispectral magnetic resonance imaging for identifying lipid-rich necrotic cores and intraplaque hemorrhage in advanced human carotid plaques. *Circulation*. 2001;104:2051-2056.
21. Dempster AP, Laird NM, Rubin DB. Maximum likelihood from incomplete data via the em algorithm. *J R Stat Soc B*. 1977;39:1-38.
22. Franklin SS, Jacobs MJ, Wong ND, L'Italien GJ, Lapuerta P. Predominance of isolated systolic hypertension among middle-aged and elderly us hypertensives: Analysis based on national health and nutrition examination survey (nhanes) iii. *Hypertension*. 2001;37:869-874.
23. Franklin SS, Khan SA, Wong ND, Larson MG, Levy D. Is pulse pressure useful in predicting risk for coronary heart disease? The framingham heart study. *Circulation*. 1999;100:354-360.
24. Benetos A, Rudnichi A, Safar M, Guize L. Pulse pressure and cardiovascular mortality in normotensive and hypertensive subjects. *Hypertension*. 1998;32:560-564.
25. Domanski MJ, Davis BR, Pfeffer MA, Kastantin M, Mitchell GF. Isolated systolic hypertension : Prognostic information provided by pulse pressure. *Hypertension*. 1999;34:375-380.
26. Somes GW, Pahor M, Shorr RI, Cushman WC, Applegate WB. The role of diastolic blood pressure when treating isolated systolic hypertension. *Arch Intern Med*. 1999;159:2004-2009.
27. Wung BS, Cheng JJ, Hsieh HJ, Shyy YJ, Wang DL. Cyclic strain-induced monocyte chemotactic protein-1 gene expression in endothelial cells involves reactive oxygen species activation of activator protein 1. *Circ Res*. 1997;81:1-7.
28. Lehoux S, Esposito B, Merval R, Tedgui A. Differential regulation of vascular focal adhesion kinase by steady stretch and pulsatility. *Circulation*. 2005;111:643-649.
29. Lee RT, Yamamoto C, Feng Y, Potter-Perigo S, Briggs WH, Landschulz KT, Turi TG, Thompson JF, Libby P, Wight TN. Mechanical strain induces specific changes in the synthesis and organization of proteoglycans by vascular smooth muscle cells. *J Biol Chem*. 2001;276:13847-13851.

30. Shaw A, Xu Q. Biomechanical stress-induced signaling in smooth muscle cells: An update. *Curr Vasc Pharmacol*. 2003;1:41-58.
31. Kolodgie FD, Narula J, Yuan C, Burke AP, Finn AV, Virmani R. Elimination of neoangiogenesis for plaque stabilization: Is there a role for local drug therapy? *J Am Coll Cardiol*. 2007;49:2093-2101.
32. O'Rourke MF, Hashimoto J. Mechanical factors in arterial aging: A clinical perspective. *J Am Coll Cardiol*. 2007;50:1-13.
33. Hashimoto J, Ito S. Some mechanical aspects of arterial aging: Physiological overview based on pulse wave analysis. *Ther Adv Cardiovasc Dis*. 2009;3:367-378.
34. Ishikawa T, Hashimoto J, Morito RH, Hanazawa T, Aikawa T, Hara A, Shintani Y, Metoki H, Inoue R, Asayama K, Kikuya M, Ohkubo T, Totsune K, Hoshi H, Satoh H, Imai Y. Association of micro-albuminuria with brachial-ankle pulse wave velocity: The ohasama study. *Am J Hypertens*. 2008;21:413-418.
35. Cicha I, Worner A, Urschel K, Beronov K, Goppelt-Struebe M, Verhoeven E, Daniel WG, Garlichs CD. Carotid plaque vulnerability: A positive feedback between hemodynamic and biochemical mechanisms. *Stroke*. 2011;42:3502-3510.
36. Schad JF, Meltzer KR, Hicks MR, Beutler DS, Cao TV, Standley PR. Cyclic strain upregulates vegf and attenuates proliferation of vascular smooth muscle cells. *Vasc Cell*. 2011;3:21.
37. Cooke JP. Angiogenesis and the role of the endothelial nicotinic acetylcholine receptor. *Life Sci*. 2007;80:2347-2351.
38. Heeschen C, Jang JJ, Weis M, Pathak A, Kaji S, Hu RS, Tsao PS, Johnson FL, Cooke JP. Nicotine stimulates angiogenesis and promotes tumor growth and atherosclerosis. *Nat Med*. 2001;7:833-839.
39. Li ZY, Taviani V, Tang T, Sadat U, Young V, Patterson A, Graves M, Gillard JH. The mechanical triggers of plaque rupture: Shear stress vs pressure gradient. *Br J Radiol*. 2009;82 Spec No 1:S39-45.
40. Jankowski P, Bilo G, Kawecka-Jaszcz K. The pulsatile component of blood pressure: Its role in the pathogenesis of atherosclerosis. *Blood Press*. 2007;16:238-245.

Chapter 2.2

Arterial stiffness is associated with carotid intraplaque hemorrhage in the general population: The Rotterdam Study

Mariana Selwaness
Quirijn van den Bouwhuijsen
Francesco Mattace-Raso
Germaine C Verwoert
Albert Hofman
Oscar H Franco
Jacqueline CM Witteman
Aad van der Lugt
Meike W Vernooij
Jolanda Wentzel

Abstract

Background: The relation between arterial stiffness and atherosclerosis, and specifically the influence of arterial stiffness on plaque composition is largely unknown. In a population-based study, we investigated the association between arterial stiffness and the presence and composition of carotid atherosclerotic plaques.

Materials and methods: Arterial stiffness was measured in 6,527 participants (67.0±8.6 years) using aortic pulse wave velocity (PWV). Presence of carotid atherosclerotic plaques was assessed with ultrasound. Subsequently, 1,059 of subjects with carotid plaques (>2.5mm) underwent magnetic resonance imaging to assess plaque composition (presence of intra-plaque hemorrhage, lipid and calcification). Generalized estimation equation analyses, adjusted for age, sex, mean arterial pressure, heart rate, carotid wall thickening, pulse pressure and traditional cardiovascular risk factors were used to study the association between PWV and the presence and composition of carotid atherosclerotic plaques.

Results: In multivariable analysis, higher PWV was independently related to higher prevalence of carotid atherosclerotic plaque on ultrasound (OR for highest quartile of PWV compared to lowest quartile 1.24; 95% confidence interval (1.02-1.51)). Furthermore, higher PWV was associated with IPH (age- and sex-adjusted OR per SD increase in PWV: 1.20 (1.04-1.38) and calcification 1.18 (1.03-1.35), but not with lipid. After adjustment for cardiovascular risk factors, PWV remained significantly associated with IPH (1.20; 1.01-1.43). Additional adjustment for pulse pressure did not materially affect the effect estimate (1.19;1.00-1.42).

Conclusions: Higher PWV is associated with presence and composition of carotid atherosclerotic plaques, in particular with IPH. These findings provide further clues for understanding the development of vulnerable atherosclerotic plaque.

Introduction

Atherosclerosis located in the carotid arterial wall is an important cause of stroke. Carotid atherosclerotic plaques can be composed of various components, such as a lipid pool (with/without necrosis), calcification and intraplaque hemorrhage (IPH), and are covered by a layer of fibrous material (the fibrous cap).[1] Plaques that contain a large necrotic core, IPH or thin fibrous cap, so-called vulnerable plaques, have been described to increase the risk of cardiovascular events.[2-4] In the past decade, the relation between carotid IPH and an increased risk of acute neurologic events has been demonstrated.[2,4-7] This underlines the importance to examine factors that may lead to atherosclerosis and in specific affect vulnerable plaque development.

Aortic pulse wave velocity (PWV), an established measure of arterial stiffness, was previously shown as an independent risk factor for stroke and cardiovascular mortality.[8-11] Although arterial stiffness and atherosclerosis share some common determinants, such as increasing age, sex and hypertension,[12] it is unknown whether a gradual stiffening of the arterial wall may accelerate development of vulnerable plaque components, such as IPH. In a previous study, we showed that a single, cross-sectional measurement of the pulsatile component of blood pressure was associated with IPH.[13] Arterial stiffness is the principal cause of increasing systolic blood pressure and pulsatility of flow, and therefore, PWV may reflect the cumulative damage on the arterial wall. Several studies have investigated the relation between arterial stiffness and aortic or coronary calcifications.[14-16] However, the relationship between arterial stiffness and carotid plaque components -either calcification or vulnerable plaque components- has received less attention. By examining the roll of vascular wall properties in the context of atherosclerosis formation, we aim to gain more insight in the etiology of the vulnerable plaque.

Magnetic resonance imaging (MRI) has emerged as a non-invasive imaging modality that enables accurate identification of the main components of the atherosclerotic plaque.[17,18] The objective of this study was to investigate the association between arterial stiffness, as assessed by PWV, and the presence and various components of carotid atherosclerotic plaque in a large population-based cohort, using both ultrasound and MRI assessment of plaques.

Materials and methods

Study population

The Rotterdam Study I (RS-I) is a prospective population-based cohort study among 7,983 participants aged ≥55 years which started in 1990-1993 and aimed at investigating determinants of various chronic diseases. In 2000-2001, the Rotterdam Study was expanded (RS-

II) with 3,011 participants who had become ≥55 years of age or had moved into the study district. In 2006, a further extension of the cohort was initiated (RS-III) in which 3,932 subjects were included, aged ≥45 years, fulfilling the same inclusion criteria as the original cohort. All participants are invited every three to four years to the research center for follow-up examinations, including carotid ultrasonography. Arterial stiffness measurements by means of PWV were conducted in 1997-2001 (RS-I and RS-II) and in 2006-2007 (RS-III). Since 2007, carotid MRI scanning has been performed in the Rotterdam Study. All participants with carotid wall thickening on a previous ultrasound examination were invited for carotid MRI scanning. The Medical Ethics Committee of Erasmus Medical Center approved the study protocol and written informed consent was obtained from all participants. The study procedures were in accordance with institutional guidelines.

Pulse wave velocity

Aortic PWV was measured with subjects in supine position. Measurements of PWV were performed during the morning or afternoon (no specific time) and the subjects were non-fasting. The PWV was assessed with an automatic device (Complior Artech Medical, Pantin, France)[19] that measures the time delay between the rapid upstroke of the feet of simultaneously recorded pulse waves in the carotid artery and the femoral artery. The distance between the recording sites in the carotid and the femoral artery was measured with a measurement tape over the surface of the body. The PWV was calculated as the ratio between distance and the foot-to-foot time delay, and was expressed in meters per second. Mean arterial pressure (MAP) and heart rate (HR) were recorded simultaneously as described previously.[11]

Ultrasound measurements

Ultrasonography of the common carotid artery, carotid bifurcation and internal carotid artery of the left and right carotid arteries was performed using a 7.5-MHz linear-array transducer (ATL Ultra-Mark IV). The ultrasonography protocol and reading has been described in detail previously.[20] For each individual, carotid wall thickening was determined as the maximum near and far wall measurements. Carotid wall thickening was reported as present if intima-media wall thickness (IMT) ≥2.5mm was observed in at least one of the carotid arteries.

Magnetic resonance imaging

Carotid MRI scanning was performed on a 1.5 Tesla scanner with a bilateral phased-array surface coil. Two-dimensional (2D) time-of-flight MR angiography was performed to cover the carotid bifurcation at both sides ranging from 15 mm caudal to 30 mm cranial from the point of bifurcation. High-resolution images were obtained using a 30 minutes standardized pro-

tocol that included four 2D axial sequences, (a) PDw Fast Spin Echo (FSE) Black-blood (BB) sequence with fat suppression; (b) PDw-FSE-BB sequence with an increased in-plane resolution; (c) a PDw-EPI sequence; (d) T2w-EPI sequence, and two 3D sequences (I) 3D-T1w-GRE sequence parallel to the common carotid artery, and (II) 3D phased-contrast MR-Angiography. Sequence parameters have been described in detail elsewhere.[21] The quality of all MRI sequences was rated on a fi e-point scale (1=worst; 5=best).[18] Scans were included in the analyses if the image quality was scored ≥3 on all MRI sequences. All carotid arteries were reviewed for presence of atherosclerotic plaques (≥2.0 mm on MRI) and we subsequently assessed each plaque for the presence of IPH, calcification and lipid as p eviously described.[21]

Covariates

Information on covariates was collected through home interviews or was measured at the study center visit as described previously.[22] Based on weight and height, the body mass index (BMI) was calculated. Blood pressure was measured using a random-zero sphygmomanometer at the study center visit and pulse pressure was calculated as the difference between the systolic and diastolic blood pressure. Serum total cholesterol and high-density lipoprotein (HDL) cholesterol values were measured using standard laboratory techniques. Smoking status was classified as current, past and never. Diabetes mellitus was considered to be present when fasting blood glucose exceeded 7.0 mmol/L, when non-fasting glucose exceeded 11.0 mmol/L, or when antidiabetic medication was used. Hypertension was defined as the use of antihypertensive medication or a blood pressure of 140/90 mmHg or above.[23] Antihypertensive drugs included diuretics, betablocking agents, calcium blockers and ACE inhibitors. History of myocardial infarction or stroke was assessed until date of inclusion as previously described.[24]

Population for analysis

PWV measurements were available in 6,915 the of Rotterdam Study participants, which is 60% of the eligible subjects (n=11,740) in this cohort. Missing information on PWV measurements was almost entirely due to logistic reasons, in particular malfunctioning equipment or unavailability of technicians. Among persons with PWV measurements, ultrasonography of the carotid arteries was available for 6,527 subjects (94%). Of these, 2,517 subjects had an atherosclerotic plaque ≥2·5mm in at least one of the carotid arteries. At the time of the present study, of these subjects, 1,439 had been invited for MRI of the carotid arteries. Of these, 380 subjects were not scanned because of claustrophobia, contraindications for MRI, refused to participate, or were excluded because of a scan with insufficient image quality. In the 1,059 subjects with an interpretable MRI scan, 1,979 carotid arteries had an atherosclerotic plaque (>2.0 mm on MRI) and were used for further analyses.

Statistical analysis

Data are expressed as mean±standard deviation (SD) for quantitative variables and percentages for discrete variables. We used logistic regression models to assess the association between PWV and carotid wall thickening on ultrasound. PWV was analyzed both in quartiles of its distribution (categorical) and per SD increase (continuous) in these models. For the analyses with PWV in quartiles of its distribution, the first quartile, indicating the lowest arterial stiffness, was used as the reference category. The model was first adjusted for age and sex (model 1) and additionally for MAP, HR, antihypertensive medication (model 2), pulse pressure (model 3) and cardiovascular risk factors (BMI, total cholesterol, HDL, smoking, diabetes and prevalent cardiovascular diseases (model 4).

Table 1. Baseline characteristics of the study population

	(I)	(II)		(III)	
Variable	**No plaque on US IMT <2.5mm (n=4,010)**	**Plaque on US IMT≥2.5mm (n=2,517)**	**P***	**MRI population (n=1,059)**	**P****
Age (years)	66.5 ± 9.0	67.7 ± 7.8	<0.001	66.2 ± 6.6	<0.001
Women	2451 (61.1)	1246 (49.5)	<0.001	495 (46.7)	0.1
Body mass index, (kg/m^2)	27.6 ± 3.8	27.7 ± 3.7	0.4	27.2 ± 3.5	<0.001
Total cholesterol (mmol/l)	5.6 ± 0.9	5.6 ± 1.0	0.5	5.6 ± 1.0	0.06
HDL-cholesterol (mmol/l)	1.5 ± 0.4	1.4 ± 0.4	<0.001	1.4 ± 0.4	0.3
Systolic blood pressure	146.4 ± 20.2	149.5 ± 20.8	<0.001	146.9 ± 20.1	<0.001
Diastolic blood pressure	81.8 ± 10.2	80.2 ± 10.7	<0.001	79.9 ± 10.9	0.02
Current smokers	899 (22.4)	764 (30.4)	<0.001	320 (30.2)	0.4
Past smokers	1453 (36.2)	1065 (42.3)	<0.001	471 (44.5)	0.1
Diabetes mellitus	538 (13.4)	455 (18.1)	<0.001	150 (14.2)	<0.001
Hypertension	3047 (76.0)	2093 (83.2)	<0.001	832 (78.6)	0.001
Antihypertensive medication	1620 (40.4)	1203 (47.8)	<0.001	456 (43.1)	0.07
History of myocardial infarction	304 (7.6)	310 (12.3)	<0.001	110 (10.4)	0.2
History of stroke	99 (2.5)	98 (3.9)	0.001	32 (3.0)	0.05
Mean arterial pressure (mmHg)	105.0 ± 13.3	106.6 ±12.7	<0.001	104.7 ± 12.4	<0.001
Heart rate (bpm)	73.0 ± 14.3	72.7 ± 14.1	0.1	71.5 ± 14.2	0.001
Aortic pulse wave velocity (m/s)	12.5 ± 3.0	13.1 ± 3.1	<0.001	12.6 ± 2.7	<0.001

Values are means ±standard deviation for continuous variables and percentages for dichotomous variables. US=ultrasound, IMT=intima-media thickness, HDL=high-density lipoprotein.
*age-adjusted p-values for difference between group I and II. ** age-adjusted p-values for difference between group II and III.

To study the association of PWV with different atherosclerotic plaque components on MRI, ORs were estimated per SD increase in PWV. To adjust for the correlation between plaques in the two carotid arteries of the same participant, we performed Generalized Estimation Equation (GEE) with an unstructured working correlation matrix including two levels per participant, namely the left and right carotid artery. All analyses were initially adjusted for age at PWV measurement, sex, time interval between PWV and MRI scan (model 1), MAP,

HR, antihypertensive medication and carotid wall thickness (model 2), and subsequently also for pulse pressure (model 3). In models 4 and 5, we additionally added cardiovascular risk factors to the models without pulse pressure (model 2) and with pulse pressure (model 3), respectively.

Because of the population composition, participants with PWV measurements conducted in 1997-2001 (RS-I and RS-II) had a longer time interval between PWV measurement and MRI compared to persons with PWV measurements in 2006-2007 (RS-III) (mean interval 10.9±0.2 years and 0.8±2.3 years, respectively). To study the effect of this time interval, we additionally analyzed the association between PWV and plaque composition stratified for time interval and tested for effect modification. All analyses were carried out using SPSS Statistical Package version 20.0 (Chicago, IL, USA). Missing values in the covariates were imputed using the Expectation Maximization method.[25]

Results

Amongst the 6,527 subjects (67.0±8.6 years) that underwent carotid ultrasonography, 2,527 (39.6%) subjects had one or more carotid plaques of ≥2.5 mm. Table 1 shows population characteristics of participants with ultrasound carotid plaques compared to those without plaques. Comparison of both groups showed that subjects with atherosclerotic plaque had a higher prevalence of various cardiovascular risk factors, including lower HDL-cholesterol, higher systolic blood pressure, lower diastolic blood pressure, higher prevalence of smoking, diabetes mellitus, hypertension, antihypertensive medication use, history of myocardial infarction and stroke (P<0.001). Of all persons with carotid plaque on ultrasound, to date, for 1,059 subjects carotid MRI scanning was available (Table 1). Although the MRI population was significantly younger, had lower BMI, systolic and diastolic blood pressure, lower prevalence of diabetes mellitus, and hypertension compared to subjects with carotid plaque ≥2.5 mm on US, the differences of the absolute values were small.

Table 2 shows the association between PWV and presence of plaque on ultrasound. In all models, higher quartiles of PWV were significantly associated to presence of plaque, when compared to the lowest quartile of PWV. Associations attenuated when additionally adjusted for pulse pressure (model 3), but remained significant for the second, third and fourth quartile of PWV compared to the first quartile, with respective ORs (95%CI) of 1.18 (1.01-1.37), 1.41 (1.19-1.66) and 1.27 (1.05-1.54). Subsequently, we investigated whether PWV was linearly related with the presence of plaque, but the linear trend for the association between PWV (per SD increase) and presence of plaques was not significant in the full model (OR of 1.06 (0.99-1.14)).

Table 3 describes the MRI plaque characteristics in 1,979 carotid arteries with wall thickening on MRI. Median (interquartile range) of carotid wall thickness on MRI and degree

Table 2. The association of arterial stiffness, as measured by pulse wave velocity, with presence of plaque on ultrasound (n=6,527)

Variable	PWV 1st quartile	PWV 2nd quartile		PWV 3th quartile		PWV 4th quartile		PWV (per SD)
		OR (95%CI)	P	OR (95%CI)	P	OR (95%CI)	P	
Model 1	1.00 (reference)	1.27 (1.10-1.47)	0.001	1.60 (1.37-1.86)	<0.001	1.48 (1.25-1.76)	<0.001	1.13 (1.07-1.20) <0.001
Model 2	1.00 (reference)	1.26 (1.08-1.46)	0.003	1.56 (1.33-1.84)	<0.001	1.44 (1.19-1.74)	<0.001	1.11 (1.04-1.19) 0.002
Model 3	1.00 (reference)	1.18 (1.01-1.37)	0.04	1.41 (1.19-1.66)	<0.001	1.27 (1.05-1.54)	0.02	1.07 (1.00-1.14) 0.06
Model 4	1.00 (reference)	1.24 (1.07-1.45)	0.005	1.50 (1.27-1.77)	<0.001	1.40 (1.15-1.69)	0.001	1.10 (1.02-1.17) 0.008
Model 5	1.00 (reference)	1.17 (1.00-1.36)	0.05	1.36 (1.15-1.61)	0.02	1.24 (1.02-1.51)	0.03	1.06 (0.99-1.14) 0.1

Model 1: adjusted for age and sex.
Model 2: adjusted as in model 1 + mean arterial pressure, heart rate + antihypertensive medication.
Model 3: adjusted as in model 2 + pulse pressure.
Model 4: adjusted as in model 2 + body mass index, total cholesterol, HDL-cholesterol, smoking, diabetes, history of myocardial infarction or stroke.
Model 5: adjusted as in model 3 + body mass index, total cholesterol, HDL-cholesterol, smoking, diabetes, history of myocardial infarction or stroke.
PWV=pulse wave velocity, OR=Odds ratio, CI=confidence interval, SD=standard deviation.

of stenosis was 3.0 (2.6-3.6) mm and 4.3 (0-20.6)%, respectively. MRI revealed presence of IPH in 520 (26.3%), lipid in 552 (27.9%) and calcification in 1,444 (73%) of carotid plaques.

Table 4 shows the association of PWV (per SD increase) with presence of the various MRI-defined plaque components. PWV was significantly associated with presence of IPH (age-, sex- and interval-adjusted OR per SD increase in PWV 1.20 (1.04-1.38)) (model 1). Additional adjustments for MAP, HR, antihypertensive medication, carotid wall thickness (model 2) and pulse pressure (model 3) only slightly attenuated this association. In the fully adjusted model (model 5), each SD increase in PWV increased the likelihood of IPH by approximately 20% (OR 1.19, 95%CI 1.00-1.42, *P*=0.05). The OR for the association between PWV and lipid was 1.13 (0.97-1.31), but lacked statistical significance. The association between PWV and calcification was inconclusive; although in model 1 the association was significant OR 1.18, 95%CI 1.03-1.35, *p*=0.02), in multivariable analyses the effect size decreased, and was no longer significant (OR 1.10 95%CI 0.93-1.31, p=0.2).

The analyses stratified for time interval between PWV and MRI showed no effect modification by time interval (supplementary table I). In both strata, the association between PWV and IPH was similar. Only for calcification, the effect estimate between PWV and presence of calcification was larger in the stratum with short time interval compared to long time interval (OR 1.59 versus 1.10; p-interaction = 0.8). (suppl table I).

Table 3. Plaque characteristics on MRI (n=1,979 carotid arteries)

Plaque characteristics on MRI (n=1,979 carotid arteries)	
Carotid wall thickening on MRI (mm)	3.0 (2.6-3.6)
Degree of stenosis (%)	4.3 (0-20.6)
Presence of IPH	520 (26.3)
Presence of lipid	552 (27.9)
Presence of calcificatio	1444 (73.0)

Values are presented as median (interquartile range) for continuous variables and percentages for dichotomous variables.

Table 4. Association between pulse wave velocity (per increase in standard deviation) and various plaque components (n=1,979 carotid plaques).

Model	**Intraplaque haemorrhage**			**Lipid**			**Calcification**		
	OR	**(95%CI)**	***P***	**OR**	**(95%CI)**	***P***	**OR**	**(95%CI)**	***P***
Model 1	1.20	(1.04-1.38)	0.01	1.06	(0.92-1.21)	0.4	1.18	(1.03-1.35)	0.02
Model 2	1.22	(1.03-1.45)	0.03	1.10	(0.95-1.28)	0.2	1.14	(0.97-1.35)	0.1
Model 3	1.21	(1.01-1.44)	0.03	1.12	(0.96-1.30)	0.2	1.12	(0.95-1.32)	0.2
Model 4	1.20	(1.01-1.43)	0.04	1.11	(0.96-1.29)	0.2	1.13	(0.95-1.33)	0.2
Model 5	1.19	(1.00-1.42)	0.05	1.13	(0.97-1.31)	0.1	1.10	(0.93-1.31)	0.3

Model 1: adjusted for age, sex and time interval between PWV and MRI measurement.

Model 2: adjusted as in model 1 + mean arterial pressure, heart rate, antihypertensive medication and carotid wall thickness

Model 3: adjusted as in model 2 + pulse pressure,.

Model 4: adjusted as in model 2 + body mass index, total cholesterol, HDL-cholesterol, smoking, diabetes, history of myocardial infarction or stroke.

Model 5: adjusted as in model 3 + body mass index, total cholesterol, HDL-cholesterol, smoking, diabetes, history of myocardial infarction or stroke.

OR=Odds ratio, CI=confidence interval, PWV = pulse wave velocity, MRI=magnetic resonance imaging.

DISCUSSION

In this large, population based cohort, we provide evidence that arterial stiffness is associated with presence and composition of carotid atherosclerotic plaques in the general population. By measuring aortic PWV, we found that arterial stiffness was independently associated with presence of plaques in the carotid arteries. Furthermore, among individuals with a plaque in the carotid arteries, arterial stiffness was an important determinant of IPH, independent of plaque size, pulse pressure and other cardiovascular risk factors. Associations between arterial stiffness and lipid or calcification were less pronounced.

Our finding that PWV is associated with presence of carotid atherosclerosis is in agreement with the Atherosclerosis Risk in Communities (ARIC) Study. In over 10,000 subjects, reduced arterial elasticity was significantly associated with carotid intima-media thickness (IMT) in the 90th percentile.[26] Also within the Rotterdam Study, it was previously shown that mean PWV was higher in subjects with moderate and severe carotid plaque score as compared to those without plaque.[27] However, our study extended this previous study population with on average younger subjects of additional cohort extensions (RS-II and RS-III) and we restricted definition of carotid atherosclerosis to IMT of ≥2.5 mm. Carotid intimal thickening represents one of the earliest manifestations of subclinical atherosclerosis. It has been suggested that lower degrees of IMT an adaptive response to local hemodynamic changes may be reflected rather than atherosclerotic thickening, which is represented beyond a certain level.[28] According to the Cardiovascular Health Study, 0.9 mm was considered as the threshold for the association with an increased risk of myocardial infarction and stroke in participants older than 65 years.[29] Our definition of plaque (IMT ≥2.5 mm) might thus be regarded as a more advanced manifestation of atherosclerosis. This is supported by earlier works in which, in 564 healthy subjects, arterial stiffness independently correlated with carotid atherosclerotic plaques, but not with diffuse common carotid intimal thickening at the plaque free sites.[30]

Additionally, we found arterial stiffness to be differently associated with different plaque components, suggesting involvement of vascular wall properties in the formation of the various plaque components. Studies investigating the relation between arterial stiffness and plaque composition are scarce. Moreover, ultrasonography, the most commonly used imaging modality for carotid plaque evaluation, is limited to a differentiation between echogenic and echolucent plaques.[15,31,32] The use of MRI for the assessment of plaque composition has now been widely accepted, and MRI has the ability to reliably assess presence of IPH, lipid and calcification.[17,18] One study that investigated arterial stiffness, measured as carotid distensibility, and plaque composition as detected with MRI found no association between carotid distensibility and plaque composition.[32] A difference between that study and ours is that local distensibility was measured instead of the global parameter pulse wave velocity.

The most interesting finding of our present study is that arterial stiffness is associated with the presence of IPH in the general population. This is important as IPH is considered as a risk indicator for plaque instability.[4-7] Several mechanisms may explain the association between arterial stiffness and IPH. Arterial stiffening may lead to early pulse wave reflection causing an increase in central systolic blood pressure, a decrease in diastolic blood pressure, and a subsequent increase in pulse pressure.[11] We have previously shown that out of several blood pressure components, pulse pressure was the strongest determinant of IPH[13]. When we controlled our current analyses for pulse pressure in model 3, associations attenuated somewhat, but we found PWV to be still associated with both plaque presence and with IPH. This indicates that PWV is associated with IPH independent of pulse pressure. Yet, we

should note that there is a complex relation between pulse pressure and arterial stiffness. There is some evidence[33] that this relationship may be bidirectional and may be amplified by atherosclerosis: on one hand the presence of atherosclerotic changes may impair the elastic properties of the wall, while on the other hand a reduced large artery compliance enhances wave reflection and augmentation of the pulsatile component of blood pressure, leading to the progression of atherosclerotic changes. Therefore, pulse pressure can be considered both a cause and consequence of arterial stiffness.[34] In this sense, adjustment for pulse pressure may have been an overadjustment and our models that included pulse pressure may have somewhat underestimated the association of PWV with plaque presence and plaque components.[35] Therefore, for all analyses we provide a full model with and without the addition of pulse pressure (model 4 and 5).

The functions of the arterial system are to deliver blood to the periphery and to transform the left ventricular ejection into a continuous flow.[36] High pulsatility as consequence of a less distensible aorta may be transferred down to arterioles[37] and possibly, also to the microcirculation. Subsequently, it can be hypothesized that higher flow pulsations due to arterial stiffness may extend more deeply into the fragile neovasculature within the vulnerable plaque, causing IPH. This hypothesis is consistent with several studies that showed a relation between reduced compliance in large arteries and pathologic conditions that are related with flow disturbances in the microcirculation.[38-41] In a cross-sectional population study, increased brachial-ankle PWV affected the microcirculation in brains and kidneys in a way leading to respectively cerebral asymptomatic lacunar infarction[40] and renal albuminuria.[41] In another population study that included 443 healthy subjects, PWV was significantly associated with silent cerebral microbleeds on brain MRI.[38] Also, one study reported a relation between arterial stiffness and microangiopathy in a diabetes type 1 population.[39]

On a local level, another aspect that needs to be considered is the fluid dynamics, which can underlie the connection between arterial stiffness and atherosclerotic plaque. Although flow in the common carotid artery has a laminar profile, this can evolve to velocity profile skewing at the carotid bifurcation, leading to regions in which the wall shear stress is low.[42] Atherosclerotic plaques tend to occur preferentially in these low wall shear stress sites.[43] These plaques can lead to stiffer walls, which in its turn may influence the plaque composition, and especially IPH as discussed before. Subsequently, the wall stiffening may also lead to alterations in the local wall shear stress. Although the connection between wall shear stress and IPH may be indirect, computational fluid dynamic models could be used to address this complex relationship.

Our finding that PWV was relatively weaker associated with lipid than with presence of calcification is supported by a previous study that investigated the carotid arteries of 561 healthy volunteers on ultrasound.[31] PWV was shown to be independently associated with echogenic, but not with echolucent plaques. Echogenic plaques are presumed to have higher contents of fibrous tissue and calcification.[44] Changes in the ratio of collagen to

elastin rather than deposition of lipid have been known to affect the elastic behavior and function of the arterial wall.[45,46] It has been suggested that degeneration of elastin renders the arterial wall to be more susceptible to calcification[15] and thus leads to less distensibility. Nevertheless, we did not find a pronounced association between arterial stiffness and plaque calcification, although this would have been expected from the biomechanical perspective that calcification leads to vessel stiffening. One explanation may be that PWV reflects global arterial stiffness and not necessarily vessel stiffness on the calcified site. Also, it is known that carotid calcification load only moderately correlates with aortic calcification.[47] Previous studies found inconsistent associations between arterial stiffness and plaque calcification.[32,48] A previous cross-sectional study within the Rotterdam Study found an independent association of arterial stiffness, measured as carotid-femoral PWV and carotid distensibility coefficient, with carotid calcification.[49] In contrast to our study, calcification was measured using computed tomography (CT) and quantified according to the Agatston score. Whereas with MRI we can only distinguish between presence or absence of calcification, with CT and the Agatston score more detailed and quantitative information is captured about the amount of calcification. Furthermore, PWV was measured on average 4.7 years prior to the CT, but up to 10.9 years before the MRI scanning. Although we found no significant effect modification of the time interval between PWV measurement and MRI, the lack of a pronounced association between PWV and calcification in the present study may have been influenced by the relatively long interval in part of our population, as the association with calcification tended to be weaker with increasing distance between measurements.

This study is limited by several methodological aspects which need to be discussed. Firstly, identification of plaque characteristics within very small plaques (<2 mm) was not feasible due to constraints in spatial resolution of MRI. This may have resulted in an underreporting of the prevalence of the different plaque components.

Secondly, we cannot completely exclude a possible link between arterial stiffness and lipid plaques, because application of contrast enhanced MRI, which improves identification of lipid, was not possible in this population-based setting.

Third, we did not measure arterial stiffness and plaque calcification on the same location, which may have reduced the association of arterial stiffness with this plaque component.

In conclusion, our study shows that pulse wave velocity is associated with presence of atherosclerotic plaques and with plaque composition, in particular IPH. These findings provide further clues for understanding the development of vulnerable atherosclerotic plaque.

Sources of Funding
This study was supported by the Netherlands Heart Foundation, (2009B044) and the Netherlands Organization for Scientific Research (NWO/ZonMwVici,918-76-619).

Acknowledgements
None.

Disclosures
None.

References

1. Toussaint JF, LaMuraglia GM, Southern JF, Fuster V, Kantor HL. Magnetic resonance images lipid, fibrous, calcified, hemorrhagic, and thrombotic components of human atherosclerosis in vivo. Circulation. 1996;94:932-938.
2. Hellings WE, Peeters W, Moll FL, Piers SR, van Setten J, Van der Spek PJ, de Vries JP, Seldenrijk KA, De Bruin PC, Vink A, Velema E, de Kleijn DP, Pasterkamp G. Composition of carotid atherosclerotic plaque is associated with cardiovascular outcome: a prognostic study. Circulation. 2010;121:1941-1950.
3. Teng Z, He J, Degnan AJ, Chen S, Sadat U, Bahaei NS, Rudd JH, Gillard JH. Critical mechanical conditions around neovessels in carotid atherosclerotic plaque may promote intraplaque hemorrhage. Atherosclerosis. 2012;223:321-326.
4. Underhill HR, Yuan C, Yarnykh VL, Chu B, Oikawa M, Dong L, Polissar NL, Garden GA, Cramer SC, Hatsukami TS. Predictors of surface disruption with MR imaging in asymptomatic carotid artery stenosis. AJNR Am J Neuroradiol. 2010;31:487-493.
5. Altaf N, Daniels L, Morgan PS, Auer D, MacSweeney ST, Moody AR, Gladman JR. Detection of intraplaque hemorrhage by magnetic resonance imaging in symptomatic patients with mild to moderate carotid stenosis predicts recurrent neurological events. J Vasc Surg. 2008;47:337-342.
6. Kolodgie FD, Gold HK, Burke AP, Fowler DR, Kruth HS, Weber DK, Farb A, Guerrero LJ, Hayase M, Kutys R, Narula J, Finn AV, Virmani R. Intraplaque hemorrhage and progression of coronary atheroma. N Engl J Med. 2003;349:2316-2325.
7. Michel JB, Virmani R, Arbustini E, Pasterkamp G. Intraplaque haemorrhages as the trigger of plaque vulnerability. Eur Heart J. 2011.
8. Sutton-Tyrrell K, Najjar SS, Boudreau RM, Venkitachalam L, Kupelian V, Simonsick EM, Havlik R, Lakatta EG, Spurgeon H, Kritchevsky S, Pahor M, Bauer D, Newman A, Health ABCS. Elevated aortic pulse wave velocity, a marker of arterial stiffness, predicts cardiovascular events in well-functioning older adults. Circulation. 2005;111:3384-3390.
9. Laurent S, Boutouyrie P, Asmar R, Gautier I, Laloux B, Guize L, Ducimetiere P, Benetos A. Aortic stiffness is an independent predictor of all-cause and cardiovascular mortality in hypertensive patients. Hypertension. 2001;37:1236-1241.
10. Lehmann ED, Hopkins KD, Jones RL, Rudd AG, Gosling RG. Aortic distensibility in patients with cerebrovascular disease. Clin Sci (Lond). 1995;89:247-253.
11. Mattace-Raso FU, van der Cammen TJ, Hofman A, van Popele NM, Bos ML, Schalekamp MA, Asmar R, Reneman RS, Hoeks AP, Breteler MM, Witteman JC. Arterial stiffness and risk of coronary heart disease and stroke: the Rotterdam Study. Circulation. 2006;113:657-663.
12. Cecelja M, Chowienczyk P. Dissociation of aortic pulse wave velocity with risk factors for cardiovascular disease other than hypertension: a systematic review. Hypertension. 2009;54:1328-1336.
13. Selwaness M, van den Bouwhuijsen QJ, Verwoert GC, Dehghan A, Mattace-Raso FU, Vernooij M, Franco OH, Hofman A, van der Lugt A, Wentzel JJ, Witteman JC. Blood pressure parameters and carotid intraplaque hemorrhage as measured by magnetic resonance imaging: The Rotterdam Study. Hypertension. 2013;61:76-81.

14. Oei HH, Vliegenthart R, Hofman A, Oudkerk M, Witteman JC. Risk factors for coronary calcification in older subjects. The Rotterdam Coronary Calcification Study. Eur Heart J. 2004;25:48-55.
15. Cecelja M, Jiang B, Bevan L, Frost ML, Spector TD, Chowienczyk PJ. Arterial stiffening relates to arterial calcification but not to noncalcified atheroma in women. A twin study. J Am Coll Cardiol. 2011;57:1480-1486.
16. Sekikawa A, Shin C, Curb JD, Barinas-Mitchell E, Masaki K, El-Saed A, Seto TB, Mackey RH, Choo J, Fujiyoshi A, Miura K, Edmundowicz D, Kuller LH, Ueshima H, Sutton-Tyrrell K. Aortic stiffness and calcification in men in a population-based international study. Atherosclerosis. 2012;222:473-477.
17. Bitar R, Moody AR, Leung G, Symons S, Crisp S, Butany J, Rowsell C, Kiss A, Nelson A, Maggisano R. In vivo 3D high-spatial-resolution MR imaging of intraplaque hemorrhage. Radiology. 2008;249:259-267.
18. Yuan C, Mitsumori LM, Ferguson MS, Polissar NL, Echelard D, Ortiz G, Small R, Davies JW, Kerwin WS, Hatsukami TS. In vivo accuracy of multispectral magnetic resonance imaging for identifying lipid-rich necrotic cores and intraplaque hemorrhage in advanced human carotid plaques. Circulation. 2001;104:2051-2056.
19. Asmar R, Benetos A, Topouchian J, Laurent P, Pannier B, Brisac AM, Target R, Levy BI. Assessment of arterial distensibility by automatic pulse wave velocity measurement. Validation and clinical application studies. Hypertension. 1995;26:485-490.
20. Iglesias del Sol A, Bots ML, Grobbee DE, Hofman A, Witteman JC. Carotid intima-media thickness at different sites: relation to incident myocardial infarction; The Rotterdam Study. Eur Heart J. 2002;23:934-940.
21. van den Bouwhuijsen QJ, Vernooij MW, Hofman A, Krestin GP, van der Lugt A, Witteman JC. Determinants of magnetic resonance imaging detected carotid plaque components: the Rotterdam Study. Eur Heart J. 2012;33:221-229.
22. Hofman A, van Duijn CM, Franco OH, Ikram MA, Janssen HL, Klaver CC, Kuipers EJ, Nijsten TE, Stricker BH, Tiemeier H, Uitterlinden AG, Vernooij MW, Witteman JC. The Rotterdam Study: 2012 objectives and design update. Eur J Epidemiol. 2011;26:657-686.
23. European Society of Hypertension-European Society of Cardiology Guidelines C. 2003 European Society of Hypertension-European Society of Cardiology guidelines for the management of arterial hypertension. J Hypertens. 2003;21:1011-1053.
24. Leening MJ, Kavousi M, Heeringa J, van Rooij FJ, Verkroost-van Heemst J, Deckers JW, Mattace-Raso FU, Ziere G, Hofman A, Stricker BH, Witteman JC. Methods of data collection and definitions of cardiac outcomes in the Rotterdam Study. Eur J Epidemiol. 2012;27:173-185.
25. Dempster AP, Laird NM, Rubin DB. Maximum Likelihood from Incomplete Data via the EM Algorithm. J R Stat Soc B. 1977;39:1-38.
26. Riley WA, Evans GW, Sharrett AR, Burke GL, Barnes RW. Variation of common carotid artery elasticity with intimal-medial thickness: the ARIC Study. Atherosclerosis Risk in Communities. Ultrasound Med Biol. 1997;23:157-164.
27. van Popele NM, Grobbee DE, Bots ML, Asmar R, Topouchian J, Reneman RS, Hoeks AP, van der Kuip DA, Hofman A, Witteman JC. Association between arterial stiffness and atherosclerosis: the Rotterdam Study. Stroke. 2001;32:454-460.

28. Bots ML, Hofman A, Grobbee DE. Increased common carotid intima-media thickness. Adaptive response or a reflection of atherosclerosis? Findings from the Rotterdam Study. Stroke. 1997;28:2442-2447.
29. O'Leary DH, Polak JF, Kronmal RA, Manolio TA, Burke GL, Wolfson SK, Jr. Carotid-artery intima and media thickness as a risk factor for myocardial infarction and stroke in older adults. Cardiovascular Health Study Collaborative Research Group. N Engl J Med. 1999;340:14-22.
30. Zureik M, Temmar M, Adamopoulos C, Bureau JM, Courbon D, Thomas F, Bean K, Touboul PJ, Ducimetiere P, Benetos A. Carotid plaques, but not common carotid intima-media thickness, are independently associated with aortic stiffness. J Hypertens. 2002;20:85-93.
31. Zureik M, Bureau JM, Temmar M, Adamopoulos C, Courbon D, Bean K, Touboul PJ, Benetos A, Ducimetiere P. Echogenic carotid plaques are associated with aortic arterial stiffness in subjects with subclinical carotid atherosclerosis. Hypertension. 2003;41:519-527.
32. Canton G, Hippe DS, Sun J, Underhill HR, Kerwin WS, Tang D, Yuan C. Characterization of distensibility, plaque burden, and composition of the atherosclerotic carotid artery using magnetic resonance imaging. Med Phys. 2012;39:6247-6253.
33. Dart AM, Kingwell BA. Pulse pressure--a review of mechanisms and clinical relevance. J Am Coll Cardiol. 2001;37:975-984.
34. Kopec G, Podolec P. Central pulse pressure: is it really an independent predictor of cardiovascular risk? Hypertension. 2008;52:e4; author reply e5.
35. Witteman JC, D'Agostino RB, Stijnen T, Kannel WB, Cobb JC, de Ridder MA, Hofman A, Robins JM. G-estimation of causal effects: isolated systolic hypertension and cardiovascular death in the Framingham Heart Study. Am J Epidemiol. 1998;148:390-401.
36. Vlachopoulos C, Alexopoulos N, Stefanadis C. Aortic stiffness: prime time for integration into clinical practice? Hellenic J Cardiol. 2010;51:385-390.
37. O'Rourke MF, Hashimoto J. Mechanical factors in arterial aging: a clinical perspective. J Am Coll Cardiol. 2007;50:1-13.
38. Ochi N, Tabara Y, Igase M, Nagai T, Kido T, Miki T, Kohara K. Silent cerebral microbleeds associated with arterial stiffness in an apparently healthy subject. Hypertens Res. 2009;32:255-260.
39. Rogowicz-Frontczak A, Araszkiewicz A, Pilacinski S, Zozulinska-Ziolkiewicz D, Wykretowicz A, Wierusz-Wysocka B. Carotid intima-media thickness and arterial stiffness in type 1 diabetic patients with and without microangiopathy. Arch Med Sci. 2012;8:484-490.
40. Hashimoto J, Ito S. Some mechanical aspects of arterial aging: physiological overview based on pulse wave analysis. Ther Adv Cardiovasc Dis. 2009;3:367-378.
41. Ishikawa T, Hashimoto J, Morito RH, Hanazawa T, Aikawa T, Hara A, Shintani Y, Metoki H, Inoue R, Asayama K, Kikuya M, Ohkubo T, Totsune K, Hoshi H, Satoh H, et al. Association of microalbuminuria with brachial-ankle pulse wave velocity: the Ohasama study. Am J Hypertens. 2008;21:413-418.
42. Ku DN, Giddens DP, Zarins CK, Glagov S. Pulsatile flow and atherosclerosis in the human carotid bifurcation. Positive correlation between plaque location and low oscillating shear stress. Arteriosclerosis. 1985;5:293-302.

43. Wentzel JJ, Chatzizisis YS, Gijsen FJ, Giannoglou GD, Feldman CL, Stone PH. Endothelial shear stress in the evolution of coronary atherosclerotic plaque and vascular remodelling: current understanding and remaining questions. Cardiovasc Res. 2012;96:234-243.
44. Wolverson MK, Bashiti HM, Peterson GJ. Ultrasonic tissue characterization of atheromatous plaques using a high resolution real time scanner. Ultrasound Med Biol. 1983;9:599-609.
45. Intengan HD, Schiffrin EL. Vascular remodeling in hypertension: roles of apoptosis, inflammation, and fibrosis. Hypertension. 2001;38:581-587.
46. Greenwald SE. Ageing of the conduit arteries. J Pathol. 2007;211:157-172.
47. Odink AE, van der Lugt A, Hofman A, Hunink MG, Breteler MM, Krestin GP, Witteman JC. Association between calcification in the coronary arteries, aortic arch and carotid arteries: the Rotterdam study. Atherosclerosis. 2007;193:408-413.
48. Cecelja M, Hussain T, Greil G, Botnar R, Preston R, Moayyeri A, Spector TD, Chowienczyk P. Multimodality imaging of subclinical aortic atherosclerosis: relation of aortic stiffness to calcification and plaque in female twins. Hypertension. 2013;61:609-614.
49. Odink AE, Mattace-Raso FU, van der Lugt A, Hofman A, Hunink MG, Breteler MM, Krestin GP, Witteman JC. The association of arterial stiffness and arterial calcification: the Rotterdam study. J Hum Hypertens. 2008;22:205-207.

Supplementary table I. Association between pulse wave velocity and different plaque components stratified for time interval between both measurements

Variable	Number of carotid plaques	Median (IQR) time interval (years)	Intraplaque haemorrhage OR, (95%CI), P-value	Lipid OR, (95%CI), P-value	Calcification OR, (95%CI), P-value
Short interval	313	0.8 (0.2)	1.18 (0.97-1.95) 0.5	0.91 (0.55-1.48) 0.7	1.59 (0.92-2.78) 0.1
Long interval	1,666	10.9 (2.3)	1.21 (1.01-1.45) 0.04	1.08 (0.92-1.27) 0.3	1.10 (0.93-1.30) 0.2
p-value for interaction			0.7	0.5	0.8

Interval presented as median (interquartile range) in years. Model adjusted for age, sex, time interval between PWV and MRI, MAP, HR and carotid wall thickness.
OR=Odds ratio.

Chapter 3

Atherosclerotic plaques in the left carotid artery are more vulnerable than on the contralateral side

Mariana Selwaness
Quirijn van den Bouwhuijsen
Robert S van Onkelen
Albert Hofman
Oscar H Franco
Aad van der Lugt
Jolanda J Wentzel
Meike W Vernooij

Abstract

Background: Ischemic stroke is more often diagnosed in the left hemisphere than in the right. It is unknown whether this asymmetrical prevalence relates to differences in carotid atherosclerosis. We compared atherosclerotic plaque prevalence, severity and composition between left and right carotid arteries.

Materials and methods: In a population-based cohort, carotid MRI scanning was performed in 1414 stroke-free participants (≥45 years). Using a multisequence MR protocol, we assessed the prevalence, stenosis and thickness of the plaque and its predominant component, i.e. lipid core, intraplaque haemorrhage (IPH), calcification, or fibrous tissue in each carotid artery. Differences between left and right side were tested using paired *t* tests, McNemar's test and Generalized Estimating Equation analyses.

Results: The majority (85%) of the participants had bilateral carotid plaques. Unilateral plaques were twice more prevalent on the left than on the right side (67% vs. 33%, $P<0.001$). Plaque thickness was also greater on the left (3.1±1.2 vs. 2.9±1.3 *mm*; $P<0.001$); degree of stenosis did not differ. IPH and fibrous tissue were more prevalent on the left (9.1 vs. 5.9%; $P<0.001$ and 45.0 vs. 38.5%; $P<0.001$), while calcification occurred more often on the right (37.4 vs. 31.6% at the left; $P<0.001$). Lipid was equally distributed.

Conclusions: Carotid atherosclerotic plaque size and composition are not symmetrically distributed. Predominance of IPH in left-sided carotid plaques suggests a greater vulnerability as opposed to right-sided plaques, which are more calcified and therefore considered more stable.

Introduction

Atherosclerotic disease in the carotid arteries is a major cause of ischemic cerebrovascular events.[1] In patient-based series, a significantly higher proportion of ischemic events is diagnosed in the left hemisphere than in the right.[2-4] Infarctions in the left hemisphere are more likely to be recognized, because most people have a dominant left hemisphere for language processing, while infarctions in the right hemisphere may be accompanied by a more easily overlooked cognitive deficit or apraxia.[3-5] Yet, an alternative hypothesis for the higher incidence of events in the left hemisphere may be related to a higher prevalence, severity or vulnerability of atherosclerotic disease in the left carotid artery.

Although atherosclerosis is considered a systemic disease, its distribution across the vascular system is not uniform, and it is thought to depend on several factors, including vessel geometry.[6,7] Furthermore, it is feasible that not only plaque severity, but also plaque composition vary according to location.[8] Some plaque components, such as intraplaque hemorrhage (IPH), are presumed to enhance vulnerability of the plaque, whilst calcification may promote plaque stability.[9] Asymmetry in plaque characteristics between the left and right carotid artery has been poorly investigated, in particular with respect to vulnerable plaque components. Most studies that focused on plaque asymmetry were conducted within clinical or patient-based settings and are therefore often subject to selection bias. A population-based study with asymptomatic individuals is therefore the best setting to study the natural history of plaques.

In this study, we assessed in 1414 stroke-free individuals with magnetic resonance imaging (MRI) the prevalence, severity and composition of atherosclerotic carotid plaque and investigated whether these characteristics differed between the left and right carotid artery.

Materials and methods

Study population

The Rotterdam Study is a prospective population-based cohort study in subjects aged ≥45 years, as detailed elsewhere.[10] All study participants routinely undergo carotid ultrasonography to assess carotid intima-media thickness (measured as maximum distance between the near and far wall).[11] Of 10073 participants with carotid ultrasound, 3795 participants (38%) had wall thickness ≥2.5 mm in at least one carotid. Participants who passed away, moved out of the study area or were physically disabled (n=701) or had known MRI contraindications (n=428) could not be invited. In total, 2666 participants were invited for carotid MRI scanning. Subsequently, 684 participants did not undergo MRI scanning, because of claustrophobia (n=57), physical restrictions (n=191), contraindications (n=115), refusal to participate (n=272), no show or lost to follow-up (n=49). The remaining 1982 participants

(74% of those initially invited) underwent MRI of both carotids. Scans were excluded if image quality was bad (n=95), if no plaques ≥2mm were observed on both sides (n=41) or if scanning was incomplete due to claustrophobia (n=106). We furthermore excluded 87 participants with a history of transient ischemic attack or stroke. For 238 scans, analyses were not completed at the time of this study. This resulted in 1414 complete carotid MRI scans. The Medical Ethics Committee approved the study and all participants gave written informed consent.

MRI acquisition

Scans were obtained with a 1.5-Tesla scanner (GE Healthcare, Milwaukee, WI, USA) with a bilateral phased-array surface coil (Machnet, Eelde, the Netherlands). 2D time-of-flight MR angiography covered the carotid bifurcation on both sides, ranging from 15 mm caudally to 30 mm cranially from the bifurcation. All exams were found to have sufficient coverage bilaterally. A standard scanning protocol was used and included: proton density-weighted (PDw)-fast spin echo (FSE)-black blood (BB) sequence; PDw-echo planar imaging (EPI) sequence; T2w-EPI sequence, 3D-T1w-gradient echo (GRE) sequence and 3D phased-contrast MR angiography.[12] Total scanning time was approximately 30 minutes.

Image review

Image quality was assessed and found sufficient in 95% of scans.[13] In both carotids, PDw-FSE images were used to measure maximum carotid wall thickness, minimal luminal diameter and the distal luminal diameter.[14] Luminal stenosis was then calculated according to the North American Symptomatic Carotid Endarterectomy Trial (NASCET) criteria.[15] Plaques were visually reviewed for prevalence of three different plaque components; calcification, intraplaque haemorrhage, and lipid core. Intraplaque hemorrhage was defined as a hyperintense region in the atherosclerotic plaque on the 3D-T1w-GRE sequence. Calcification was defined as a hypointense region on all sequences, but mainly on the magnitude images of the 3D-PC-MRA sequence. Lipid was defined as a region not classified as intraplaque haemorrhage or calcification on PDw-FSE, PDw-EPI and T2w-EPI images, and with a relative signal-intensity drop in the plaque on the T2w-EPI sequence.[13,16,17] Prevalence of multiple components was permissible within one plaque. Furthermore, one of these components was also selected as the most predominant component, which we defined as a single main component that covered the largest proportion of the plaque based on visual assessment. Hereby, fibrous tissue was added as an additional option if other components were absent or only minimally present.[16,17] Plaques were reviewed for plaque characteristics with a standardized evaluation protocol by one of two trained observers (MS and QvdB), blinded to all participant characteristics, overseen by a Radiologist (AvdL) with 12 years of experience. In cases of doubt or disagreement, the judgment by the expert was considered definite.

Inter-rater agreement for predominant and prevalent component (n=60 carotid arteries) was excellent (κ 0.88-0.94)[12]

Cardiovascular risk factors

Information on cardiovascular risk factors was obtained from the closest research center visit prior to the MRI scanning and measured as described previously.[12] Hypertension was defined as the use of antihypertensive medication or blood pressure of ≥140/90 mmHg. Serum total cholesterol was measured using standard laboratory techniques. Smoking status was classified as ever or never. Diabetes mellitus was considered present when fasting blood glucose exceeded 7.0 mmol/L, when non-fasting glucose exceeded 11.0 mmol/L, or when antidiabetic medication was used. A history of cardiovascular disease was defined as a history of myocardial infarction until date of MRI.[18]

Statistical analysis

Differences in prevalence, stenosis, thickness and composition of atherosclerotic plaques between the left and right carotid arteries were tested using paired *t*-tests for continuous variables and McNemar's test for categorical variables. A value of zero was substituted for plaque thickness and degree of stenosis if atherosclerotic plaque was absent on one side. To adjust for confounders and take into account within-subject correlations between the two carotid arteries, we used Generalized Estimation Equation analyses. These analyses were modeled with an unstructured working correlation matrix that included two levels per participant, i.e. left and right carotid artery. We studied effect modification by age, by entering an interaction term in the model. Odds ratios (ORs) and corresponding 95% confidence intervals (CIs) adjusted for age, sex and carotid wall thickness were estimated per predominant component. All analyses were carried out using the Statistical Package for Social Sciences (SPSS) version 20.0 (Chicago, IL, USA).

Results

Carotid atherosclerotic plaque characteristics on MRI were available for 1414 asymptomatic participants (table 1), with mean age of 72.0±9.6 years and 749 men (53%). Overall, 1196 subjects (85%) had plaque in both carotid arteries. Among the 218 subjects with unilateral plaque, left-sided plaques were twice as prevalent as right-sided plaques (145 vs. 73, $P<0.001$). This did not differ across men and women (72 left-sided vs. 31 right-sided in men; $P<0.001$ and 73 vs. 42 in women; $P<0.001$). However, individuals with unilateral left-sided plaques were significantly younger than participants with unilateral right-sided plaques (68.3±10.0 vs. 71.2±10.4 years; P 0.04).

Asymmetry of plaque severity and plaque composition is presented in table 2. Whereas overall carotid wall thickness was slightly greater on the left than on the right (3.1±1.2 mm vs. 2.9±1.3 mm, *P*<0.001), the degree of luminal stenosis did not differ. Also, the degree of clinically relevant stenosis did not differ between sides: 64 (4.5%) participants had stenosis >50% on the left side vs. 72 (5.1%) on the right side (p=0.4). Lipid and IPH were both more frequent in left carotid artery plaque than on the right (lipid 27.6% vs. 23.4%; *P* 0.006 and IPH 23.1% vs. 19.7%; *P* 0.01), while calcification was equal on both sides.

When we assigned just a single component as the most predominant component, we found IPH and fibrous tissue both to be more often predominant on the left than on the right (9.1 vs. 5.9%; *P*<0.001 and 45.0 vs. 38.5%; *P*<0.001; Table 2). In contrast, calcification was the predominant component more on the right than on the left (37.4 vs. 31.6%; *P*<0.001). Lipid was distributed equally. Similar trends were found for men and women (Table 2). There was no interaction between plaque characteristics and age (data not shown). An example of asymmetry in predominant plaque components is presented in figure 1.

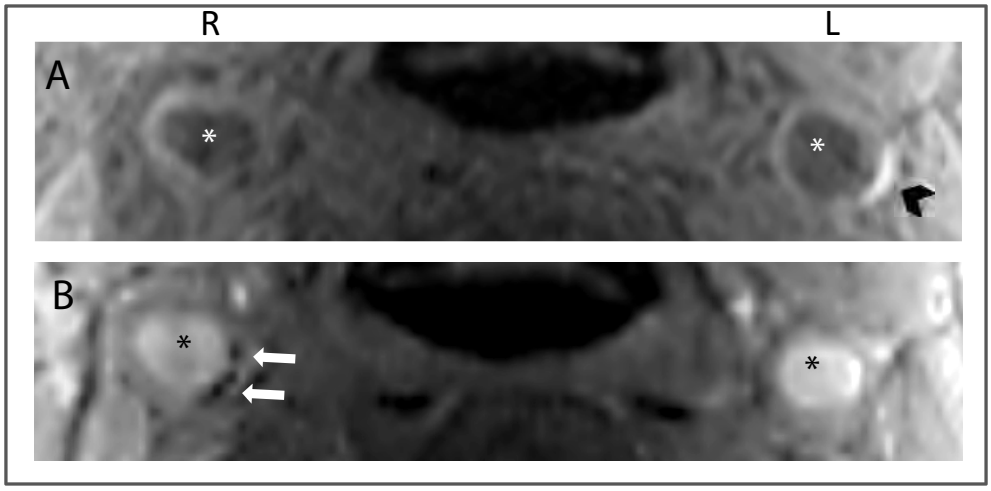

Figure 1. Axial magnetic resonance images of a participant with left-sided intraplaque hemorrhage and right-sided calcification. The carotid arterial lumen is marked with an asterisk. A. T1w-gradient echo sequence: black arrowhead indicates hyperintense signal corresponding with intraplaque hemorrhage. B. Phased-contrast magnetic resonance angiography: white arrow indicates hypointense signal corresponding with calcification.

Figure 2 shows the odds ratios for the predominance of a specific plaque component on the left side, adjusted for age, sex and maximal wall thickness. The right side was used as the reference. The OR for IPH or fibrous tissue on the left side was 1.5 [95%CI 1.1-1.9] and 1.1 [95%CI 1.1-1.4] respectively, and was 0.7 for calcification [0.6-0.8].

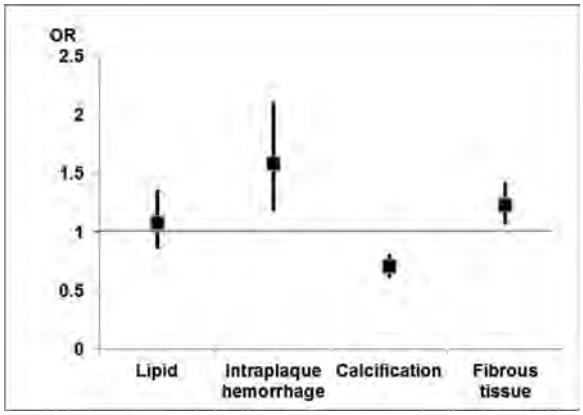

Figure 2. Overall odds ratio's for the predominance of a specific plaque component in the left carotid artery. The right carotid artery was used as the reference.
*P-value <0.05 estimated adjusted for age, sex and carotid wall thickness.

Discussion

Within a large cohort of stroke-free individuals, we demonstrated that plaque prevalence, severity and composition are not equally distributed among the left and right carotid arteries. Although most individuals had bilateral carotid disease, unilateral plaque was more usually located on the left, and left-sided plaques were also thicker than the contralateral side. Whereas IPH and lipid were most prevalent in left-sided plaques, these plaques were predominantly composed of IPH and fibrous tissue. In contrast, right-sided plaques were predominantly composed of calcification, which is considered more stable and therefore less likely to result in thromboembolic complications. These findings suggest that atherosclerotic plaques on the left are more vulnerable than on the right.

Table 1. Baseline characteristics of the population

Variable	All (n=1414)	Men (n=749)	Women (n=665)	*P-value*
Age, years±SD	72.0±9.6	71.4±9.4	72.8±9.7	0.008
Hypertension, n (%)	1057 (74.8)	570 (76.1)	487 (73.2)	0.05
Total cholesterol mmol/L±SD	5.7±1.0	5.4±1.0	5.9±1.0	<0.001
Ever smoking, n (%)	1047 (74.0)	637 (85.0)	410 (61.7)	<0.001
Diabetes mellitus, n (%)	200 (14.1)	124 (16.6)	76 (11.4)	0.005
Statin use (%)	375 (26.5)	229 (30.6)	146 (22.0)	<0.001
History of cardiovascular disease, n (%)	128 (9.1)	91 (12.1)	37 (5.6)	<0.001

Categorical variables are presented as numbers (%). Continuous variables are presented as mean±SD. P-values indicate age-adjusted difference between men and women.

IPH=intraplaque hemorrhage. SD=standard deviation. Note that percentages of prevalent components do not add up to 100%, because multiple components per plaque could be present. Percentages of predominant component, expressed as proportion of the 1414 carotid arteries, do not add up to 100%, because a proportion of carotid arteries did not have an atherosclerotic plaque.

Table 2. Asymmetry of plaque severity and plaque components

Plaque characteristics	Overall			Men			Women		
	Right	Left	*P-value*	Right	Left	*P-value*	Right	Left	*P-value*
Wall thickness (mm) mean±SD	2.9±1.3	3.1±1.3	<0.001	3.0±1.4	3.2±1.2	0.001	2.7±1.2	3.0±1.1	<0.001
Stenosis (%), mean±SD	11.9±17.7	11.4±16.7	0.4	12.9±19.3	12.4±17.8	0.5	10.8±15.6	10.3±15.3	0.5
Prevalent component									
Lipid, n (%)	331 (23.4)	390 (27.6)	0.006	197 (26.3)	240 (32)	0.01	134 (20.2)	150 (22.6)	0.3
IPH, n (%)	279 (19.7)	327 (23.1)	0.01	190 (25.4)	199 (26.6)	0.6	89 (13.4)	128 (19.2)	0.002
Calcification, n (%	900 (63.6)	920 (65.1)	0.4	483 (64.5)	496 (66.2)	0.5	417 (62.7)	424 (63.8)	0.7
Predominant component									
Lipid, n (%)	113 (8.0)	130 (9.2)	0.2	62 (8.3)	86 (11.5)	0.03	51 (7.7)	44 (6.6)	0.5
IPH, n (%)	83 (5.9)	128 (9.1)	<0.001	62 (8.3)	94 (12.6)	0.004	21 (3.2)	34 (5.1)	0.07
Calcification, n (%	529 (37.4)	447 (31.6)	<0.001	265 (35.4)	221 (29.5)	0.008	264 (39.7)	226 (34.0)	0.02
Fibrous tissue, n (%)	544 (38.5)	636 (45.0)	<0.001	288 (38.5)	317 (42.3)	0.09	256 (38.5)	319 (48.0)	<0.001

Important strengths of this study are its population-based design and the large number of stroke-free individuals who underwent carotid plaque characterization with MRI. Yet, not all participants with atherosclerotic plaque on carotid ultrasound underwent carotid MRI scanning, due to both logistical and participant-related reasons. Although this may have led to selection bias, we expect this to be non-differential. Restricting our study to a stroke-free population allowed us to generalize our findings to asymptomatic individuals. Because of this inclusion criterion, persons with highly vulnerable plaques may have had symptoms and been excluded from the study. Due to the preponderance of left-sided strokes among symptomatic persons, it is thus feasible that we may have underestimated left-sided vulnerable plaques.

Although MRI is currently regarded as the most reliable method for in vivo assessment of plaque composition, small plaques (<2.0 mm) could not be characterized due to constraints in spatial resolution of MRI. Furthermore, we could not apply contrast-enhanced sequences because we are investigating healthy subjects. Hence, distinguishing lipid from fibrous tissue was more difficult,[19] possibly resulting in an underestimation of the presence of lipid or an overestimation of fibrous tissue, although we do not expect a predilection for a particular side. A further limitation is that fibrous tissue was defined per exclusionem of other components, which may have led to underestimation of this component. Image reviewing was performed by two observers, who were not blinded to the side of the carotid artery. We should therefore consider potential observer bias, though the observers were at

time of rating unaware of potential left-right differences, and inter-rater reliability was very high.

The higher prevalence of subjects with left-sided unilateral plaques and the significantly younger age of these subjects support a predisposition of atherosclerotic plaques in the left carotid artery. We found a slight but significant difference in wall thickness between the left and right carotid artery. This finding is consistent with a previous study that found a thicker intima-media thickness in the left common carotid artery than in the right using B-mode ultrasonography.[20] A greater wall thickness may indicate more plaque growth.

In asymptomatic subjects with mild stenosis, plaque growth might be accompanied by outward remodelling of the plaque.[21] This may explain why we did not find a difference in (clinically relevant) luminal stenosis between both sides. Yet, it is important to realize that a substantial proportion of strokes are caused by stenosis[22,23], probably due to variations in plaque composition rather than lumen narrowing.[1]

Regarding plaque composition, we found that IPH occurred predominantly and more often on the left side. IPH is considered an important indicator of vulnerable plaques.[1] Vulnerable plaques, and in particular IPHs, are gaining importance because they may lead to plaque rupture and subsequent ischemic stroke.[24-26] Whereas left-sided plaques have a more vulnerable phenotype, right-sided plaques were predominantly composed of calcification. Calcifications have been suggested to increase plaque stability, because they are associated with lower risks of cerebrovascular complications[27-29], and therefore considered as a more favorable phenotype of carotid atherosclerosis. Atherosclerotic plaques can remain stable for many years without surface rupture and subsequent cerebrovascular complications.[26] In studies that compared carotid atherosclerotic plaques in symptomatic and asymptomatic subjects, calcified plaques were less likely to be symptomatic than non-calcified plaques and asymptomatic patients had a higher calcification content than symptomatic patients.[27-29]

We found more predominant fibrous tissue and prevalent lipid on the left, which may also reflect higher vulnerability, although their contributions to plaque instability are less conclusive than IPH. Enlargement of the lipid pool may result in development of a necrotic core, initiating a cascade with fibrous cap erosion or rupture.[1] However, the role of lipid and fibrous tissue in plaque instability, in health subjects, has not been determined.

Few studies have compared plaque components between the left and right carotid arteries and usually only distinguish between calcified and non-calcified plaques.[30,31] In fifty pairs of carotid arteries from cadaveric donors, plaque calcification, quantified using electron beam computed tomography, was found to be similarly distributed between both carotid arteries.[31] Whereas the authors used cumulative volume of calcification for comparison, we assessed the prevalent and predominant component. It should be noted that abso-

lute volumes do not reflect the proportion of specific components within a plaque. We overcame this by defining a predominant plaque component, which can be more easily assessed.

Whereas sex differences regarding the severity of atherosclerosis are widely known, studies that assess gender differences in plaque composition are scarce. In a recent MRI study amongst 96 patients with mild stenosis, vulnerable plaque characteristics, such as a thin or ruptured fibrous cap and IPH, were significantly higher in men than in women.[32] We also found asymmetry in plaque composition across sexes, although IPH was more prevalent on the left in women and more predominant on the left in men.

Differences in plaque thickness and composition between both carotid arteries may be explained by geometrical factors, such as bifurcation angle, the configuration of the left carotid artery to the aortic arch or because of the direct connection of the left carotid artery to the aortic arch as opposed to the right carotid artery that arises from the brachiocephalic artery. Vessel anatomy in turn influences the hemodynamic forces and as such the left carotid artery may be exposed to higher arterial pressures.[6,33] Flow models have shown that atherosclerotic plaques preferentially develop in areas with low wall shear stress, such as at bifurcations or inner curves.[34] Wall shear stress and stress inside the vessel wall may affect plaque formation and composition by causing alterations in wall structure and metabolism.[34-36] The role of these local factors has been scarcely investigated in vivo. However, we believe that studying their contributions may help understand the variation between left and right carotid atherosclerosis and should be considered in future studies.

This study was initiated because of the reported high incidence of left-sided strokes,[2-4] which has been explained by the fact that left-sided strokes cause more apparent symptoms. Although we found an asymmetry in plaque prevalence and composition between the left and right carotid artery, these side-differences seem to be too small to explain the higher incidence of left-sided strokes. Nevertheless, it is important to identify local or systemic factors underlying these asymmetrical differences in plaque composition, and to gain insight into the factors that lead to development of side-specific vulnerable plaque characteristics. Understanding these pathways could improve risk prediction of stroke, and contribute to the prevention of stroke in primary care.

Sources of Funding

This study was supported by the Netherlands Heart Foundation, (2009B044) and the Netherlands Organization for Scientific Research (NWO/ZonMwVici,918-76-619).

Disclosures

None.

References

1. Seeger JM, Barratt E, Lawson GA, Klingman N. The relationship between carotid plaque composition, plaque morphology, and neurologic symptoms. *J Surg Res*. 1995;58:330-336
2. Hedna VS, Bodhit AN, Ansari S, Falchook AD, Stead L, Heilman KM, et al. Hemispheric differences in ischemic stroke: Is left-hemisphere stroke more common? *J Clin Neurol*. 2013;9:97-102
3. Naess H, Waje-Andreassen U, Thomassen L, Myhr KM. High incidence of infarction in the left cerebral hemisphere among young adults. *J Stroke Cerebrovasc Dis*. 2006;15:241-244
4. Foerch C, Misselwitz B, Sitzer M, Berger K, Steinmetz H, Neumann-Haefelin T, et al. Difference in recognition of right and left hemispheric stroke. *Lancet*. 2005;366:392-393
5. Fink JN. Underdiagnosis of right-brain stroke. *Lancet*. 2005;366:349-351
6. Phan TG, Beare RJ, Jolley D, Das G, Ren M, Wong K, et al. Carotid artery anatomy and geometry as risk factors for carotid atherosclerotic disease. *Stroke*. 2012;43:1596-1601
7. Odink AE, van der Lugt A, Hofman A, Hunink MG, Breteler MM, Krestin GP, et al. Association between calcification in the coronary arteries, aortic arch and carotid arteries: The rotterdam study. *Atherosclerosis*. 2007;193:408-413
8. Herisson F, Heymann MF, Chetiveaux M, Charrier C, Battaglia S, Pilet P, et al. Carotid and femoral atherosclerotic plaques show different morphology. *Atherosclerosis*. 2011;216:348-354
9. Virmani R, Burke AP, Kolodgie FD, Farb A. Pathology of the thin-cap fibroatheroma: A type of vulnerable plaque. *J Interv Cardiol*. 2003;16:267-272
10. Hofman A, van Duijn CM, Franco OH, Ikram MA, Janssen HL, Klaver CC, et al. The rotterdam study: 2012 objectives and design update. *Eur J Epidemiol*. 2011;26:657-686
11. Iglesias del Sol A, Bots ML, Grobbee DE, Hofman A, Witteman JC. Carotid intima-media thickness at different sites: Relation to incident myocardial infarction; the rotterdam study. *Eur Heart J*. 2002;23:934-940
12. van den Bouwhuijsen QJ, Vernooij MW, Hofman A, Krestin GP, van der Lugt A, Witteman JC. Determinants of magnetic resonance imaging detected carotid plaque components: The rotterdam study. *Eur Heart J*. 2012;33:221-229
13. Yuan C, Mitsumori LM, Ferguson MS, Polissar NL, Echelard D, Ortiz G, et al. In vivo accuracy of multispectral magnetic resonance imaging for identifying lipid-rich necrotic cores and intraplaque hemorrhage in advanced human carotid plaques. *Circulation*. 2001;104:2051-2056
14. Mani V, Aguiar SH, Itskovich VV, Weinshelbaum KB, Postley JE, Wasenda EJ, et al. Carotid black blood mri burden of atherosclerotic disease assessment correlates with ultrasound intima-media thickness. *J Cardiovasc Magn Reson*. 2006;8:529-534
15. Staikov IN, Arnold M, Mattle HP, Remonda L, Sturzenegger M, Baumgartner RW, et al. Comparison of the ecst, cc, and nascet grading methods and ultrasound for assessing carotid stenosis. European carotid surgery trial. North american symptomatic carotid endarterectomy trial. *J Neurol*. 2000;247:681-686
16. Cappendijk VC, Cleutjens KB, Kessels AG, Heeneman S, Schurink GW, Welten RJ, et al. Assessment of human atherosclerotic carotid plaque components with multisequence mr imaging: Initial experience. *Radiology*. 2005;234:487-492

17. Saam T, Ferguson MS, Yarnykh VL, Takaya N, Xu D, Polissar NL, et al. Quantitative evaluation of carotid plaque composition by in vivo mri. *Arterioscler Thromb Vasc Biol*. 2005;25:234-239
18. Leening MJ, Kavousi M, Heeringa J, van Rooij FJ, Verkroost-van Heemst J, Deckers JW, et al. Methods of data collection and definitions of cardiac outcomes in the rotterdam study. *Eur J Epidemiol*. 2012;27:173-185
19. Cai J, Hatsukami TS, Ferguson MS, Kerwin WS, Saam T, Chu B, et al. In vivo quantitative measurement of intact fibrous cap and lipid-rich necrotic core size in atherosclerotic carotid plaque: Comparison of high-resolution, contrast-enhanced magnetic resonance imaging and histology. *Circulation*. 2005;112:3437-3444
20. Rodriguez Hernandez SA, Kroon AA, van Boxtel MP, Mess WH, Lodder J, Jolles J, et al. Is there a side predilection for cerebrovascular disease? *Hypertension*. 2003;42:56-60
21. Glagov S, Weisenberg E, Zarins CK, Stankunavicius R, Kolettis GJ. Compensatory enlargement of human atherosclerotic coronary arteries. *N Engl J Med*. 1987;316:1371-1375
22. Kwee RM, van Oostenbrugge RJ, Prins MH, Ter Berg JW, Franke CL, Korten AG, et al. Symptomatic patients with mild and moderate carotid stenosis: Plaque features at mri and association with cardiovascular risk factors and statin use. *Stroke*. 2010;41:1389-1393
23. Flaherty ML, Kissela B, Khoury JC, Alwell K, Moomaw CJ, Woo D, et al. Carotid artery stenosis as a cause of stroke. *Neuroepidemiology*. 2013;40:36-41
24. Hellings WE, Peeters W, Moll FL, Piers SR, van Setten J, Van der Spek PJ, et al. Composition of carotid atherosclerotic plaque is associated with cardiovascular outcome: A prognostic study. *Circulation*. 2010;121:1941-1950
25. Takaya N, Yuan C, Chu B, Saam T, Underhill H, Cai J, et al. Association between carotid plaque characteristics and subsequent ischemic cerebrovascular events: A prospective assessment with mri--initial results. *Stroke*. 2006;37:818-823
26. Thapar A, Jenkins IH, Mehta A, Davies AH. Diagnosis and management of carotid atherosclerosis. *BMJ*. 2013;346:f1485
27. Nandalur KR, Baskurt E, Hagspiel KD, Phillips CD, Kramer CM. Calcified carotid atherosclerotic plaque is associated less with ischemic symptoms than is noncalcified plaque on mdct. *AJR Am J Roentgenol*. 2005;184:295-298
28. Shaalan WE, Cheng H, Gewertz B, McKinsey JF, Schwartz LB, Katz D, et al. Degree of carotid plaque calcification in relation to symptomatic outcome and plaque inflammation. *J Vasc Surg*. 2004;40:262-269
29. Miralles M, Merino J, Busto M, Perich X, Barranco C, Vidal-Barraquer F. Quantification and characterization of carotid calcium with multi-detector ct-angiography. *Eur J Vasc Endovasc Surg*. 2006;32:561-567
30. Sabetai MM, Tegos TJ, Nicolaides AN, El-Atrozy TS, Dhanjil S, Griffin M, et al. Hemispheric symptoms and carotid plaque echomorphology. *J Vasc Surg*. 2000;31:39-49
31. Adams GJ, Simoni DM, Bordelon CB, Jr., Vick GW, 3rd, Kimball KT, Insull W, Jr., et al. Bilateral symmetry of human carotid artery atherosclerosis. *Stroke*. 2002;33:2575-2580
32. Ota H, Reeves MJ, Zhu DC, Majid A, Collar A, Yuan C, et al. Sex differences of high-risk carotid atherosclerotic plaque with less than 50% stenosis in asymptomatic patients: An in vivo 3t mri study. *AJNR Am J Neuroradiol*. 2013;34:1049-1055, S1041

33. Schulz UG, Rothwell PM. Major variation in carotid bifurcation anatomy: A possible risk factor for plaque development? *Stroke*. 2001;32:2522-2529
34. Malek AM, Alper SL, Izumo S. Hemodynamic shear stress and its role in atherosclerosis. *JAMA*. 1999;282:2035-2042
35. Chatzizisis YS, Jonas M, Coskun AU, Beigel R, Stone BV, Maynard C, et al. Prediction of the localization of high-risk coronary atherosclerotic plaques on the basis of low endothelial shear stress: An intravascular ultrasound and histopathology natural history study. *Circulation*. 2008;117:993-1002
36. Lee RT, Schoen FJ, Loree HM, Lark MW, Libby P. Circumferential stress and matrix metalloproteinase 1 in human coronary atherosclerosis. Implications for plaque rupture. *Arterioscler Thromb Vasc Biol*. 1996;16:1070-1073

Chapter 4

The relation of carotid atherosclerotic plaque characteristics on MRI with a history of ischemic stroke and coronary heart disease: a population-based approach

Mariana Selwaness
Quirijn van den Bouwhuijsen
Marileen L Portegies
Mohammed A Ikram
Albert Hofman
Oscar H Franco
Aad van der Lugt
Jolanda J Wentzel
Meike W Vernooij

Chapter 5

Carotid plaque burden determinants and measurements

Chapter 5.1

Carotid wall volume quantification from magnetic resonance images using deformable models and learning-based correction of systematic errors

Mariana Selwaness
Reinhard Hameeteman
Ronald van 't Klooster
Quirijn van den Bouwhuijsen
Albert Hofman
Oscar H Franco
Wiro J Niessen
Stefan Klein
Meike W Vernooij
Jolanda J Wentzel
Aad Van der Lugt

Abstract

We present a method for carotid vessel wall volume quantification from Magnetic Resonance Imaging (MRI).

The method combines lumen and outer wall segmentation based on deformable model fitting with a learning-based segmentation correction step. After selecting two initialization points, the vessel wall volume in a region around the bifurcation is automatically determined. The method was trained on 8 datasets (16 carotids) from a population-based study in the elderly for which one observer manually annotated both the lumen and outer wall. Evaluation was done on a separate set of 19 datasets (38 carotids) from the same study for which two observers made annotations. Wall volume and normalized wall index measurements resulting from the manual annotations were compared to the automatic measurements.

Our experiments show that the automatic method performs comparably to the manual measurements.

All image data and annotations used in this study together with the measurements are made available through the website http://ergocar.bigr.nl.

Introduction

The prevalence of cardiovascular diseases (CVDs) is rising and heart disease is the leading cause of death in the western world, claiming approximately one out of every five lives (Roger *et al* 2011). Atherosclerosis, a disease of the vessel wall, is the primary cause of CVD. Atherosclerotic wall thickening in the carotid arteries can cause a narrowing or total occlusion of the lumen. Atherosclerotic plaque that does not cause occlusion may still lead to clinical events because of rupture and development of thromboembolism, which may subsequently lead to cerebral ischemia (Glagov *et al* 1987). Consequently, much research is aimed at finding parameters that describe the plaque, and which can be used for improving risk stratification and for monitoring the progression of atherosclerotic disease. One of those parameters is the size of the plaque and its relation to the size of the vessel.

Magnetic resonance imaging (MRI) is an important means to monitor and quantify the state of the vessel wall and lumen. Several studies have shown the possibility to visualize the vessel lumen and outer wall on MRI (Dehnavi *et al* 2007, Takaya *et al* 2006, Varghese *et al* 2005, Zhang *et al* 2003, Kang *et al* 2000, Yuan *et al* 1998). Annotation of both the lumen border and the outer vessel wall is a laborious task. Therefore, several researchers have proposed automatic wall segmentation methods (Yuan *et al* 1999, Van 't Klooster *et al* 2012). Although calculating the volume of the vessel wall is straightforward once a segmentation is performed, a comparison between automatic and manual wall volume measurements has, to the best of our knowledge, not yet been done.

In this paper, we present an automatic method to measure carotid wall volume from MR images. The contribution is fivefold.

(i) Theautomatic method combines a deformable model approach (Van'tKloosteretal2012) with a learning-based postprocessing step in which systematic segmentation errors of the deformable model fitting are corrected. The idea behind this segmentation correction was developed by Wang *et al* (2011). However, the method described in Wang *et al* (2011) was designed for the brain structure segmentation, we modified it such that it can handle vessel-shaped structures.

(ii) An intensity inhomogeneity correction method is designed to compensate for the nonuniform sensitivity pattern of the RF surface coils.

(iii) A training set of eight subjects with manual annotations is used to exhaustively optimize a number of algorithm parameters.

(iv) The final algorithm is evaluated on a different set of 19 subjects, and the automatic results are compared with manual vessel wall volume measurements and inter-observer variability.

(v) All image data used in this study together with the manual and automatic measurements are made available through the website http://ergocar.bigr.nl. The remainder of this paper is organized as follows. First, section 2 explains the deformable

model fitting and learning-based segmentation correction (LBSC), and the wall volume quantification. Section 3 describes the image data and the preprocessing steps. Section 4 describes the experiments that were conducted to optimize the parameters of the method and evaluate the wall volume quantification. The results of the experiments are given in section 5. Discussion and conclusion are given in sections 6 and 7, respectively.

Materials and methods

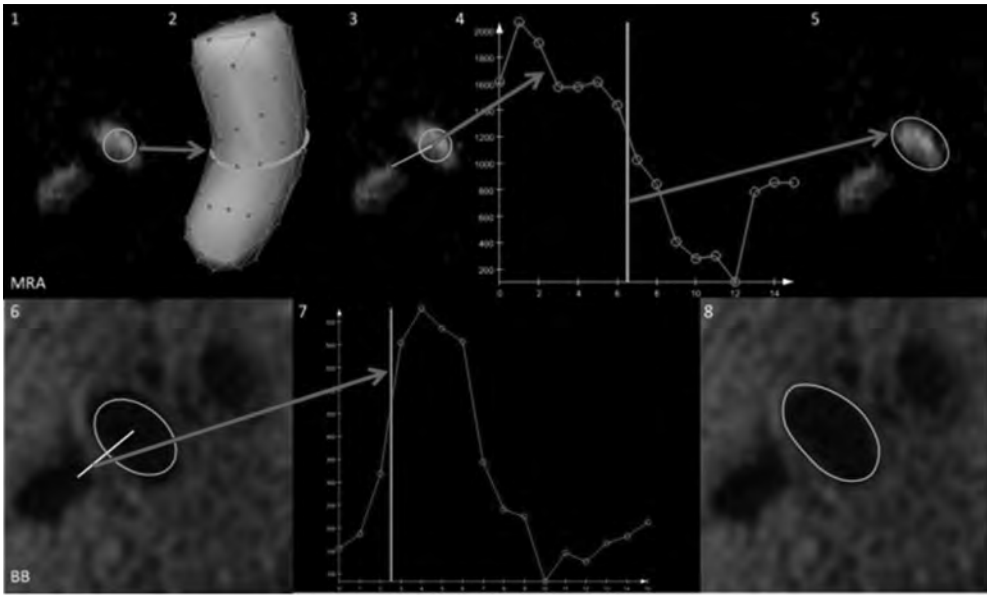

Figure 1. Graphical summary of the deformable model fitting method. An MRA segmentation based on wavefront propagation (1) is used to initialize a NURBS surface (2), which is fitted to the lumen boundary by searching for a maximum gradient magnitude (4) along an intensity profile (3). The resulting segmentation is used as an initialization in the BB image (6) where it is optimized (7,8) in the same manner as done in the MRA image.

Deformable model fitting

The method described by Van 't Klooster *et al* (2012) was used to create an initial segmentation of the lumen and outer wall. This method requires an MR angiography (MRA) image and a black blood (BB) image. The MRA image is used to obtain a robust initial segmen-

tation of the carotid lumen. This segmentation is copied to the BB image and based on this initialization, the lumen and outer wall are segmented. The MRA and BB images are assumed to be co- registered (see section 3.3). The only required user input consists of two initialization points. Based on these, the method fully automatically fits a deformable surface model of the lumen and the outer wall to the image data. Below, a brief description of this method is given which is summarized in figure 1. For further details, we refer to Van 't Klooster *et al* (2012).

The method starts with a two-point initialization: one in the common carotid artery (CCA) and one in the internal carotid artery (ICA). These two points are used to initialize a wave-front propagation (De Koning *et al* 2003) in the MRA image which results in an approximate centerline with an associated lumen diameter estimate (green curve in frame 1 of figure 1) at each centerline position. This centerline together with the diameters is used to initialize a NURBS surface (De Koning *et al* 2003) (blue surface lines in frame 2). The method then performs an optimization step in which the boundaries of the NURBS surface are more precisely fitted to the lumen boundaries in the MRA image by searching for the maximum gradient magnitude in an intensity profile with a specified length (dLMRA) perpendicular to the lumen surface (frame 3 shows the location of a profile, frame 4 shows the corresponding intensities along the profile and frame 5 shows an update of the initial contour). Only those edges are selected which have a high value (bright) inside the model and a low value (dark) outside the model. This optimization step is performed for a given number of iterations (nLMRA).

The lumen NURBS surface found in the MRA image is used to initialize the lumen segmentation in the BB image (frame 6). Here, the same optimization of the surface fitted to the lumen boundary is performed as in the MRA image (frames 7 and 8), using again a specified length (dLBB) of the intensity profile and a number of iteration steps (nLBB). The edge direction in this step is set from dark inside the model to bright outside the model.

The estimated lumen surface is expanded and used to initialize the search for the outer wall. This is done in the same manner as for the BB lumen segmentation, by searching for the maximum gradient magnitude in an intensity profile with a specified length (dWBB) for a number of iterations (nWBB). For this segmentation step, the edge direction is set from bright inside the model to dark outside the model.

Learning-based correction of systematic errors

Using a deformable model to acquire an automatic segmentation limits the precision of the final segmentation to the flexibility of the used (NURBS) model. In the areas where there is a sudden change in the shape of the vessel, this may lead to errors. Also, the deformable model approach described in the previous section was originally designed and optimized

for one particular set of images. To compensate for the limitation of the deformable model and to adjust for the differences in image characteristics when using a different scanner, surface coil and/or different MR acquisition parameter settings, we propose to use a post-processing step in which the segmentation is tailored to a new set of images. The idea behind this method was developed by Wang *et al* (2011). We will refer to this method as the LBSC method. As the LBSC method was designed for the brain structure segmentation, we modified it to be able to handle vessel structures. We will refer to this modified method as the learning-based vessel segmentation correction (LBVSC) method.

The LBSC method uses a ground-truth segmentation (in our case manual annotations) to train a classifier that modifies a binary segmentation made by a host segmentation method (in our case the result from the deformable model fitting described in section 2.1). The LBSC method classifies all voxels in a region of interest (ROI), which is created by dilating the host segmentation. For each voxel, a feature vector is computed, consisting of

- all image values in a 5×5×5 neighborhood of the voxel in the MR image (125 features),
- all values in a 5×5×5 neighborhood of the voxel in the host segmentation (125 features),
- *x-, y-* and *z-coordinates* of the voxel relative to the center of mass of the host segmentation (three features) and
- product of the neighborhood and coordinate features ($3 \times (125 + 125)$ features).

This leads to a total of 1003 features. The LBSC method trains a classifier on the difference between the host segmentation and the manual annotation. It thus learns to correct the errors made by the host segmentation. AdaBoost is chosen as a classifier, which combines many weak classifiers (regression stumps) into a single strong classifier (Freund and Schapire 1997). The AdaBoost classifier has previously been shown to be successful in the context of medical image segmentation (Tu *et al* 2007, Morra *et al* 2008).

For our application, a number of modifications are proposed: we use the signed distance to the host segmentation's border and the *z-index* as spatial features. Since the carotid artery is roughly perpendicular to the transversal plane, the latter feature is an approximation of the position along the centerline. For elongated structures like vessels, these two spatial features seem more appropriate than the distance to the center of mass. In addition to these spatial features, we used the intensity of the BB image and its gradient magnitude. Instead of using a 5×5×5 neighborhood, we used a 7×7×3 neighborhood. The effect of this neighborhood size ($fLx \times fLy \times fLz$ and $fWx \times fWy \times fWz$ for the lumen and outer wall feature neighborhood, respectively) on the segmentation accuracy was determined experimentally (see section 4.2.2). Thus, the two spatial features of the LBVSC method are the following.

- Signed distance to the boundary host segmentation (one feature).
- Relative *z-index* (one feature).

The 441 appearance features are the 7×7×3 neighborhood voxels of

- the host segmentation (i.e. 0 or 1) (147 features)
- the BB image (147 features)
- the gradient magnitude of the BB image (147 features).

Similar to the LBSC method, we also used the product of the spatial and appearance features as additional features ($2 \times (147 + 147 + 147)) = 882$, leading to a total of $2 + 441 + 882 = 1325$ features.

Since most errors in the host segmentation are near the boundary of the segmentation, our LBVSC method only classifies the voxels within an ROI around this boundary. This region is defined by a morphological dilation minus an erosion of the binary host segmentation using a spherical kernel with radii *rLdilation* and *rLerosion* for the lumen and *rWdilation* and *rWerosion* for the outer wall segmentation. The binary host segmentation of the outer wall includes the lumen area.

When the classifier is trained on the difference between the host segmentation and the manual annotation (as in the original LBSC method), only the voxels that are not correctly segmented in the host segmentation obtain a negative label. If the host segmentation has a large overlap with the manual annotation, this leads to many positive samples and only a few negative samples. To prevent these unequal class sizes, we trained the AdaBoost classifier directly on the label from the manual annotation, which leads to a better balance between the classes. To make the classification tractable, only half of the randomly selected voxels within the ROI are used as samples.

While the output of the deformable model fitting described in section 2.1 is smooth, the output of the LBVSC method may have holes or isolated voxels. Therefore, a morphological closing with a kernel radius of two voxels is applied to the output of the LBVSC method and isolated voxels are removed using a connected component analysis.

Vessel wall volume quantification

The vessel wall volume *Vwall* is quantified in a region of 25 mm in the transversal direction centered at the bifurcation. The bifurcation point is manually annotated and defined as the first transversal plane on which two separate lumens (one of the ICA and one of the external carotid artery (ECA)) are visible. In cases where part of the evaluation region falls outside the scan range, the evaluation region is restricted by the image boundaries.

The application of the LBVSC method results in a binary mask for the lumen and the outer wall. The difference of these two masks is defined as the vessel wall. The vessel wall volume

is computed by voxel counting and multiplying the result with the volume of one voxel.

Besides the volume, *Vwall,* a clinically used parameter to quantify the vessel wall is the normalized wall index (NWI) which is defined as follows:

$$\mathrm{NWI} = \frac{V_{\mathrm{wall}}}{V_{\mathrm{lumen}} + V_{\mathrm{wall}}},$$

where *Vlumen* is the volume of the vessel lumen. Bigger plaques thus lead to a higher NWI.

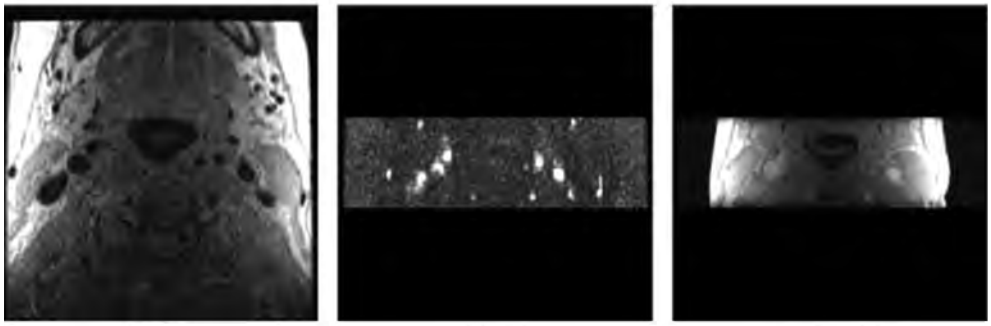

Figure 2. Example slice near the bifurcation of the three different MR sequences used in this study.

Data specific preprocessing

Data description

The image data of this study are taken from a prospective, population-based study among subjects aged 45 years and older. This study has been described in detail elsewhere (Hofman *et al* 2011). All participants having a maximum intima–media thickness of more than 2.5 mm (determined using ultrasound (Van den Bouwhuijsen *et al* 2012)) in at least one carotid artery were invited for a carotid MRI exam. In total, 1072 participants were scanned.

MRI of the carotid arteries was performed on a 1.5 T MR scanner (Signa Excite, GE Healthcare, Milwalkee, USA) with a bilateral phased-array surface coil. To reduce motion artifacts, subjects were stabilized in a custom-designed head holder. The total scanning time was about 30 min in which, among others, the following sequences were acquired (see Van den Bouwhuijsen *et al* (2012) for acquisition details):

- Proton density weighted fast spin echo BB.
- Phase contrast (PC) sequence which consists of an image showing flow in any direction, a magnitude image (PCMag) and three images for the flow in the *x-, y-* and *z-directions.*

The PC is used as the MRA image for the deformable model fitting (see section 2.1) and the PCMag image is used to register the PC image to the BB image (see section 3.3). Figure 2 shows an example slice of each of these MR sequences.

Inhomogeneity correction

The bilateral phased-array surface coils cause severe intensity inhomogeneity within the neck. The sensitivity near the skin is much higher than in the middle of the neck. Figure 3(c) shows a typical example of the intensity profile across the neck in a BB image. Many popular intensity inhomogeneity correction methods have strong assumptions on the distribution of the modeled bias field. For example, N3 (Sled *et al* 1998) and N4 (Tustison *et al* 2010) assume the distribution of the bias field intensities to be log-normal. Other methods like the one proposed by Brinkmann *et al* (1998) and Cohen *et al* (2000) assume a slowly varying bias field. These methods do not result in a satisfactory correction of the intensity inhomogeneities in the case of phased-array surface coils. The method proposed by Salvado *et al* (2006), called local entropy minimization with a bicubic spline model (LEMS), was designed to deal with inhomogeneities caused by phased-array surface coils.

The original LEMS method was designed for 2D images. To ensure a smooth bias field across slices, we extended the method to 3D with the following modifications.

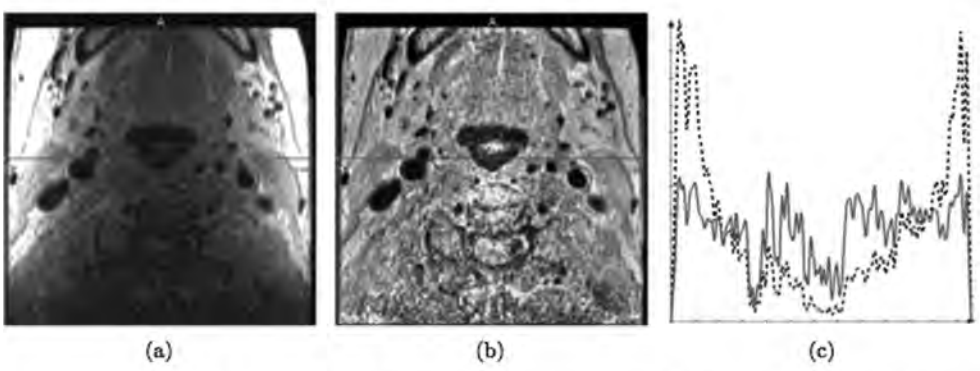

Figure 3. Example of the intensity inhomogeneities caused by a surface coil (a), the same image after applying the LEMS method (b) and the intensity profiles of the red line in the original (black, dashed line) and the corrected (gray, solid line) image (c).

LEMS tries to identify the voxels that do not have any signal as they cannot be used to estimate the bias field. We estimated the background voxels using the whole 3D image. Furthermore, the 2D slice-based estimation of the bias field is smoothed in the slice direction using Gaussian blurring with a σ of three slices.

This way, a spatially smooth bias field is obtained as can be seen in figure 4.

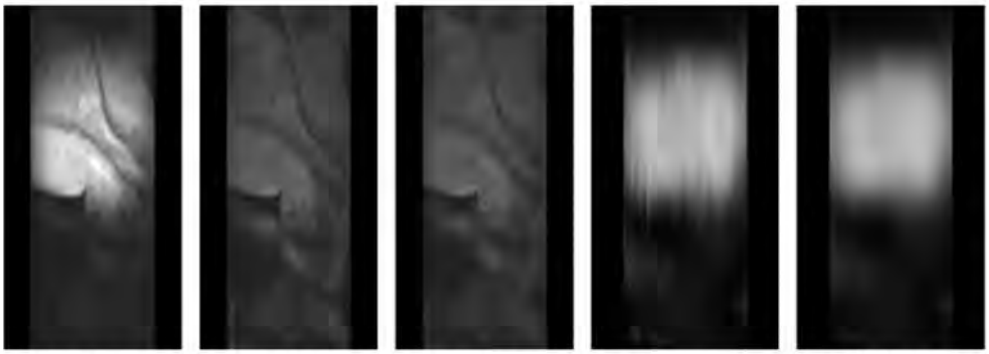

Figure 4. Inhomogeneity correction using LEMS and smoothing the estimated correct field. Sagittal slice of (a) the original BB image, (b) after correction using standard LEMS (c), using LEMS with a smoothed bias field, (d) estimated bias field of the standard LEMS method and (e) estimated bias field with smoothing in the slice direction.

Because the LEMS method uses a multiplicative bias field model, the correction is performed by dividing the original image by the estimated bias field. This can lead to very large intensity values in the corrected image in regions where the estimated bias field has small values. The registration between the BB and MRA images (see section 3.3) is hampered by a few extremely high intensity values within the image; therefore, the highest 1% of the intensities of the corrected image are clamped. Figures 3(a) and (b) show an example of the BB image before and after inhomogeneity correction, respectively, and the effect of the correction on the intensity profile can be seen in figure 3(c).

Registration

As stated in section 3.1, the complete MRI exam takes approximately 30 min. Although the position of the head of the subjects is stabilized using a head holder, they still have the ability to move their body, which can cause twisting of the neck. Moreover, cardiac and breathing motion can also lead to the displacement of the arteries in the neck. This motion leads to small misregistrations between the different sequences. The lumen and vessel wall segmentation method described in section 2.1 requires a registered BB and MRA image. We perform an intensity-based registration method to align the images. The PC image contains very little anatomical information as can be seen in figure 2(b) and is therefore not very well suited for an intensity-based registration. The PCMag image (shown in figure 2(c)) which is simultaneously acquired with the PC image contains much more anatomical information. Therefore, the PCMag image was registered to the BB image and the resulting deformation was applied to the PC image.

The registration first performs a rigid registration step to compensate for global displacements. Because the BB image and the PCMag image contain different anatomical regions, a mask was used for both the fixed and the moving images to indicate the regions where there should be overlapping information. The rigid registration was followed by a B-spline registration (Rueckert *et al* 1999) using mutual information as a similarity metric (The ´venaz and Unser 2000). For the optimization, we used an adaptive stochastic gradient descent optimizer (Klein *et al* 2009). The registration was performed in a multi-resolution framework with three resolution levels and was achieved using the ITK-based (Ibanez *et al* 2005) registration toolbox elastix (Klein *et al* 2010).

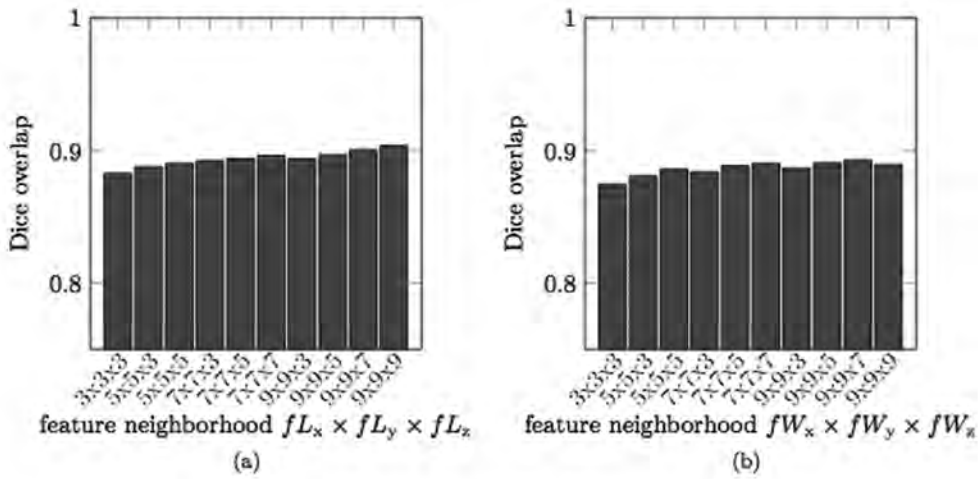

Figure 5. Influence of the feature neighborhood size on the final Dice overlap with the manual segmentation for (a) the lumen and (b) the outer wall.

Table 1. Average surface distance $\delta L_{surface}$ for the various settings of profile length dL_{BB} and the number of iterations nL_{BB} used in the BB lumen segmentation. The minimum value is shown in bold font.

nL_{BB} \ dL_{BB} (mm)	5	7	9	11	13	15	17	19	21	23	25
5	0.84	0.77	0.73	0.70	0.69	0.69	0.71	0.90	0.91	0.92	0.93
10	0.76	0.62	0.54	0.51	0.50	0.50	0.51	0.72	0.73	0.74	0.74
15	0.70	0.54	0.46	0.44	0.43	0.43	0.45	0.66	0.66	0.66	0.67
25	0.65	0.47	0.40	0.39	**0.39**	0.39	0.42	0.63	0.63	0.64	0.65
50	0.70	0.53	0.49	0.46	0.45	0.43	0.46	0.52	0.63	0.71	0.87
75	0.68	0.52	0.48	0.45	0.46	0.45	0.48	0.56	0.78	0.82	0.94
100	0.67	0.50	0.48	0.45	0.46	0.47	0.49	0.59	0.78	0.92	0.96
150	0.65	0.50	0.47	0.45	0.47	0.47	0.51	0.64	0.80	1.30	0.96

Table 2. Average surface distance $\delta W_{surface}$ for the various settings of the profile length dW_{BB} and the number of iterations nW_{BB} used in the BB outer wall segmentation. The minimum value is shown in bold font.

nW_{BB} \ dW_{BB} (mm)	5	7	9	11	13	15
0	0.54	0.54	0.54	0.54	0.54	0.54
1	0.52	0.51	0.50	0.50	0.50	0.50
2	0.51	0.50	0.49	0.49	0.49	0.49
3	0.49	0.49	0.50	0.54	0.58	0.62
5	**0.48**	0.50	0.57	0.67	0.75	0.84
7	0.49	0.53	0.66	0.81	0.93	1.05
10	0.51	0.61	0.82	1.02	1.19	1.34
25	0.62	0.90	1.27	1.59	1.87	2.11
50	0.74	1.12	1.55	1.95	2.28	2.57
75	0.81	1.23	1.69	2.11	2.50	2.83

Table 3. Average lumen Dice overlap values of the final segmentation for various sizes of the region around the host segmentation border which is defined by the dilation $rL_{dilation}$ and erosion $rL_{erosion}$ radius. The maximum value is in bold font. The value for zero dilation and erosion is the Dice overlap value for the uncorrected segmentation.

$rL_{dilation}$ (voxels) \ $rL_{erosion}$ (voxels)	0	1	2	3	4	5	6	7	8	9
0	78.9	80.4	80.6	80.8	80.8	80.8	80.8	80.7	80.8	80.8
1	85.1	84.7	85.0	85.2	85.2	85.2	85.2	85.2	85.1	85.1
2	86.2	85.7	86.0	86.1	86.1	86.2	86.1	86.2	86.2	86.2
3	87.2	86.8	87.1	87.1	87.1	87.2	87.2	87.2	87.2	87.2
4	88.2	87.9	88.1	88.0	88.1	88.1	88.0	88.1	88.2	88.2
5	88.6	88.5	88.8	89.1	88.9	**89.1**	88.8	88.9	88.8	88.8
6	88.8	88.3	88.9	88.6	88.7	88.6	88.7	88.9	89.0	89.0
7	88.8	88.0	88.3	88.7	88.6	88.9	88.8	88.7	88.9	88.9
8	88.5	87.7	88.2	88.5	88.3	88.5	88.5	88.5	88.5	88.5
9	88.2	87.6	87.9	88.0	88.1	88.1	88.3	88.2	88.1	88.0

Table 4. Average outer wall Dice overlap values of the final segmentation for various sizes of the region around the host segmentation border which is defined by the dilation $rW_{dilation}$ and erosion $rW_{erosion}$ radius. The maximum value is in bold font. The value for zero dilation and erosion is the Dice overlap value for the uncorrected segmentation.

$rW_{dilation}$ (voxels) \ $rW_{erosion}$ (voxels)	0	1	2	3	4	5	6	7	8	9
0	81.3	82.2	82.3	82.4	82.3	82.3	82.4	82.3	82.4	82.4
1	85.5	85.6	85.5	85.5	85.5	85.6	85.5	85.6	85.5	85.4
2	86.4	86.4	86.4	86.4	86.4	86.4	86.4	86.4	86.5	86.4
3	87.2	87.3	87.3	87.3	87.3	87.3	87.3	87.3	87.1	87.3
4	87.8	87.9	88.0	87.9	87.9	87.9	88.0	87.9	87.9	88.0
5	88.3	88.3	88.3	88.2	88.3	88.3	88.3	**88.3**	88.3	88.2
6	88.2	88.2	88.1	88.2	88.2	88.1	88.3	88.3	88.1	88.1
7	87.8	87.9	87.9	87.9	87.9	87.9	88.1	88.0	88.0	88.1
8	87.8	87.7	87.4	87.8	87.7	87.9	87.9	87.6	87.7	87.5

Experiments

For the experiments, 27 subjects were randomly selected from the full database. This evaluation set was split in a training set of eight subjects and a test set of 19 subjects. The training set was used to optimize the parameters of the deformable model fitting (dLMRA, *nLMRA, dLBB, nLBB, dWBB* andnWBB)andtheLBVSCmethod(rLdilation,rLerosion,rWdilation,rWerosion, *fLx*×*fLy*×*fLz* and *fWx* × *fWy* × *fWz)*. The test set was used to evaluate the vessel wall volume and NWI quantification.

Manual annotations

On the complete set of 27 subjects, the lumen and outer wall of both the left and the right carotid arteries were annotated manually by observer 1 (ob1). On the test set, observer 2 (ob2) performed the same annotations. The manual annotation started with an accurate definition of the centerline after which longitudinal contours along this centerline were drawn in a curved planar reformatted image for both the lumen and the outer wall. These longitudinal contours were used to create cross-sectional contours perpendicular to the centerline. The cross-sectional contours were then adjusted to fit the lumen and the outer wall. More details on the annotation process can be found in Hameeteman *et al* (2011). The manual annotations were converted into binary masks for calculating the Dice (Dice 1945) overlap coefficient and using the masks in the LBVSC step. The mask generation was achieved by fitting a surface through the contour points using variational interpolation (Heckel *et al* 2011) and voxelizing this closed surface. The mask of the outer wall contains everything within the outer wall including the lumen.

The manual annotations of the ICA do not incorporate the external part in the bifurcation region. Because the automatic method does not differentiate between ICA and ECA in the bifurcation region, the automatic segmentation may cover a larger part of the lumen area within the bifurcation region. This larger automatic segmentation is not wrong, but would result in errors during the evaluation because the manual ground truth does not contain the ECA. To make sure that this does not influence the evaluation results, the ECA region of the bifurcation was masked out and no evaluation was done in that region.

Parameter optimization

4.2.1. Surface distance. Since there is no ground-truth definition in the MRA sequence, the values of profile length *dLMRA* and the number of iterations *nLMRA* were chosen such that the resulting segmentation visually provided a good initialization for the BB lumen segmentation.

For the parameter optimization of the deformable model fitting in the BB image, a distance measure was computed between the NURBS surface and the manual contours. First, the surface was intersected with the MPR plane (perpendicular to the centerline) in which the contours were drawn. This created a contour for the automatic segmentation. Then, the symmetric average Euclidean distance between the manual and automatic contours was calculated. This distance was calculated for all manual contours and the average was computed for each carotid artery. The average over all carotid artery segmentations in the training set (denoted by δLsurface and δWsurface for the lumen and outer wall segmentation, respectively) was used as an optimization objective.

The *dLBB, nLBB, dWBB* and *nWBB* parameters were selected by an exhaustive search, minimizing δLsurface and δWsurface. First, the lumen parameters were optimized and then the outer wall parameters. The value of *dLBB* was optimized between 5 and 25 mm in steps of 2 mm. The number of iterations *nLBB* was optimized over the following set: {5,10,15,25,50,75,100,150}. The outer wall parameter *dWBB* was optimized between 5 and 15 mm in steps of 2 mm and *nWBB* over the following set: {0,1,2,3,5,7,10,25,50,75}. Each combination of profile length and number of iterations was tested, leading to 88 lumen experiments and 60 outer wall experiments.

Learning-based vessel segmentation correction.

The influence of the neighborhood size of the features, $fLx \times fLy \times fLz$ and $fWx \times fWy \times fWz$, on the resulting segmentation was determined for the following values: 3×3×3, 5×5×3, 5×5×5, 7×7×3, 7×7×5, 7×7×7, 9×9×3, 9×9×5, 9×9×7, 9×9×9. For each of these feature neighborhoods, the optimal combination of *rLdilation* and *rLerosion,* and *rWdilation* and *rWerosion* was determined. These LBVSC parameters were optimized with respect to the Dice overlap of the resulting segmentation with the manual segmentation. For each combination of neighborhood size dilation and erosion radius, a new classifier was trained. As the training of each classifier took several hours, performing cross validation on the training set would take too much time. Therefore, each classifier was trained on the complete training set and the evaluation of the resulting segmentation was also performed on the complete training set. This may lead to an overestimation of the performance of the LBVSC method. This is of minor importance since these experiments are only meant to optimize the dilation and erosion parameters, and the true performance will be evaluated on the test set (see section 5.3). The dilation and erosion radii were varied over the interval [0, 9] mm in steps of 1 mm. The AdaBoost classifier was trained using 400 iterations.

Evaluation on the test set

The algorithm was evaluated on the 38 carotids of the 19 datasets in the test set. We evaluated the final segmentation of the lumen and the outer wall by calculating the Dice coefficient for each. This evaluation was performed both without the segmentation correction step, and applying the original LBVC method and our modification, the LBVSC method. The significance of the difference caused by applying the segmentation correction methods was tested using a paired *t-test*.

The vessel wall volumes and NWI from the manual annotations were computed in the same way as for the automatic segmentation (see section 2.3). This was done for both observers that annotated the test set.

The manual and automatic wall volumes were compared by calculating the average difference between the two volumes, the average difference of the NWI and the standard deviation of these two difference measures. Also, the Pearson and intra-class correlation (Shrout and Fleiss 1979) coefficient were calculated.

In these evaluations on the test set, both observers were compared to each other and to the automatic method.

The influence of the number of training sets for the LBVSC method was determined by increasing this number from 10 until 18 in steps of 2. Because for the eight datasets in the training set no manual segmentations of the second observer were available, we only used the manual annotations of the first observer for the evaluation. For each training set size (10, 12, 14, 16 and 18 datasets), ten different random selections of the 38 datasets were made and the results of these ten experiments were averaged. Just as in the other evaluations on the test set, we calculated the Dice coefficient between the automatic segmentation of the lumen and the outer wall.

Results

Parameter optimization

5.1.1. Deformable model fitting. The PC MRA images used in this study have a lower contrast compared to the TOF images used in Van 't Klooster *et al* (2012). In particular in the bifurcation area, the optimization of the MRA lumen surface generated a small or 'half- moon'-shaped vessel surface leading to a bad initialization for the BB lumen segmentation. To handle this problem, we drastically reduced the number of iterations, *nLMRA,* to 1 and kept the profile length *dLMRA* to the minimum of five voxels. This gives the NURBS surface less freedom to adjust and results in a more circular cross-section of the segmented lumen.

Tables 1 and 2 show the results of the optimization experiments for the lumen and outer wall parameters, respectively. The red cell (in bold) indicates the optimal value, i.e. the minimal average surface distance δLsurface and δWsurface. We did not perform any experiments using a profile length of less than 5 mm as this would require the estimation of a gradient on less than three voxels.

Table 5. Optimal lumen and outer wall method parameters.

Lumen		Outer wall	
Parameter	Value	Parameter	Value
nL_{MRA}	1	nW_{BB}	5
dL_{MRA}	5	dW_{BB}	5
nL_{BB}	25	$fW_x \times fW_y \times fW_z$	$7 \times 7 \times 3$
dL_{BB}	13	$rW_{dilation}$	5
$fL_x \times fL_y \times fL_z$	$7 \times 7 \times 3$	$rW_{erosion}$	7
$rL_{dilation}$	5		
$rL_{erosion}$	5		

Table 6. Dice overlap between the different measurements of the test set without segmentation correction and using the LBSC and LBVSC methods.

	Lumen					Outer wall				
	No correction	LBSC	p-value	LBVSC	p-value	No correction	LBSC	p-value	LBVSC	p-value
ob1-ob2	0.90	0.90	–	0.90	–	0.90	0.90	–	0.90	–
ob1-auto	0.83	0.84	0.45	0.86	0.03	0.85	0.86	0.02	0.87	<0.01
ob2-auto	0.84	0.83	0.64	0.84	0.86	0.83	0.85	0.11	0.86	0.01

Learning-based vessel segmentation correction.

Figure 5 shows for each neighborhood size the maximum Dice overlap (obtained with optimum settings of the erosion and dilation parameters, which may be different for each neighborhood size). As can be seen from figure 5, the influence of the feature neighborhood size on the segmentation accuracy is relatively small for both lumen and outer wall. As the computational costs increase significantly with a growing feature neighborhood, we chose a neighborhood size of 7×7×3, which is computationally feasible and accounts for the anisotropic voxel size.

Tables 3 and 4 show the Dice overlap values for the 7×7×3 feature neighborhood size for different combinations of dilation and erosion radii, *rLdilation, rLerosion,* and *rWdilation* and *rWerosion* for the lumen and outer wall, respectively. The maximum Dice coefficients are shown in bold font. The values for a dilation and erosion with zero radius show the Dice overlap without applying the LBVSC method. The tables for the other feature neighborhood

sizes can be found on the website http://ergocar.bigr.nl. In tables 3 and 4, the value for zero dilation and erosion is the smallest. On the training set, the LBVSC method improved the segmentation result of the deformable model fitting: with any setting of *rLdilation, rLerosion, rWdilation* and *rWerosion*, the results were better than *rLdilation* = *rLerosion* = 0 or *rWdilation* = *rWerosion* = 0.

Optimal parameters

Table 5 summarizes the optimal method parameters for both the lumen and the outer wall segmentation.

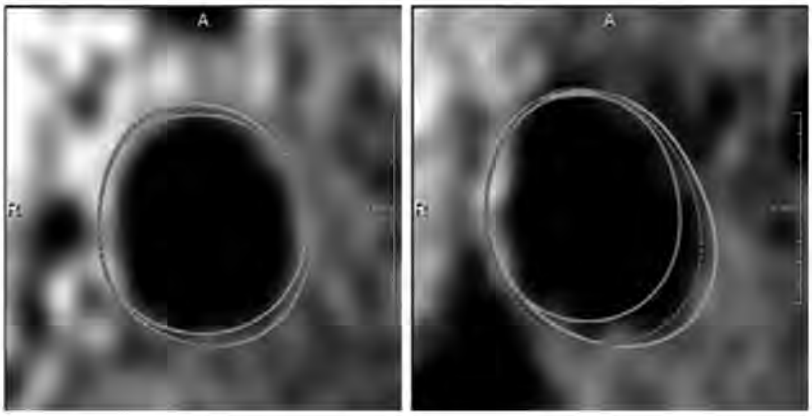

(a) (b)

Figure 6. Two examples of the effect of the LBVSC method on the outer wall segmentation. The green solid line depicts the annotation by ob1, the blue solid line depicts the segmentation from the deformable model fitting method and the dashed red line depicts the segmentation after applying the LBVSC method.

Table 7. Average ± standard deviation of vessel wall volume (ml) and normalized wall index measurements (ml/ml).

	ob1	ob2	No correction	LBSC	LBVSC
V_{wall} (ml)	0.80 ± 0.21	1.1 ± 0.20	0.78 ± 0.13	0.83 ± 0.11	0.89 ± 0.17
NWI (ml/ml)	0.48 ± 0.05	0.59 ± 0.05	0.51 ± 0.05	0.51 ± 0.05	0.54 ± 0.08

Evaluation on the test set

The average Dice similarity coefficients for the lumen and outer wall are listed in table 6. The average Dice overlap between the automatic segmentation and both observers is comparable to the Dice between the two observers. The overlap with the first observer is higher, which is expected as the automatic method was trained using the segmentations of this observer. The LBSC method only improved the outer wall segmentation of the observer

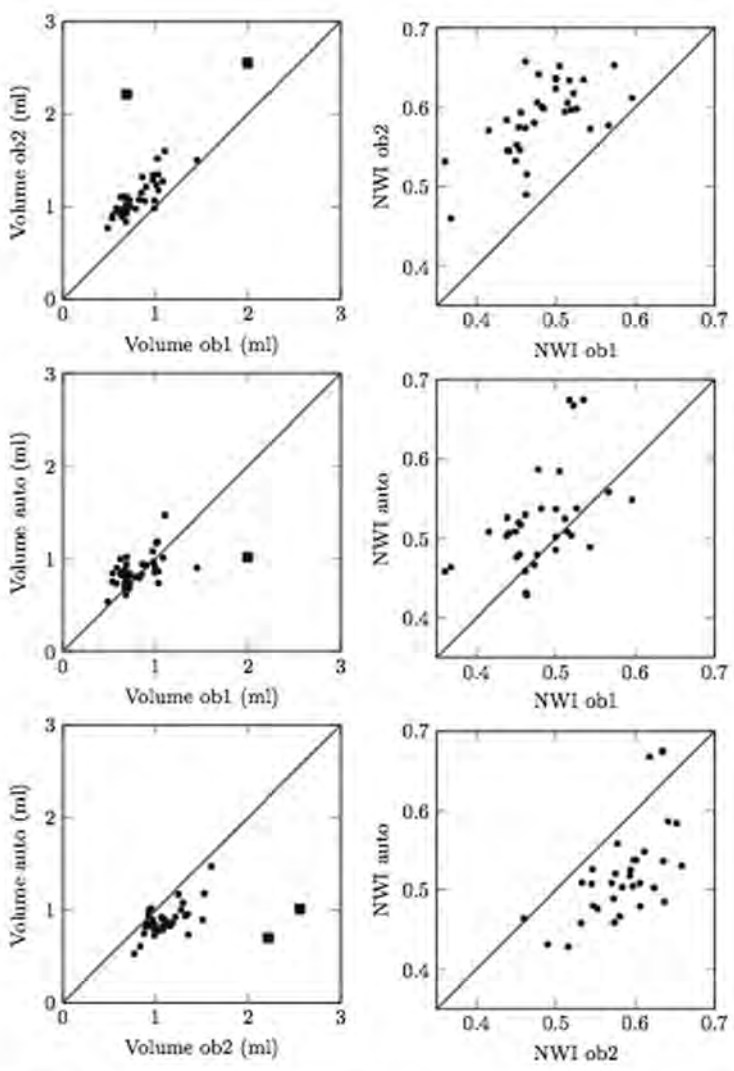

Figure 7. Scatter plot of the volume measurements (left column) and normalized wall index (right column) for ob1 versus ob2 (top row), ob1 versus automatic method (middle row) and ob2 versus automatic method (bottom row). In the volume measurement graphs, two outliers are present and shown with big markers. These outliers are not shown in the NWI graphs because they would stretch the scale too much.

on which it was trained. There was no significant difference for the lumen segmentation. The LBVSC method significantly increased the average lumen overlap for ob1, whereas it remained the same for ob2. For the outer wall, the LBVSC method has a positive effect on the Dice overlap with respect to both observers.

The difference in effect of the LBVSC method between the training (tables 3 and 4) and test set (table 6) is explained by the fact that in the former, the training set was used to both train the classifier of the LBVSC method and measure the effect of the LBVSC method on the Dice overlap of the resulting segmentation (see also section 4.2.2).

Figure 6 gives a visual impression of the effect of the LBVSC method on the outer wall segmentation. The LBVSC method (the dashed red contour) here clearly improved the segmentation of the deformable model fitting method (smallest blue solid contour): it is closer to the manual annotation (solid green contour).

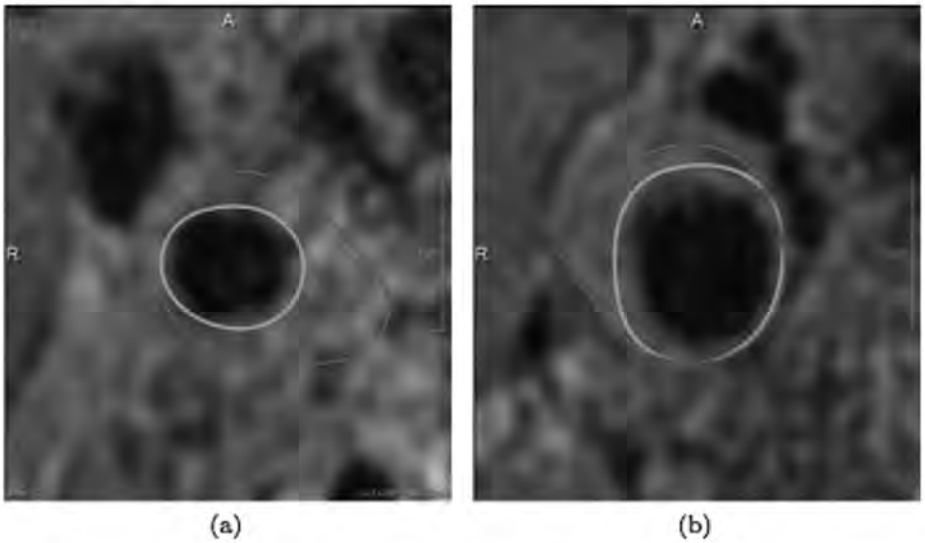

(a) (b)

Figure 8. Example slice from the two outlier datasets. The green contour is from ob1 and the red contour from ob2.

Table 8. The average volume differences, the Pearson and intra-class correlation coefficients of the volume and NWI measurements between the two observers and the automatic method.

	V_{wall}			NWI		
	ΔV_{wall} (ml)	Pearson	icc	ΔNWI (ml/ml)	Pearson	icc
ob2-ob1	0.30 ± 0.19	0.83	0.58	0.10 ± 0.04	0.51	0.32
auto-ob1	0.08 ± 0.20	0.51	0.62	0.05 ± 0.07	0.50	0.52
auto-ob2	-0.21 ± 0.15	0.57	0.57	-0.05 ± 0.07	0.54	0.56

In figure 7, the scatter plots of the volume and NWI measurements by ob1, ob2 and the automatic method are shown. The two large markers in the volume measurements indicate two outliers where ob1 and ob2 disagree. Figure 8 gives an example slice of these outliers. The contours shown in figure 8 are the manual annotations of the outer wall for both observers. It is obvious from these segmentations that in this dataset, it is very hard to determine the location of the outer vessel wall and both observers made a different choice on what to include in the vessel wall. In the subsequent analysis, we removed these outliers.

Table 7 gives the average vessel wall volume and NWI measurements of both observers and the automatic method without applying the segmentation correction and with the LBSC and LBVSC methods. As can be seen, the automatic segmentation slightly overestimated the vessel wall volume when compared to ob1 and underestimated the volume when compared to ob2. Ob2 on average made larger volume measurements than ob1. The average vessel wall volume of the automatic method is between the volumes estimated by ob1 and ob2, but was on average closer to ob1 on which it was trained. The p-values of the differences between the automatic method with and without the LBVSC method are 0.0005 and 0.1 for *Vwall* and NWI, respectively.

Table 8 shows the differences, Pearson and intra-class correlations of the volume and NWI measurements. The average difference in the wall volume measurements of the automatic method with respect to both observers is smaller than the average difference between the observers. Although the Pearson correlation coefficient of the volume measurements between the observers and the automatic method is not as good as the correlation between the two observers, the intra-class correlation with both observers is better than (ob1) or almost the same as (ob2) between the two observers.

Looking at the clinically used NWI, the average difference between the measurements of automatic method and both observers is again smaller than the average difference between the two observers. Also, the correlation coefficients between the automatic method and both observers are better than or almost the same as the correlations between the measurements of the two observers.

Table 9 shows the Dice overlap between the manual segmentation of the first observer and the automatic method for different size of the training set. The table shows that increasing the size of the training set leads to a small increase in overlap.

Table 9. Influence of the number of training sets used for training the LBVSC method on the Dice overlap of the lumen and the outer wall, and the NWI.

Number of training sets	10	12	14	16	18
Dice lumen	0.84	0.84	0.84	0.85	0.86
Dice outer wall	0.85	0.84	0.84	0.85	0.86

Discussion

The inter-observer measurements presented in this study show that the systematic difference between the outer vessel wall annotations of the two observers can be considerable (see the scatter plots in figure 7). As we do not have manual annotations of the second observer on the training set, it is impossible to train the automatic method on both observers, or generate a new reference standard based on the combined annotations of these two observers without compromising the size of the test set. However, the annotation protocol for both observers was the same and the variation between the two observers can also be expected in clinical practice. The method described in this paper was designed in order to analyze the MRI data acquired in the context of a population study. This population study uses a 1.5 T MRI scanner and a BB sequence which may not be the best possible sequence for imaging the vessel wall. Despite these limitations, the described automatic method performs comparable to the observers. In future research, it would be interesting to study the effect of different acquisition settings (1.5 T versus 3 T, different MR sequences, the use of a head stabilizer) on the vessel wall quantification. The evaluation described in this study was performed on 19 subjects. For the future, we plan a quantification of the vessel wall volume and normalized wall index on all 1072 subjects that participated in this study. Manual measurements on this number of subjects become infeasible. The deformable model fitting method enforces a NURBS model on the lumen and wall boundary, and uses a single image feature (the maximum gradient magnitude) to fit the model. For the lumen border, this is an adequate image feature. The gradient of the outer wall is less strong, which makes the application of this image feature less successful. The LBVSC method is not limited to the use of a single image feature, but instead uses many features to classify the outer wall voxels. This explains the difference in effect of the LBVSC method on the lumen and outer wall segmentation.

As long as there is a training set on which the LBVSC can be trained, the method described in this paper can easily be adapted to other images, acquired on a higher field MR scanner or using different protocols. If there is a training set consisting of a ground-truth definition of multiple observers, these could be combined using existing methods like consensus reading or STAPLE (Warfield *et al* 2004), but they can also be used to train multiple classifiers and combine these classifiers into a single stronger classifier using methods described in Tax *et al* (2000).

Conclusion

In conclusion, we presented a method that can automatically quantify the wall volume and normalized wall index of the carotid artery in a region around the bifurcation. The method consists of a deformable model fitting step and a learning-based correction of systematic errors. Intensity inhomogeneities in the MR images were reduced using a 3D-extended version of the LEMS method. The parameters of both the deformable model fitting and the LBVSC method have been optimized by extensive experiments using the manual annotations of a single observer on a training set. The evaluation was performed with respect to annotations of two observers on a separate test set. Our experiments justify the conclusion that the automatic method performs comparably to the manual annotations in terms of wall volume and normalized wall index measurements and can therefore be used to replace the manual measurements.

All image data, annotations and results from this study are made available through the website http://ergocar.bigr.nl. We challenge every one to improve our automatic vessel wall volume and normalize wall index measurements on these datasets and publish their results.

References

1. Brinkmann B, Manduca A and Robb R 1998 Optimized homomorphic unsharp masking for MR grayscale inhomogeneity correction *IEEE Trans. Med. Imaging* 17 161–71
2. Cohen M, DuBois R and Zeineh M 2000 Rapid and effective correction of RF inhomogeneity for high field magnetic resonance imaging *Hum. Brain Mapp.* 10 204–11
3. De Koning P, Schaap J, Janssen J, Westenberg J, Van der Geest R and Reiber J 2003 Automated segmentation and analysis of vascular structures in magnetic resonance angiographic images *Magn. Reson. Med.* 50 1189–98
4. Dehnavi R, Doornbos J, Tamsma J, Stuber M, Putter H, van der Geest R, Lamb H and de Roos A 2007 Assessment of the carotid artery by MRI at 3T: a study on reproducibility *J. Magn. Reson. Imaging* 25 1035–43
5. Dice L 1945 Measures of the amount of ecologic association between species *Ecology* 26 297–302 Freund Y and Schapire R E 1997 A decision-theoretic generalization of on-line learning and an application to boosting *J. Comput. Syst. Sci.* 55 119–39
6. Glagov S, Weisenberg E, Zarins C, Stankunavicius R and Kolettis G 1987 Compensatory enlargement of human atherosclerotic coronary arteries *New Engl. J. Med.* 316 1371–5
7. Hameeteman K *et al* 2011 Evaluation framework for carotid bifurcation lumen segmentation and stenosis grading *Med. Image Anal.* 15 477–88
8. Heckel F, Konrad O, Hahn H and Peitgen H 2011 Interactive 3D medical image segmentation with energy-minimizing implicit functions *Comput. Graph.* 35 275–87
9. Hofman A *et al* 2011 The Rotterdam study: 2012 objectives and design update *Eur. J. Epidemiol.* 26 657–86
10. Ibanez L, Schroeder W, Ng L and Cates J 2005 *The ITK Software Guide* 2nd edn (Clifton Park, NY: Kitware) ISBN 1-930934-15-7 www.itk.org/ItkSoftwareGuide.pdf
11. Kang X, Polissar N, Han C, Lin E and Yuan C 2000 Analysis of the measurement precision of arterial lumen and wall areas using high-resolution MRI *Magn. Reson. Med.* 44 968–72
12. Klein S, Pluim J, Staring M and Viergever M 2009 Adaptive stochastic gradient descent optimisation for image registration *Int. J. Comput. Vis.* 81 227–39
13. Klein S, Staring M, Murphy K, Viergever M and Pluim J 2010 elastix: a toolbox for intensity-based medical image registration *IEEE Trans. Med. Imaging* 29 196–205
14. Morra J H, Tu Z, Apostolova L G, Green A E, Toga A W and Thompson P M 2008 Automatic subcortical segmentation using a contextual model *Med. Image Comput. Comput. Assist. Interventions* 11 194–201 (PMID: 18979748)
15. Roger V *et al* 2011 Heart disease and stroke statistics—2011 update: a report from the American Heart Association *Circulation* 123 e18–209
16. Rueckert D, Sonoda L, Hayes C, Hill D, Leach M and Hawkes D 1999 Nonrigid registration using free-form deformations: application to breast MR images *IEEE Trans. Med. Imaging* 18 712–21
17. Salvado O, Hillenbrand C, Zhang S and Wilson D 2006 Method to correct intensity inhomogeneity in MR images for atherosclerosis characterization *IEEE Trans. Med. Imaging* 25 539–52
18. Shrout P E and Fleiss J L 1979 Intraclass correlations: uses in assessing rater reliability *Psychol. Bull.* 86 420–8

19. Sled J, Zijdenbos A and Evans A 1998 A nonparametric method for automatic correction of intensity nonuniformity in MRI data *IEEE Trans. Med. Imaging* 17 87–97
20. Takaya N *et al* 2006 Association between carotid plaque characteristics and subsequent ischemic cerebrovascular events: a prospective assessment with MRI–initial results *Stroke* 37 818–23
21. Tax D M, van Breukelen M, Duin R P and Kittler J 2000 Combining multiple classifiers by averaging or by multiplying? *Pattern Recognit.* 33 1475–85
22. The ´venaz P and Unser M 2000 Optimization of mutual information for multiresolution image registration *IEEE Trans. Image. Process.* 9 2083–99
23. Tu Z, Zheng S, Yuille A L, Reiss A L, Dutton R A, Lee A D, Galaburda A M, Dinov I, Thompson P M and Toga A W 2007 Automated extraction of the cortical sulci based on a supervised learning approach *IEEE Trans. Med. Imaging* 26 541–52
24. Tustison N, Avants B, Cook P, Zheng Y, Egan A, Yushkevich P and Gee J 2010 N4ITK: improved N3 bias correction *IEEE Trans. Med. Imaging* 29 1310–20
25. Van den Bouwhuijsen Q, Vernooij M, Hofman A, Krestin G, van der Lugt A and Witteman J 2012 Determinants of magnetic resonance imaging detected carotid plaque components: the Rotterdam Study *Eur. Heart J.* 33 221–9
26. Van 't Klooster R, de Koning P, Dehnavi R, Tamsma J, de Roos A, Reiber J and van der Geest R 2012 Automatic lumen and outer wall segmentation of the carotid artery using deformable three-dimensional models in MR angiography and vessel wall images *J. Magn. Reson. Imaging* 35 156–65
27. Varghese A, Crowe L, Mohiaddin R, Gatehouse P, Yang G, Firmin D and Pennell D 2005 Inter-study reproducibility of 3D volume selective fast spin echo sequence for quantifying carotid artery wall volume in asymptomatic subjects *Atherosclerosis* 183 361–6
28. Wang H, Das S, Suh J, Altinay M, Pluta J, Craige C, Avants B, Yushkevich P and Initiative A D N 2011 A learning-based wrapper method to correct systematic errors in automatic image segmentation: consistently improved performance in hippocampus, cortex and brain segmentation *Neuroimage* 55 968–85
29. Warfield S K, Zou K H and Wells W M 2004 Simultaneous truth and performance level estimation (STAPLE): an algorithm for the validation of image segmentation *IEEE Trans. Med. Imaging* 23 903–21
30. Yuan C, Beach K, Smith L and Hatsukami T 1998 Measurement of atherosclerotic carotid plaque size in vivo using high resolution magnetic resonance imaging *Circulation* 98 2666–71
31. Yuan C, Lin E, Millard J and Hwang J 1999 Closed contour edge detection of blood vessel lumen and outer wall boundaries in black-blood MR images *Magn. Reson. Imaging* 17 257–66
32. Zhang S, Cai J, Luo Y, Han C, Polissar N, Hatsukami T and Yuan C 2003 Measurement of carotid wall volume and maximum area with contrast-enhanced 3D MR imaging: initial observations *Radiology* 228 200–5

Chapter 5.2

Cardiovascular risk factors of carotid plaque burden as measured by MRI in the general population

Mariana Selwaness
Reinhard Hameeteman
Ronald van 't Klooster
Quirijn van den Bouwhuijsen
Albert Hofman
Oscar H Franco
Wiro J Niessen
Stefan Klein
Meike W Vernooij
Aad van der Lugt
Jolanda J Wentzel

Chapter 6

Intraplaque hemorrhage progression and measurements

Chapter 6.1

Semiautomatic carotid intraplaque hemorrhage segmentation and volume quantification by in vivo MRI

Hui Tang
Mariana Selwaness
Reinhard Hameeteman
Anouk C van Dijk
Aad van der Lugt
Jacqueline CM
Witteman
Wiro J Niessen
Lucas J van Vliet
Theo van Walsum

Abstract

Background: Intra-plaque hemorrhage (IPH) is associated with plaque instability. Therefore, the presence and volume of IPH in carotid arteries may be relevant in predicting the progres- sion of atherosclerotic disease and the occurrence of clini- cal events. The aim of our work was to develop and eval- uate a method for semi-automatic IPH segmentation in T1- weighted (T1w)-magnetic resonance imaging (MRI).

Materials and methods: IPH segmentation is performed by a regional level set method that models the intensity of the IPH and the background in T1w-MRI to be smoothly varying. The method only requires minimal user interaction, i.e., one or more mouse clicks inside the hemorrhage serve as initialization. The parameters of the method are optimized using a leave-one-out strategy by maximizing the Dice simi- larity coefficient (DSC) between manual and semi-automatic segmentations. We evaluated the IPH segmentation method on 22 carotid arteries; 10 of which were annotated by two observers and 12 were scanned twice within a 2 week period.

Results: We obtained a DSC of 0.52 between the manual and level set segmentations on all 22 carotids. The inter-observer DSC on 10 arteries is 0.57, which is comparable to the DSC between the method and the manual segmentation (0.55). The correlation between the IPH volumes extracted from the level set segmentation and the manual segmentation is 0.88, which is close to the inter-observer volume correlation of 0.92. The reproducibility after rescanning 12 carotids yield an IPH vol- ume correlation of 0.97. The robustness with respect to the initialization by manually clicking two sets of seed points in these 12 carotid artery pairs yields a volume correlation of 0.99.

Conclusion: Semi-automatic segmentation and quantification of IPHs are feasible with an accuracy in the range of the inter- observer variability. The method has excellent reproducibil- ity with respect to rescanning and manual initialization.

Introduction

Atherosclerosis is one of the main underlying causes of cardiovascular events such as ischemic stroke, and a major cause of mortality and morbidity [8]. Atherosclerosis progresses with age and often remains asymptomatic prior to clinical events [8]. Many studies investigated the relation between plaque growth and various other factors, such as vessel geometry and plaque composition [6, 15, 17]. Recently, intraplaque hemorrhage (IPH) was found to be associated with the increase in size of the necrotic core and lesion instability in coronary plaques [11] and therefore, IPH is considered as a high risk component of the vulnerable plaques [14]. IPH was also reported to be related to (recurrent) neurological events during follow-up [1]. Takaya et al. [16] found that the presence of IPH in carotid atherosclerotic plaques accelerated plaque progression over an 18-month period. The association between the size of IPH and plaque progression has not been investigated previously. MRI can be used for visualizing IPH [20]. It has been shown that high resolution MR has excellent capabilities for differentiating IPH from other carotid plaque tissues [3,4]. To study the association between IPH size and plaque progression, an MRI study was designed as part of a population-based study [9]. Purpose of our work was to develop a method for the precise and robust quantification of IPH volume from MRI data and evaluate it on those data.

Manual quantification of IPH (or other plaque characteristics) is a tedious procedure, prone to inter- and intra-observer variability. Therefore, there is a large interest in automated procedures for plaque assessment. Pattern recognition and machine learning methods play an important role in (semi-) automatic segmentation of plaque components [10, 13, 19]. Hofman et al. [10] quantified the relative area of all detected atherosclerotic plaque components, including IPH, using supervised classification techniques. Their method needs manual annotation of the inner and outer vessel wall to obtain a mask of the plaque and thus requires a significant amount of user interaction. Liu et al. [13] seg- mented plaque components based on morphology enhanced probability maps from in vivo magnetic resonance imaging (MRI), but IPH is not included in their work. Van Engelen et al. [19] segmented the plaque composition in ex vivo MRI using a machine learning method. Similar to the work by Hofman et al. [10] and Liu et al. [13], this method requires manual annotation of the inner and outer vessel wall.

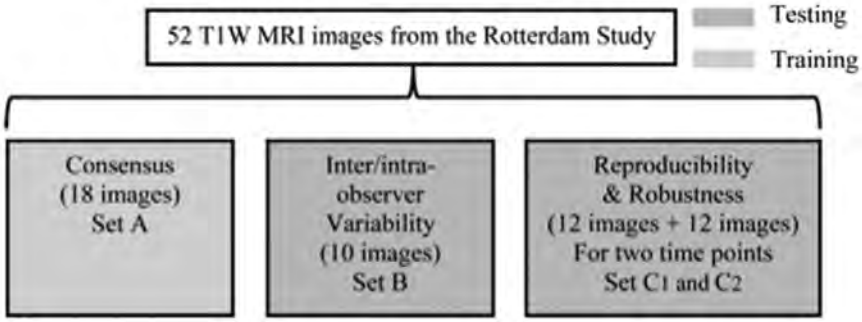

Fig. 1 Description of image data

In this paper, we present a semi-automatic approach to quantify the carotid IPH volume using manually selected seed points. The seed points are used to initialize a piecewise-

Fig. 2 An example of a manually drawn contour and the partial volume image generated from the manual contour

smooth regional level set method that segments the IPH. Our main contributions are (1) we demonstrate the feasibility of precise IPH segmentation without vessel wall annotation and (2) we perform an extensive validation study to investigate the accuracy, and inter-scan reproducibility and robustness of the proposed semi-automatic IPH segmentation approach.

Materials and methods

Materials

Data description The data in this work are obtained from a prospective cohort study to investigate the prevalence, incidence, and risk factors of chronic diseases in an asymptomatic group of elderly aged 45 years and older [9]. In this study, 1,006 participants with a vessel wall thickness larger than 2.5mm at plaque locations (determined by 2D ultra- sound) underwent MR imaging of the carotid arteries [18]. The study procedures and consent forms were reviewed and approved by The Medical Ethics Committee of Erasmus MC, University Medical Center Rotterdam.

From this data set, we randomly selected 52 T1-weighted (T1w) MRI images (see Fig. 1) of 40 carotid arteries from 27 subjects among the participants who contain IPH. The 52 images were further divided into subsets, denoted by *A, B, C1,* and *C2,* based on the availability of manual reference data and re-scan data. Set *A* consists of 18 carotid arteries from 12 subjects with a consensus annotation by two observers. This set is used for parameter optimization. Ten data sets (set *B)* from six subjects have intra-/inter-observer annotations, and for 12 carotid arteries, we have images at two time points (C1 and *C2),* with <2weeks between the acquisitions. The accuracy of the proposed method was evaluated using sets *B* and *C1* (22 data sets). The reproducibility and robustness of the method were evaluated

on the 12 carotid arteries (24 image data sets) from 10 subjects for which two images are available (C1 and *C2)* and for which two observers provided seed points. An overview of the data used in this paper is shown in Fig. 1.

All scans were obtained with a 1.5-T scanner (GE Signa Excite II; GE Healthcare, Milwaukee, WI, USA) with a bi- lateral phased-array surface coil. The MRI acquisition parameters for the T1w MRI scans are as follows: a 3D Gradient Recalled Echo sequence, scanned in the coronal plane, parallel to the common carotid artery, repetition time / echo time: 15.7 / 1.8 ms, field of view (FOV): 18 × 18 cm2, matrix size: 192 × 180 in the coronal plane. The slice thick- ness is 1.0 mm and the flip angle is 40˚. The stenosis is measured manually using the NASCET (North American Symptomatic Carotid Endarterectomy Trial) criteria [2] and ranges from 0 to 90 % (23% on average). All scans were reviewed by two independent physicians, both with 2 years experience in reading MRI, under supervision of a neuroradiologist with more than 8 years of experience in MRI plaque analysis.

Reference standard The IPHs were manually annotated in axial slices using in-house developed software. Observers were able to zoom in and out and delineate the border by drawing contours around the IPHs per slice. For Set A, two readers, R1 and R2, annotated the IPH border in consensus, yielding annotation OA consencus 1. For Set B, reader R performed the annotation two times, resulting in two annotations labeled as OB_{11} and OB_{12} , which enables the assessment of the intra-observer variability. The time interval between the two annotations is over 2 months. Reader *R2* performed the annotation once, resulting in one annotation labeled as *O2B* to allow the assessments of the inter-observer variability. Reader *R1* also annotated sets *C1* and *C2* twice. The manual contours were used to create a partial volume image by calculating the fraction of the voxel inside the contour (a polygon) for every voxel in each slice. In the partial volume image, the intensity value ranges between 0 and 1, indicating the fraction of each voxel occupied by the IPH (Fig. 2). The manual method takes around 10 min per carotid artery.

Methods

The IPH segmentation is performed by a piecewise regional level set initialized by seed points. A region of interest is automatically generated around the seed points. The size of the region is defined by a box whose size is 15 voxels larger in all directions than the smallest bounding box that encloses all seed points. Figure 3 shows a slice through the 3D volume, the projected seed points, and the automatically cropped image.

For the semi-automatic IPH segmentation, we require a method that can deal with: (1) varying size of IPHs, (2) intensity variation within the IPH due to variations in plaque composition, and (3) intra-scan intensity variations. Based on these requirements, we chose a piecewise-smooth regional level set for this purpose [12]. The level set's energy function is

$$E_{RSF}(\phi(\boldsymbol{x})) = \lambda_1 \int \int K_\sigma(\boldsymbol{y}-\boldsymbol{x})(I(\boldsymbol{y}) - f_1(\boldsymbol{x})) H_1(\phi(\boldsymbol{x}))d\boldsymbol{x}d\boldsymbol{y} + \lambda_2 \int \int K_\sigma(\boldsymbol{y}-\boldsymbol{x})(I(\boldsymbol{y}) - f_2(\boldsymbol{x})) H_2(\phi(\boldsymbol{x}))d\boldsymbol{x}d\boldsymbol{y} + v|\nabla\phi(\boldsymbol{x})|,$$

where φ (x) is a signed distance map which is negative inside the segmentation surface *S,* positive outside, and zero at the border. *H1* (φ (x)) is the Heaviside function representing the current segmentation during the iteration process which has the value 0 inside the surface S and 1 outside, and *H2* (φ (x)) is equal to 1– *H1(φ(x))*. *Kσ* (y–x) is a Gaussian function that controls the size of a spherical region in which the intensity inhomogeneity is ignored, a larger (smaller) scale σ assumes a homogenous intensity in a larger (smaller) local region and thus a less (more) severe intensity inhomogeneity. The term *fi* (x) (i = 1, 2) denotes the estimated mean intensity as a function of image location. We use a local estimate *fi(x)* instead of a global constant to estimate the mean intensity in the fore- and background, in order to take intensity inho- mogeneity into account. Li et al. used a standard gradient descent method to minimize Eq. 1, which upon convergence yields the final segmentation φ(x) = 0. In each iteration, we need to update *fi* (x), *i* = 1, 2 according to

$$f_i(\boldsymbol{x}) = \frac{K_\sigma(\boldsymbol{x}) * [H_i(\phi(\boldsymbol{x}))I(\boldsymbol{x})]}{K_\sigma(\boldsymbol{x}) * H_i(\phi(\boldsymbol{x}))}, \quad i = 1, 2$$

where denotes the convolution operation. A curvature term, weighted by v, is included to enforce the smoothness of the surface [5].

The method was implemented in itk (www.itk.org) and runs on a Linux workstation with 16 processors (AMD 6172, 12 cores, 2.1 GHz). The processing time is around 1 min per seed points. None of the processing steps uses a parallel implementation.

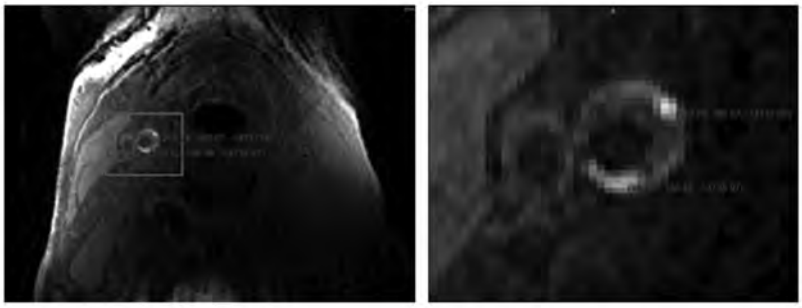

Fig. 3 (a) The original image overlaid by the automatic bounding box (red), (b) automatically cropped image using the clicked seed points.

Results

Experiments are designed to determine both inter- and intra- observer variability and to determine the difference between the semi-automatic method and the observers. First, inter- and intra-observer variabilities are assessed. Subsequently, for the semi-automatic method, parameter settings for IPH segmentation are optimized on training set *A*. Then, the segmentation results are compared with the manual reference standard. This value is further compared with the inter- /intra-variability. Finally, the robustness and inter-scan reproducibility of the method are investigated. The mean and standard deviation of the volume in all the dataset for different annotations are listed in Tables 1, 2.

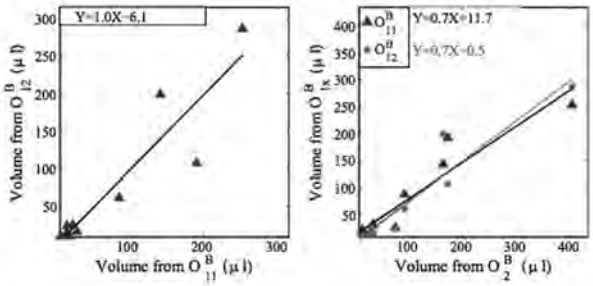

Fig. 4 Scatter plot of (a) the IPH volumes measured twice by observer one and (b) the IPH volumes measured by the first observer and second observer.

Table 1 The results after parameter training, where the second row lists the average DSC on the training set, i.e. all subjects excluding the subject in the column. The sixth and seventh rows show the DSC of the subject in the current column (test set) using these optimal parameter values. An entry listing the '–' sign indicates that the corresponding carotid artery does not have any IPHs. A DSC of '0' means that the semi-automatic segmentation method

shrinks to a size of zero volume. DSCL (DSCR): DSC between the maunal and the semi-automatic segmentation for the left (right) carotid artery.

subjectID	0	1	2	3	4	5	6	7	8	9	10	11
DSC (%)	51	48	48	41	49	49	47	49	48	48	52	48
λ_1	1	1	1	1	1	1	1	0.9	1	1	1	1
v	7e-3	7e-3	8e-3	7e-3	8e-3	8e-3	7e-3	10e-3	7e-3	8e-3	7e-3	7e-3
σ	0.1	0.1	0.1	0.1	0.1	0.1	0.1	0.1	0.1	0.1	0.1	0.1
DSC_L (%)	8	70	66	41	43	–	47	50	–	62	0	–
DSC_R (%)	48	49	–	–	56	38	76	35	–	58	48	55

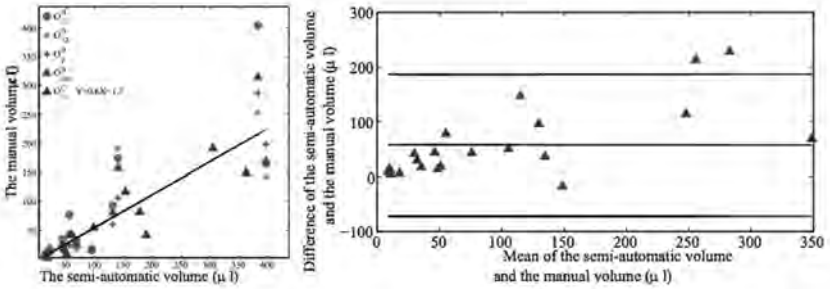

Fig. 6 (a) Scatter plot and the regression line between manual and semi-automatic volume and (b) Bland & Altman plot of the manual volume and semi-automatic volume in Set B and C_1.

Inter- and intra-observer variability

The inter-observer Dice similarity coefficient (DSC) [7] is defined as the average of the two DSC's between the first observer's and the second observer's annotations and is found to be 0.57. The intra-observer DSC is defined as the DSC between the two annotations of the first observer and is equal to 0.62. Figure 4 shows the scatter plot of volume quantifications from these annotations. The intra-observer correlation of volume is 0.92, while the average correlation of the inter- observer correlation of volume is 0.95.

Parameter optimization

The semi-automatic segmentation method includes a number of parameters: the parameter λ1 and λ2 determines the weights of the internal and external intensity dissimilarity; v determines the weight of the curvature which controls the smoothness of the segmentation, and σ is the scale of the Gaussian function which controls the size of the region. The optimal value for these parameters was determined in a leave- one-out fashion on data set *A*. Since only the relative value of the internal and external weights, λ1 and λ2, and curvature weight v matters, we fixed λ2 to be 1 and optimized the values for λ1 and v, as well as the parameter σ . The curvature weight v was trained from 0.004 to 0.010 in 7 steps. The internal weight λ1 was varied from 0.9 to 1.8 with a step size of 0.1. The Gaussian kernel scale σ was

varied between 0.1 and 1 in two steps. We set the number of iterations to 200. The initial size of the segmentation is a sphere with a radius of 1mm around the seed points. The leave-one-subject-out training results are shown in Table 3. The overall optimal values for IPH segmentation using the piecewise-smooth regional level set are

$\lambda 1 = 1, v = 0.007 \text{and} \sigma = 0.1 \text{mm}$.

Accuracy

Three IPH segmentation results on the test sets (B and *C1*) are shown in Fig. 5. We compared the automatically quan- tified volume to the average volume from three annotations in set *B* (10 images) and the only annotation in set *C1* (12 images); both are depicted by triangles in Fig. 6. We obtained a DSC of 0.53 with regard to the average manual volume in set *B* and the first observer in set *C1*. The Pearson correlation coefficient between the manual and semi-automatic volumes is 0.88. Figure 6a also shows the scatter plot of the semi- automatic volume and the three annotations in set *B*. The difference between the annotations increases with volume.

We compared our semi-automatic segmentation results for data sets *B* to the inter- and intra-observer variability. The average DSC between the semi-automatic method and the average of three annotations is 0.55, which is close to the inter-observer variability of 0.57. Figure 6 shows the scatter plot between the manual segmentation and the semi- automatic volumes, the Pearson correlation coefficient is 0.88.

Inter-scan reproducibility and robustness

Reproducibility and robustness of the method with regard to rescanning and seed point selection were assessed by apply- ing the method to the carotid arteries in sets *C1* and *C2*. The Pearson correlation coefficient between the 12 pairs of vol- umes obtained by applying the semi-automatic (manual) seg- mentation to both timepoints with the semi-automatic seg- mentation for images acquired at two time points is 0.97, which is considerably higher than that between the manual annotation of two time points (0.71). The Bland and Altman plot in Fig. 7 shows that the absolute difference between the two volumes increases with the average size of the IPH. We performed a Wilcoxon's signed rank test between the 12 pairs of volumes obtained with the semi-automatic segmen- tation (manual segmentation) acquired at two different time points, the p value is 0.38 (0.04) at a confidence level of 95 %, indicating a good (poor) reproducibility of the imaging techniques and semi-automatic (manual) segmentation methods. The mean absolute

difference between the volumes of the first and second scan obtained from the semi-automatic segmentation is 30.7µl, whereas the mean absolute difference between the volumes of the first and the follow-up scans obtained from the manual segmentation is 81.0 µl, shown in Table 3. Figure 8 shows the scatter plot of the 12 pairs of manual volumes and the Bland and Altman plot.

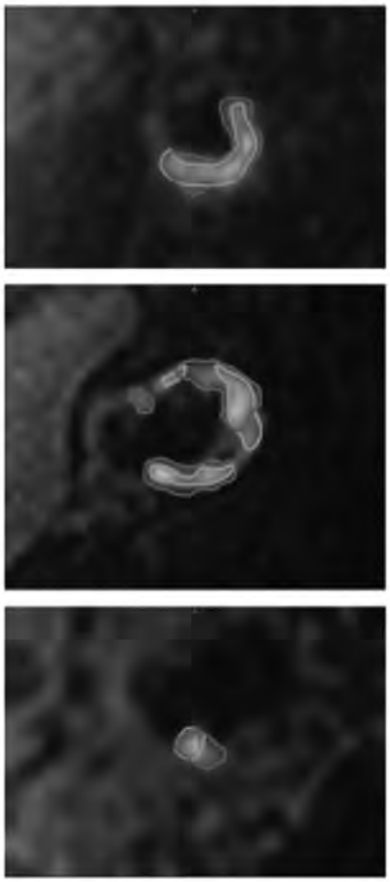

Fig. 5 IPH segmentation results; the manual segmentation in green and the semi-automatic segmentation in red, (a) Dice = 0.72, (b) Dice = 0.64, (c) Dice = 0.51

We also studied the robustness of the method with respect to manual seed point selection on sets *C1* and *C2*. Two observers independently selected two series of seed points with a time interval of more than 1 month. The Pearson correlation coefficient between volumes from two semi-automatic segmentations is 0.99, as seen in Fig. 9a. We also performed a paired *t* test between the 24 pairs of semi-automatic volumes acquired with two different initial seeds, the *p* value is 0.12 at a confidence level of 95 %, indicating a good robustness of this method with respect to the manual initialization. The average DSC between two semi-automatic segmentations is 0.88, and the mean absolute difference between the volumes obtained with two semi-automatic segmentations with two different sets of seed points is 8.1 µl, shown in Table 3.

Discussion

We presented a semi-automatic IPH segmentation and quantification method that does neither require manual annotation of the inner or outer vessel wall nor preprocessing to correct for intensity inhomogeneities. The method segments IPHs using a piecewise-smooth regional level set initialized by a set of manually clicked seed points. We trained the parameters of this segmentation using a leaving-one-out strategy on 18 images. The method is evaluated for accuracy on 34 images and for robustness and inter-scan reproducibility on 24 images.

We obtained a volume correlation of 0.88 between the semi-automatic segmentation and the manual segmentation in 10 data sets, which is slightly less than the inter-observer correlation. A robustness study with respect to the selection of seed points yielded a high volume correlation between the volumes obtained using two different seed points, which is better than the intra-observer correlation (0.92). The inter- scan reproducibility experiments showed that the segmented volumes of the semi-automatic method have a much higher reproducibility than those of the observers.

This study demonstrates that the manual annotation of IPH is subject to large observer variability. Therefore, the semi- automatic results can at best also have a moderate agreement with the manual reference standard. However, the robustness and inter-scan reproducibility of the semi-automatic method are better than the manual observations. This suggests that semi-automatic IPH volume quantification is to be preferred in clinical studies. We found three existing alternatives [10,13,19] for IPH segmentation whose accuracy was evaluated by different metrics: area correlation [13], relative area difference and correlation [10], and classification statistics (AUC, PPV, NPV, sensitivity and specificity) [19]. Even though it is difficult to compare our method with the others due to the differences in evaluation metrics and data selection, we can state the following differences with previous studies: (1) the methods by [10, 13, 19] all need a manual segmentation of the inner and outer vessel wall to define a region of inter- est. In contrast, our method needs a few seed points as user inputs, which largely reduces the user interaction. (2) We per- formed a 3D segmentation, while Liu et al. [13] and Hofman et al. [10] performed a 2D segmentation. (3) All three meth- ods [10, 13, 19] used a voxel-wise classification method to segment each plaque component, while we directly segment only the IPH using a levelset approach. The latter is expected to achieve subvoxel accuracy. Additionally, our study is the only one addresses reproducibility with respect to rescan- ning, which is essential for the application of the method in longitudinal studies.

This work has some limitations. We did not evaluate the robustness of the method with respect to scanner type. However, as there is a parameter training part involved, we expect that similar results can be obtained on different scanners, provided that a similar parameter training experiment with representative data from that scanner is performed.

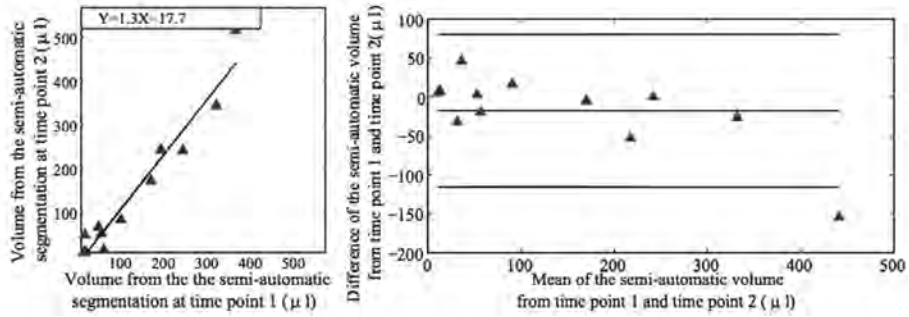

Fig. 7 (a) Scatter plot and (b) Bland & Altman plot of the semi-automatic volumes from two time points (Set C_1 and C_2).

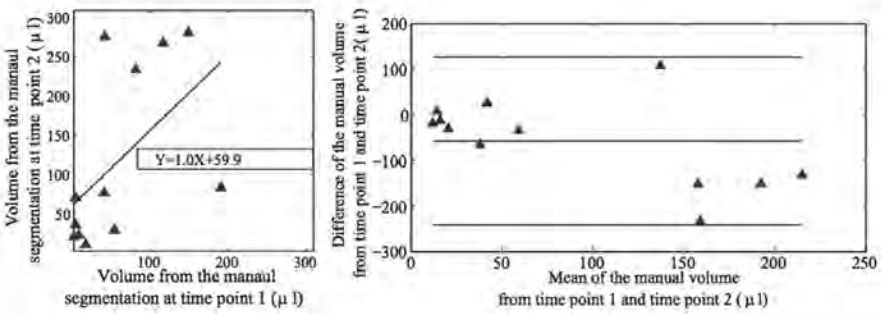

Fig. 8 (a) Scatter plot and (b) Bland & Altman plot of the manual volumes from two time points (Set C_1 and C_2).

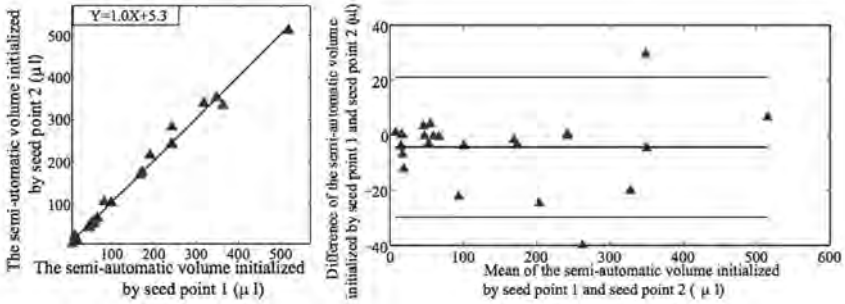

Fig. 9 (a) Scatter plot and (b) Bland & Altman plot of the semi-automatic volumes from two initializations (Set C_1 and C_2).

We presented a semi-automatic IPH segmentation method, which gives IPH volume quantifications with an accuracy similar to manual annotation. In the robustness study as well as the reproducibility study, the quantifications obtained with the semi-automatic method are shown to be more robust and reproducible than those obtained from manual annotations. We thus demonstrated the feasibility of semi-automatic quantification of IPH volumes.

Additional information

Hui Tang, Mariana Selwaness, Reinhard Hameeteman, Anouk van Dijk, Aad van der Lugt, Jacqueline C Witte- man, Wiro J Niessen, Lucas J van Vliet and Theo van Walsum declare that they have no conflict of interest. Informed consent was obtained from all patients for being included in the study.

References

1. Altaf N, Daniels L, Morgan PS, Auer D, MacSweeney ST, Moody AR, Gladman JR (2008) Detection of intraplaque hemorrhage by magnetic resonance imaging in symptomatic patients with mild to moderate carotid stenosis predicts recur- rent neurological events. J Vasc Surg 47(2):337–342. doi:10.1016/ j.jvs.2007.09.064. http://www.sciencedirect.com/science/article/ B6WMJ-4RPSH92-P/2/2bbdaed07bbb88aed06a6f8b190ddd08
2. BarnettHJ,TaylorDW,EliasziwM,FoxAJ,FergusonGG,Haynes RB, Rankin RN, Clagett GP, Hachinski VC, Sackett DL et al (1998) Benefit of carotid endarterectomy in patients with symptomatic moderate or severe stenosis. N Engl J Med 339(20):1415–1425
3. Bitar R, Moody AR, Leung G, Symons S, Crisp S, Butany J, Rowsell C, Kiss A, Nelson A, Maggisano R (2008) In vivo 3D high-spatial-resolution MR imaging of intraplaque hemorrhage. Radiology 249(1):259–267
4. Cappendijk VC, Cleutjens KBJM, Kessels AGH, Heeneman S, Schurink GWH, Welten RJTJ, Mess WH, Daemen MJAP, van Engelshoven JMA, Kooi ME (2005) Assessment of human atherosclerotic carotid plaque components with multisequence MR imaging: initial experience1. Radiology 234(2):487–492. doi:10. 1148/radiol.2342032101. http://radiology.rsna.org/content/234/2/ 487.abstract
5. CasellesV,KimmelR,SapiroG,SbertC(1997)Minimalsurfaces based object segmentation. IEEE Trans Pattern Anal Mach Intell 19:394–398
6. ChamblessLE,HeissG,FolsomAR,RosamondW,SzkloM,Shar- rett AR, Clegg LX (1997) Association of coronary heart disease incidence with carotid arterial wall thickness and major risk factors: the atherosclerosis risk in communities (ARIC) study, 1987–1993. Am J Epidemiol 146(6):483–494
7. Dice LR (1945) Measures of the amount of ecologic association between species. Ecology 26(3):297–302
8. Epstein FH, Ross R (1999) Atherosclerosis: an inflammatory dis- ease. N Engl J Med 340(2):115–126. http://dx.doi.org/10.1056/ NEJM199901143400207
9. Hofman A, van Duijn CM, Franco OH, Ikram MA, Janssen HL, Klaver CC, Kuipers EJ, Nijsten TE, Stricker BHC, Tiemeier H et al (2011) The Rotterdam study: 2012 objectives and design update. Eur J Epidemiol 26(8):657–686
10. Hofman JMA, Branderhorst W, ten Eikelder H, Cappendijk V, Heeneman S, Kooi M, Hilbers P, ter Haar Romeny B (2006) Quan- tification of atherosclerotic plaque components using in vivo MR and supervised classifiers. Magn Reson Med 55(4):790–799. http:// dx.doi.org/10.1002/mrm.20828
11. Kolodgie FD, Gold HK, Burke AP, Fowler DR, Kruth HS, Weber DK, Farb A, Guerrero L, Hayase M, Kutys R, Narula J, Finn AV, Virmani R (2003) Intraplaque hemorrhage and progression of coronary atheroma. N Engl J Med 349(24):2316–2325. http://www. nejm.org/doi/abs/10.1056/NEJMoa035655
12. Li C, Kao CY, Gore JC, Ding Z (2008) Minimization of region- scalable fitting energy for image segmentation. IEEE Trans Image Process 17(10):1940–1949
13. LiuF,XuD,FergusonMS,ChuB,SaamT,TakayaN,Hatsukami TS, Yuan C, Kerwin WS (2006) Automated in vivo segmentation of carotid plaque MRI with morphology-enhanced probability maps. Magn Reson Med 55:659–668

14. Selwaness M, van den Bouwhuijsen Q, Verwoert G et al (2013) Blood pressure parameters and carotid intraplaque hemorrhage as measured by magnetic resonance imaging: the Rotterdam study. Hypertension 61(1):76–81
15. Smedby Ö, Bergstrand L (1996) Tortuosity and atherosclerosis in the femoral artery: what is cause and what is effect? Ann Biomed Eng 24(4):474–480
16. TakayaN,YuanC,ChuB,SaamT,PolissarNL,JarvikGP,Isaac C, McDonough J, Natiello C, Small R, Ferguson MS, Hatsukami TS (2005) Presence of intraplaque hemorrhage stimulates progres- sion of carotid atherosclerotic plaques: a high-resolution magnetic resonance imaging study. Circulation 111(21):2768–2775. http:// circ.ahajournals.org/cgi/content/abstract/111/21/2768
17. Thomas JB, Antiga L, Che SL, Milner JS, Hangan Steinman DA, Spence JD, Rutt BK, Steinman DA (2005) Variation in the carotid bifurcation geometry of young versus older adults: implications for geometric risk of atherosclerosis. Stroke 36(11):2450–2456. http:// stroke.ahajournals.org/cgi/content/abstract/36/11/2450
18. Van den Bouwhuijsen QJ, Vernooij MW, Hofman A, Krestin GP, van der Lugt A, Witteman JC (2012) Determinants of magnetic resonance imaging detected carotid plaque components: the Rotterdam study. Eur Heart J 33(2):221–229
19. Van Engelen A, De Bruijne M, Klein S, Verhagen H, Groen H, Wentzel J, Van der Lugt A, Niessen W (2011) Plaque characteriza- tion in ex vivo mri evaluated by dense 3D correspondence with histology. In: SPIE medical imaging, international society for optics and photonics, p 796329
20. WassermanBA(2010)Advancedcontrast-enhancedMRIforlook- ing beyond the lumen to predict stroke: building a risk profile for carotid plaque. Stroke 41:S12–S16

Chapter 6.2

Change of carotid intraplaque hemorrhage in the general population: a 1-year follow up study

Mariana Selwaness
Quirijn van den Bouwhuijsen
Hui Tang
Anouk C van Dijk
Reinhard Hameeteman
Theo van Walsum
Wiro J Niessen
Albert Hofman
Oscar H Franco
Aad van der Lugt
Meike W Vernooij

Chapter 7

General discussion

Introduction

Atherosclerotic plaques located in the carotid arteries are an important cause of cerebrovascular events. Although atherosclerosis usually becomes symptomatic in later life, preclinical atherosclerosis begins in childhood and adolescence and progresses silently. Despite advances in treatment strategies targeting atherosclerosis or carotid atherosclerotic plaques, the incidence of cerebrovascular events remains dramatically high. Available screening and diagnostic methods are limited to symptomatology and degree of stenosis to identify the high-risk individual. Additional parameters are needed to improve risk prediction. Recent advances in the prevention of cerebrovascular events include the recognition of the vulnerable atherosclerotic plaque which can rupture, with subsequent embolisation of thrombus and/or plaque debris in the intracranial circulation. The vulnerable rupture prone plaque is characterized by a thin fibrous cap, presence of a necrotic core or an intraplaque hemorrhage (IPH).(1) In patients-based studies, cumulative evidence has indicated a strong relation of IPH to ischemic stroke and cardiovascular events.(2-6) Furthermore, even in asymptomatic individuals IPH has shown to contribute to plaque progression and destabilization.(7, 8) Although the underlying pathophysiology of IPH is still largely unknown, IPH is believed to follow from rupture or leakage of the plaque neovasculature.(6, 9) Magnetic resonance imaging (MRI) scanning of the carotid arteries is highly feasible to discriminate between the different atherosclerotic plaque components and can accurately detect IPH in atherosclerotic plaques of the carotid artery.(1, 10-12)

This thesis had several objectives. The first objective was to identify biomechanical parameters for carotid atherosclerosis and more specifically for carotid intraplaque hemorrhage. Secondly, we aimed to increase understanding of the role of biomechanical parameters in the pathophysiology of cardiovascular disease. The third objective was to develop automated segmentation methods in order to be able to reliably quantify plaque burden and changes in IPH. Finally, within a large population of asymptomatic individuals, we investigated determinants of increased carotid plaque burden and IPH progression.

In this part of the thesis, I will describe the main findings of our studies and their interpretation. Furthermore, we will discuss some methodological considerations and we will give suggestions for future research.

Review and interpretation of main findings

Hemodynamic parameters determining plaque composition

Hypertension is a highly prevalent condition and a major contributor to atherosclerotic cardiovascular disease. However, the pathophysiology of the contribution of high blood pressure to atherosclerotic plaques is still not fully elucidated. In chapter 2.1 we evaluated the association between various blood pressure parameters and the presence of IPH in carotid atherosclerotic plaques of individuals from the general population. Amongst different blood pressure parameters, the pulsatile component of blood pressure, as indicated by pulse pressure was the strongest determinant of IPH independent of carotid wall thickness and cardiovascular risk factors and independent of the other blood pressure parameters.

Several experimental models support association between cyclic hemodynamic factors and atherosclerosis progression and plaque instability. Pulsatile strain affects the endothelium, vascular smooth muscle cells, the production of elastin, collagen, glycosaminoglycans, and results in increased atherosclerotic plaque volume.(13-16) Rupture of an atherosclerotic plaque may be expected when the stress acting on the vessel wall exceeds its strength. Accordingly one would expect a greater contribution of the systolic blood pressure than pulse pressure causing rupture of the neovessels. However, our findings suggest that the pulsatile mechanical load that acts on the arterial wall, irrespectively of the absolute value of blood pressure, is at least as important in the development of IPH.

IPH is believed to develop from the disruption of thin-walled intraplaque microvessels that are lined by discontinuous endothelium without supporting-muscle cells.(17) An underlying pathophysiological mechanism linking pulse pressure to IPH could include the involvement of arterial stiffness. Large elastic arteries, such as the aorta and the carotid arteries, work predominantly as cushions, but with progressive arterial stiffening, the pulsations are not completely absorbed and may extend to the microcirculation,(18) as was previously shown in the brains(19) and the kidneys.(20) Likewise, enhanced pulsatile flow in the vasa vasorum of the carotid arteries may occur and cause hemorrhage of the neovessels in the plaque.

Furthermore, a possible role for arterial stiffness could be expected as we found that not all subjects with the same level of systolic blood pressure have the same IPH risk. Subjects with lower diastolic blood pressure, and therefore higher pulse pressure, have a higher probability of IPH. In middle-aged and elderly subjects, an increase in pulse pressure with fixed systolic blood pressure occurs solely as a function of declining diastolic blood pressure and is a consequence of a rise in large-artery stiffness.(21) In an additional study, we therefore investigated the relation of arterial stiffness to IPH using a direct measurement of arterial stiffness, namely pulse wave velocity.

In chapter 2.2, we investigated the association between arterial stiffness, as assessed by pulse wave velocity, and the presence and various components of the carotid atherosclerot-

ic plaque. The findings of this study provide evidence that arterial stiffness is associated with presence and composition of carotid atherosclerotic plaques in the general population. By measuring arterial pulse wave velocity, we found that arterial stiffness was independently associated with presence of plaques in the carotid arteries. Furthermore, among individuals with a plaque in the carotid arteries, arterial stiffness was an important determinant of IPH, independent of plaque size, pulse pressure, and other cardiovascular risk factors.

Stiffening of the arterial tree may lead to early pulse wave reflection, and as consequence an increase in central systolic blood pressure, a decrease in diastolic blood pressure, and an increase in pulse pressure.(22) Hence, the pulse wave velocity reflects the cumulative damage on the arterial wall. Although we also found that pulse wave velocity is associated with IPH independent of pulse pressure, we should note that there is a complex relation between pulse pressure and arterial stiffness. There is some evidence (23) that this relationship may be bidirectional and may be amplified by atherosclerosis: on one hand, the presence of atherosclerotic changes may impair the elastic properties of the wall, whereas on the other hand, a reduced large artery compliance enhances wave reflection and augmentation of the pulsatile component of blood pressure, leading to the progression of atherosclerotic changes. Therefore, pulse pressure can be considered both a cause and consequence of arterial stiffness.(24) Shared underlying pathological mechanisms however, may also be a possible risk factor for the associations we found between pulse pressure and arterial stiffness with intraplaque hemorrhage. Further investigations on hemodynamic risk factors provide further clues for understanding the development of vulnerable atherosclerotic plaque

Asymmetry in carotid atherosclerotic plaque prevalence and composition in the left and right carotid artery

Although atherosclerosis is considered a systemic disease, its distribution across the vascular system is not uniform. Hemodynamic and geometrical factors are likely to influence the atherosclerotic plaque severity.(25, 26) Not only plaque severity, but also plaque composition may vary according to location.(27) Some plaque components, such as intraplaque hemorrhage (IPH), are presumed to enhance vulnerability of the plaque, whilst for example calcification may promote plaque stability.(28) Asymmetry in plaque characteristics between the left and right carotid artery has been poorly investigated, in particular with respect to vulnerable plaque components. In Chapter 3, the prevalence, severity and composition of atherosclerotic carotid plaque and investigated whether these characteristics differed between the left and right carotid artery.

Our findings demonstrated that plaque prevalence, severity and composition are not equally distributed among the left and right carotid arteries. Although most individuals had bilateral carotid disease, unilateral plaque were usually located on the left, and left-sided plaques were also thicker than the contralateral side. Whereas IPH and lipid were mostly

observed in left-sided plaques, these plaques were predominantly composed of IPH and fibrous tissue. These findings suggest that atherosclerotic plaques on the left are more vulnerable than on the right. In contrast, right-sided plaques were predominantly composed of calcification, which is considered more stable and therefore less likely to result in thromboembolic complications.

Differences in plaque thickness and composition between the left and right carotid arteries might be explained by hemodynamic or geometrical factors such as wall shear stress, bifurcation angle, or because of the direct connection of the left carotid artery to the aortic arch, leading to increased exposure in arterial pressures.(25, 29) These local factors received less attention in the past. However, we believe that understanding their contributions may explain the variation between left and right carotid atherosclerosis. Also, due to these side differences, it is recommended that future studies do not focus on one carotid artery only.

In patient-based series, a significantly higher proportion of ischemic events is diagnosed in the left hemisphere than in the right.(30-32) It has been hypothesized that infarctions in the left hemisphere are more likely to be recognized, because most people have a dominant left hemisphere for language processing, while infarctions in the right hemisphere may be accompanied by a more easily overlooked cognitive deficit or apraxia.(31-33) Yet, an alternative hypothesis for the higher incidence of events in the left hemisphere may be related to a higher prevalence, severity or vulnerability of atherosclerotic disease in the left carotid artery. We now propose an alternative explanation, namely that it is partially related to the more vulnerable phenotype of left-sided carotid atherosclerotic plaques as opposed to the more calcified, and therefore stable, right-sided plaques. However, for the current study, we did not have data available to determine whether left-sided atherosclerotic plaques are indeed associated with a higher risk of stroke. Prospective population-based studies are needed to investigate a potential temporal relationship between carotid plaque compositions and symptomatic and silent brain infarctions on MRI.

Carotid atherosclerosis in relation to past coronary heart disease and stroke

The systemic nature of atherosclerosis suggests that changes in one vessel bed may reflect alterations in another vessel bed, with subsequent risk of events. The carotid artery is highly accessible for imaging, because of its superficial location, the large size and relative immobility. Imaging of the carotid arteries could therefore provide information on generalized vascular health. Numerous studies already consider carotid intima media thickness as a measure of general atherosclerosis.(34, 35) In another study, carotid irregularity of plaque-surface was found to be associated with ischemic diseases in different vascular beds.(36) The authors postulated that systemic risk factors might lead to a systemic vulnerabilty to rupture of atherosclerotic plaques. Such a predisposition to plaque instability attributable

to systemic risk factors would suggest that plaque composition and instability in the carotid arteries are a marker of plaque instability in other vessel beds. Therefore, it is useful to examine the association between non-invasive measures of atherosclerosis in various vascular beds with both coronary heart disease and cerebrovascular disease.(37)

We examined the association between carotid atherosclerotic plaque characteristics, including vulnerable components, and history of ischemic stroke and coronary heart disease. In Chapter 4, we found different atherosclerotic plaque characteristics related to coronary heart disease as compared to stroke. Whereas plaque thickness and stenosis were associated with a history of coronary heart disease and stroke, IPH was associated with history of stroke only. These associations were primarily present in men and less so in women. Pathways underlying cardiovascular events in different locations could be triggered by different plaque characteristics, and these might differ by sex.

The relation between carotid intima-media thickness as measured with B-mode ultrasound and cardiovascular disease has been well established and IMT serves as a marker of generalized atherosclerosis.(34, 35, 38) Most imaging studies used ultrasound measurements, because these measurements are relatively simple and noninvasive, but the resolution is of limited value for characterization of plaque composition.(39) By using MR imaging, we found that carotid wall thickness and stenosis are more associated with a history of CHD than any of the vulnerable carotid plaque components.

Our findings did not support the hypothesis that presence of IPH observed in one vessel bed might reflect a systemic susceptibility for vulnerable plaques in other vessel beds.(40, 41). Some previous studies suggested a relation between carotid IPH and CHD,(42-44). A possible explanation is that some of the previous studies used carotid tissue specimens derived after carotid endarterectomy or autopsy, in which it is difficult to distinguish between intraplaque hemorrhage and intraluminal thrombi after the tissue preparation. In addition, in some studies a composite endpoint of cerebral and cardiovascular disease was used or stratification for sex was not performed. (40, 41) This may have resulted in a dilution of the association between IPH with stroke and an overestimation of the association with coronary heart disease.

We focused on the independent risks of stroke and coronary heart disease separately instead of restricting the study to one end organ or using composite end points. For this extent, we used prevalent cardiovascular events in which symptoms of ischemia or treatment of the disease were clinically confirmed. Although we expect plaque characteristics to determine the outcome, the cross-sectional design of the study does not allow conclusions regarding the temporal relation between carotid plaque characteristics and clinical event. The main limitation of this study is that we used prevalent cardiovascular events as surrogate end point in order to explore the relation between carotid plaque composition and clinical event. As a consequence, fatal events, in which advanced atherosclerosis is ex-

pected, were not considered in the present study. This may have led to an underestimation of the association between vulnerable plaque characteristics and clinical events. Therefore, prospective studies that investigate the relation between carotid plaque characteristics and incident coronary heart disease and incident stroke in the general population are required.

Plaque burden and lumen volume: quantification and possible risk factors

Direct non-invasive measurements of the burden and composition of preclinical atherosclerosis have been proposed as a way to improve cardiovascular disease prevention and management. It has been suggested that plaque burden may provide more information on the extent of atherosclerosis beyond luminal stenosis.(45, 46) In Chapter 5.1, we describe a novel method for volumetric assessment of carotid plaque burden and lumen volumes. The method combines lumen and outer wall segmentation based on deformable model fitting with a learning-based segmentation correction step. The method was first trained on a set of 16 manually segmented inner and outer walls. We found that the automatic method performs comparably to the manual annotations in terms of wall volume and normalized wall index measurements and can therefore be used to replace the manual measurements. (47)

Using this automated method, we evaluated age and sex distributions of plaque burden and lumen volume in the general population and investigated relations of cardiovascular risk factors. Chapter 5.2 describes the sex-related differences in plaque burden and lumen volumes. We found that women have a larger plaque burden and smaller lumen volume than men. Also in women, age, HDL-levels and systolic blood pressure were independently associated with plaque burden and lumen volume. In men, cholesterol levels and statin use were significantly associated with plaque burden and lumen volume, whilst smoking and DM related only to lumen volume. Hence, the control of modifiable risk factors can prove beneficial in lowering plaque burden. Prospective longitudinal studies should investigate whether these cardiovascular risk factors are also associated with plaque progression.

Amongst three plaque components, intraplaque hemorrhage was found to be an additional risk factor for plaque burden. Furthermore, within the highest quartile of plaque burden, IPH was strongly associated with stenosis independent of age, sex, plaque burden and composition. Although it was suggested that the increased cardiovascular risk of IPH is due to plaque destabilization with thromboembolic complications,(48, 49) we now show that IPH also strongly affects lumen narrowing independent of plaque size. This finding is supported by Takaya et al. who found that lesions with intraplaque hemorrhage (IPH) at baseline had a greater increase in wall volume and reduction in lumen volume compared with arteries without IPH.(9)

Plaque burden reflects the effect of expansive remodeling, and takes into account the influence of mechanical flow and metabolic response of the vessel wall.(46) Glagov et al. proposed that luminal narrowing occurred after plaque burden exceeded the ability of the artery to outwardly remodel.(50) Previous studies using different imaging modalities like ultrasound or CT have demonstrated the potential to use plaque burden measurements as a direct measure of the extent and severity of atherosclerotic disease.(51). Plaque measurements in these studies have varied between estimation of the intima medial thickness and luminal stenosis on ultrasound to measurement of calcified plaque burden on CT.(45, 52, 53) Nevertheless, studies investigating the association of cardiovascular risk factors in relation to plaque burden measurements using MRI remain scarce, mainly because of the limited tissue contrast between the outer vessel wall and the surrounding soft tissues, hence limiting the accuracy of outer wall contouring. Although still challenging, success in this field of research may have an enormous impact on the diagnosis and management of cardiovascular disease.

Change in intraplaque hemorrhage over time

Manual quantification of IPH volume is a laborious procedure and may easily result in segmentation errors when measuring inter- and intra-observer variability. Therefore, there is a large interest in automated procedures for plaque assessment. In Chapter 6.1 we presented a semi-automatic IPH segmentation and quantification method that does neither require manual annotation of the inner or outer vessel wall nor preprocessing to correct for intensity inhomogeneity's. The method segments the IPH using a piecewise smooth regional level set initialized by a set of manually clicked seed points. The inter-scan reproducibility experiments showed that the segmented volumes of the semi-automatic method have a much higher reproducibility than those of the observers. In this study we demonstrated that the manual annotation of IPH is subject to large observer variability. Therefore the semi-automatic results can at best also have a moderate agreement with the manual reference standard. However, the robustness and inter-scan reproducibility of the semi-automatic method is better than the manual observations.

In Chapter 6.2 we aimed to evaluate the visual and quantitative change of IPH after one year follow up in asymptomatic subjects and to identify risk factors of IPH growth. In a nested-case-control study, we used automated segmentation to assess IPH volumes as detected on MRI. Serial imaging of IPH after one year follow up revealed in the majority of cases (96%) persistence of high signal on T1w-sequence. This finding is consistent with a previous study conducted in symptomatic individuals and 18 months follow up. In all individuals, IPH at baseline was found to be present at follow up. In the present study, we also assessed IPH change both qualitatively and quantitatively. Using visual assessment of IPH, we found

that the largest proportion of haemorrhages exhibited no visual change in size. However, we also report the novel finding that IPH may also regress or disappear. Pathophysiological pathways that may explain the course of IPH need to be investigated. Knowledge about development of IPH is predominantly derived from histologic studies. One study suggested repetitive rupture of the fragile neovasculature or continuous leakage of the microvessels.(9) It was also postulated that intraluminal blood invades the plaque through fibrous cap rupture.(49) A possible explanation for the persistence in high signal on MRI may be related with insufficient clearage of the hemorrhage. Serial MRI of the carotid arteries might allow for early identification of patients with IPH who are at highest risk of accelerated plaque growth.

Methodological considerations

The methodological considerations relevant to the above described studies have been discussed in the individual chapters. In this paragraph a more detailed discussion is presented on the study population, study design, the MRI scanning protocol and the automated segmentation tools.

The Study Population

A population-based approach

The term cohort refers to a group of individuals who share a common feature upon inclusion and who are followed in time. The described studies were conducted in the context of the Rotterdam Study, an ongoing prospective population based cohort study investigating chronic diseases in the elderly.(54) Within this population-based cohort, we identified a group of individuals who would be feasible to follow for carotid MRI scanning. First, all Rotterdam Study participants underwent carotid ultrasound. Participants who had carotid plaque thickness ≥2.5 mm were invited for MRI. The carotid ultrasound measurement is comparable with a prescreening test for preclinical carotid atherosclerosis. In most studies we also excluded individuals with a history of stroke. The benefits of this study design are that we started off with an unselected population, so it could resemble and be generalizable to the general population. Selection based on pre-MRI ultrasound ensured that only participants with plaque underwent MRI, to keep time and costs feasible.

Asymptomatic versus clinical population

The majority of previous studies on carotid atherosclerosis in vivo were either conducted in symptomatic or asymptomatic individuals. Both approaches can provide meaningful and accurate data, but distinct restrictions can be encountered or advantages gained from each method. Although the symptomatic subjects are those most at risk, the disadvantage is that the outcome has little impact on the disease burden in society, because a considerable number of cases of disease occur in people at low or moderate risk. Atherosclerosis develops over decades and has a prolonged asymptomatic phase, during which it is possible to modify the course of disease.(55) Therefore, investigating subclinical atherosclerosis in apparently healthy individuals is in part important to tackle the condition in its early stages when interventions may be more effective. Therefore, within most studies described in this thesis, we focused on identifying risk factors of subclinical atherosclerosis, in particular of the vulnerable plaque, in a stroke-free population. There are only a few other population-studies that used MR imaging to investigate carotid plaque composition.(56-58) Amongst those, the Atherosclerosis Risk in Communities (ARIC) study has the largest cohort of asymptomatic subjects, of who 60% were selected based on carotid wall thickening on ultrasound.(56) The study included 2066 participants of 65 years and older who underwent carotid plaque characterization using a 1.5T MRI scanner. In another study, a total of 946 participants of 45 years and older were evaluated in the Multi-Ethnic Study of Atherosclerosis (MESA) using MR imaging.(57) In this study, participants were randomly selected from the top 15th percentile of carotid maximum intima-media thickness of 6814 cardiovascular asymptomatic study participants. Recently, the Progression and Early detection of Subclinical Atherosclerosis (PESA) study was initiated, in which ^{18}FDG PET/MRI of the carotid arteries will be performed in order to characterize plaque composition and progression.(58) This Spanish prospective longitudinal cohort targets 4000 healthy participants between 40-54 years. Longitudinal population-studies may increase knowledge about carotid atherosclerotic plaque progression and may help to establish a more personalized management of medical care.

MR eligibility based on presence of advanced subclinical atherosclerosis

We restricted definition of carotid atherosclerosis to an intima–media thickness of ≥2.5 mm. Carotid intimal thickening represents one of the earliest manifestations of subclinical atherosclerosis. It has been suggested that with lower degrees of intima–media thickness an adaptive response to local hemodynamic changes may be reflected rather than atherosclerotic thickening, which is represented beyond a certain level.(59) According to the Cardiovascular Health Study, 0.9 mm was considered as the threshold for the association with an increased risk of myocardial infarction and stroke in participants aged >65 years.(60) Our definition of plaque (intima– media thickness ≥2.5 mm) might thus be regarded as a more advanced manifestation of atherosclerosis. Within the Rotterdam Study, we found approximately 40% of the subjects to meet this criterion.

Cross-sectional study design

The studies included in this thesis were all conducted within The Rotterdam Study, a prospective population-based cohort study. In a cohort study, a population is observed in time for the incidence of diseases. However, the studies described in this thesis were all cross-sectional in design. A cross-sectional study collects all data at the same point in time, uses a single measurement of exposure and outcome variable and does not take into account the effect of time.

In the studies on pulse pressure and pulse wave velocity and the association with atherosclerotic plaque components (chapter 2.1 and 2.2), the cross-sectional design restricted our interpretation of the data with respect to cause and consequence. Although it is theoretically possible that plaque composition, or more in general presence of atherosclerosis, leads to changes in hemodynamic factors such as pulse pressure and pulse wave velocity, a causal link is more likely to be in the opposite direction. For the study on differences in plaque composition between the left and right carotid artery (chapter 3), the cross-sectional design is most appropriate to test the hypothesis that left-sided plaques are more common and vulnerable than right-sided plaques. However, the cross-sectional design limited us to draw conclusions whether this asymmetrical distribution partly determines the higher clinical prevalence of left hemispheric stroke. Longitudinal studies are therefore indicated.

In the study on the association between plaque composition and history of stroke and coronary heart disease (chapter 4), the research question is causal and time order is important to be able to make inferences on causality. Although this study intended to explore whether risk differences exist for ischemic diseases in the brain and the heart, the strong positive findings suggest that plaque composition may be an important feature for risk stratification. Our final goal is examining the predictive value of carotid plaque composition for the risk of stroke and coronary heart disease, which should be examined in a prospective cohort study design.

Magnetic resonance imaging acquisition protocol

In this thesis, we used a standardized multisequence MR imaging protocol, which was previously validated in histologic studies with tissue specimens from endarterectomy patients. (39) The signal intensities on the different MR sequences reflect a different biochemical environment of protons hereby assisting in the differentiation of plaque components. We focused on recognizing the intraplaque hemorrhage, lipid core and calcification, which can be identified on the base of their signal intensity on the T1-weighted, T2-weigthed, and phase-contrast sequences, respectively. For the purpose of plaque characterization and wall segmentation, MRI can provide excellent contrast between the vessel wall and adjacent lumen, and, at the same time, produce tissue information that describes the vessel

wall.(10, 61) These advantages would be beneficial when identifying the unstable lesion and can be used in serial imaging studies that investigate factors related with the change of the plaque.

Detection of lipid, with or without a necrotic core, is an important aspect of the MRI data acquisition. The majority of atherosclerotic plaques consist of lipid or fibrous tissue. Cholesterol and cholesteryl esters, which have a short T2, form the essence of the lipid deposits.(62) Previous studies that investigated plaque specimens ex vivo showed that T2-weighted sequences improved the identification of lipid and allowed differentiation of lipid from fibrous tissue.(1, 63) It is important to note that, in vivo, multiple sequences with different contrast weightings are required to characterize these atherosclerotic plaque components accurately. The most reliable approach to detect lipid tissue is the comparison of T1w-sequence after contrast media injection to the T1w-sequence before injection. The non-enhancing parts of the plaque correspond to lipid tissue.(64) In our studies, we were limited to incorporate contrast-enhanced sequences in our study protocol because we were investigating healthy subjects. Such a protocol should also be applied in a medical setting because of the invasiveness and possible adverse reactions to contrast agents. Therefore, the prevalence of lipid may be underestimated which is indicated by the higher prevalence of lipid in another population study.(57)

Although MRI is currently regarded as the most reliable method for in vivo assessment of plaque composition, small plaques (<2.0 mm) could not be characterized due to constraints in spatial resolution of MRI. Most imaging of the carotid wall is performed using a 1.5-Tesla MRI protocol with an in-plane spatial resolution of approximately 0.5×0.5 mm^2, which is too large to be able to accurately visualize different plaque components in early atherosclerosis.(65) Although it is possible to increase the resolution to smaller voxel sizes, however, this will be compensated by a relatively long acquisition time.(66)

Automated segmentation

To increase knowledge about the carotid atherosclerotic plaque and its different plaque components and to detect novel risk factors for plaque burden and composition, more large, multicenter population-based studies or clinical trials are needed. As current MR imaging provide excellent means already to characterize plaque morphology,(10-12, 61, 67) it is time to move the field forward by implementing quantitative assessment and improving reproducibility of segmentation techniques. Automated methods facilitate inner wall and outer wall segmentation on axial MR images of the carotid artery and hereby provide a means of measuring the total volume of the artery segment.(68) Unlike luminal stenosis, plaque volume might be used as a direct measure of the size and severity of atherosclerotic disease.(69-71) With the excellent contrast produced between the lumen and vessel wall, we aimed to automatically segment the inner wall boundaries of the carotid artery.

Automated segmentation of the outer wall is more difficult, because of the lower contrast with surrounding tissue. Evaluating the artery both in axial slices and on the longitudinal reformats may improve the detection of the borders of the vessel wall and enable a better continuation of the transversal contours in the consecutive slices.

In the present thesis we evaluated the use of non-invasive MRI-based automated segmentation using a population-based approach. In Chapter 5.1, we introduce a custom-designed tool to determine plaque burden and lumen volume automatically and evaluated the performance by comparing the cross-sectional areas of the carotid plaques segmented manually with the automatically measured areas. In Chapter 6.1 we introduce a semiautomated segmentation method for the quantification of the IPH volumes. For both methods, we found the automated method to perform comparably to the manual annotations. However, it is important to note that segmentations in general cannot get better than the quality of the manual segmentations as automatic method is trained by the manual segmentations which are considered the "golden standard". In this thesis, either two experienced observers manually segmented the regions of interest twice or a consensus data set was used as the golden standard. Differences during manual segmentation are a consequence of the variety in window level settings. The window level settings determine the size of the image contrast between the wall of the artery or component and the adjacent tissue. In contrast to visual assessment, automated methods use a statistical algorithm to overcome this issue and are therefore much better in a way that they will always produce the same output and are more robust or reproducible.

The next step is to perform serial imaging in order to assess changes in plaque burden and composition. In this context, an important aspect that needs to be mentioned is the variations in image quality which are caused by patient reposition, movements during scanning, position of the coils and heart rate from one scan to another. However, concerns about measurements error to be larger than progression rate with repeated MRI scans impedes monitoring of the disease and evaluation of intervention strategies. This issue can be overcome by optimizing acquisition protocols, automated segmentation tools but most of all, by improving registration of repeated MRI scans. With current advances in atherosclerosis risk management, it will be important to have methods to study effects of new therapies on atherosclerosis as proof-of-principle, before going on to very large and costly studies on the basis of reduction of events.

Clinical implications and directions for future research

Intraplaque hemorrhage; most promising imaging marker for screening

One of the goals in atherosclerosis research is to identify the high-risk subject before the vascular events. For this purpose, future research should test the hypothesis that assessment of the vulnerable plaque, as opposed to simple stenosis measurements with carotid ultrasound, can better guide individual selection of optimal treatment strategies. Hereby, carotid MRI scanning could serve as an excellent non-invasive imaging technique, as it is highly feasible to discriminate plaque composition and detect IPH. In an unselected population, IPH has shown to be a promising marker for screening purposes. Not only because its strong association with cerebrovascular event risk, but IPH can also be easily distinguished from the surrounding tissue and other plaque components on MRI. However, it is unclear how IPH develops and what the best time would be to perform imaging of the artery. Furthermore, for a screening test to be useful, it should have a very high sensitivity (ability to correctly identify people who have the disease) and specificity (ability to correctly identify people who do not have the disease). Currently, more research needs to be conducted in order to increase understanding about the progression rate of IPH and to assess the sensitivity of IPH for detection of high-risk individuals.

We propose the need of additional clinical trials randomizing patients with IPH to standard and aggressive medical therapy. Initial trials may use a regression of IPH or a decrease in size of IPH as a surrogate marker for improved atherosclerotic treatment, although larger multicenter trials with sufficient patients to test for a statistically significant improvement in hard clinical end points, such as stroke and TIA, will be needed to fully test the hypothesis. In this context, MR imaging of IPH could play an important role as a surrogate endpoint and could serve as a measure of disease severity and clinical risk. In general, noninvasive characterization of plaque morphology may be used to provide surrogate endpoints for therapeutic trials. For instance, MR imaging of atherosclerosis may provide information on the responses of atherosclerosis to cholesterol-lowering treatments or other treatments that may have a stabilizing effects on the atherosclerotic plaque.

MR imaging techniques are currently able to provide morphologic information that can suggest whether a lesion is unstable, regardless of the degree of stenosis. Future applications of these imaging techniques could use the information from plaque characterization and the measurement of plaque burden to assist clinicians in the selection of an optimal treatment method for each patient, based on the vulnerability of the atherosclerotic plaque. Furthermore, imaging of IPH may better stratify risk and identify patients with mild-to-moderate carotid artery stenosis, who are at an increased risk of ipsilateral stroke and who would benefit from surgical intervention, namely carotid endarterectomy or carotid arterial stenting, but are currently not being treated as such.

Insight into carotid plaque etiology: Is there a role for local biomechanical factors?

Another important focus of atherosclerosis research is the etiologic aspects of the disease. In order to expand knowledge about development of different plaque components and to detect novel risk factors for plaque composition, population-based studies are helpful. Although atherosclerosis is viewed as a systemic process, the severity and composition of atherosclerotic plaques varies from one arterial bed to another. This variation is likely to be the result of local risk factors, such as the geometrical or hemodynamic factors as well as their interactions. A key link for the asymmetry in plaque composition between the left and right carotid artery may be provided through the quantification of wall shear stress.

Atherosclerotic plaques are preferentially located at bifurcations or inner curves. In this regions blood flow profiles induce a low wall shear stress.(72) Wall shear stress is the frictional force of the blood at the vessel wall. Stresses inside the vessel wall which are related to the blood pressure are called the wall stress. Wall shear stress and wall stress are known to influence many atherogenic processes, including cell proliferation, inflammation, thrombosis and plaque growth. They also influence the plaque composition and hereby also the plaque vulnerability.(72-74)

As a first next step to investigate these biomechanical parameters, in an ongoing study we aim to calculate the local patient-specific wall shear stress and wall stress in the carotid artery. As the 3D geometry of the lumen and wall are essential for this, we use the method described in Chapter 5.1 of this thesis to generate a 3D reconstruction model. Also, information on the composition of the vessel wall and on blood pressure and blood flow are required and has already been collected in previous studies. Using a finite element software package, it is then possible to calculate the wall shear stress and wall stress and relate that with the location and morphology of the plaque. Understanding the pathways on which this complex hemodynamic setting will translate to a biologic response would provide more insight in the development of atherosclerosis.

Next step; Serial imaging in population studies

Atherosclerosis is a slowly progressing disease. The pathophysiological mechanisms that underlie the evolvement of subclinical atherosclerotic plaques into rupture-prone lesions have not been unraveled yet. In this thesis, several risk factors were identified and associated with IPH and plaque burden in a cross-sectional study design. Yet, the predictive value was not assessed in a prospective, longitudinal study. Longitudinal assessment of risk factors for cerebrovascular disease is necessary to provide evidence that a putative risk factor or risk indicator is a true risk factor.

The next step forward would be the evaluation of the natural course of carotid atherosclerotic plaques and identification of determinants of plaque progression. We made the first steps by validating and developing post-processing tools to measure plaque volume and volume of plaque components, in particular intraplaque hemorrhage, on MRI. Currently, we consider the volume measurements sufficiently reliably for cross-sectional measurements, although we need to examine whether these measurements are accurate enough to assess changes in atherosclerotic plaque characteristics on serial images. In ongoing research, we performed repetitive MRI examination of 100 healthy participants with atherosclerotic disease after four years follow up. Using the previously described plaque segmentation tools, we will study whether follow up time is sufficient to enable us to detect plaque change. Our segmentation method has shown to be a promising and time preserving method, because manual interaction is reduced to the minimum, and because inner and outer vessel wall annotation is not required.

Another important implication of serial imaging is to monitor progression of atherosclerosis in order to adapt treatment. In clinical practice, monitoring atherosclerosis is done by monitoring stenosis, which is not equal to monitoring overall growth of plaques.(75) Therefore, in order to recognize pathologic growth of atherosclerosis, it is important to first increase the knowledge about plaque volumes as how they progress during normal aging. Only then can pathologic changes be distinguished from normal.

Conclusions

The ultimate goal of carotid vulnerable plaque research is to increase knowledge about the development of vulnerable plaques in the carotid arteries and to identify healthy patients at high-risk for cardiovascular complications. Carotid plaque MR imaging may play a large role in individual patient selection and decision making for optimal atherosclerotic treatment strategies. This thesis provides more insight into risk factors of vulnerable plaque characteristics, in particular intraplaque hemorrhage, and represents one step forward towards a more complete understanding of the complex interplay between carotid wall properties and hemodynamic forces of carotid atherosclerosis. Summarizing, the main conclusions of this thesis with respect to imaging of carotid atherosclerosis are as follows.

Among the different plaque components investigated in carotid plaque composition, IPH is the most premising parameter to play a role in preventive strategies for cerebrovascular events. We identified novel risk factors for IPH, such as increased blood pressure, pulse pressure and pulse wave velocity. Also, we found that asymmetry in plaque composition exists between the left and right carotid artery and we found measurements of carotid plaque characteristics to be differentially related to ischemic stroke and CHD. Finally, we introduced user-friendly, non-invasive MRI-based automated segmentation methods to quantify plaque burden and IPH volume.

As the understanding of the pathophysiology of cardiovascular disease has undergone a remarkable revolution, new parameters for risk prediction are anticipated. Biomechanical parameters are new promising parameters that potentially can play a role in risk stratification as we have shown that they are associated with IPH and others have demonstrated that they are crucial for plaque development, plaque rupture and embolism. The emergence of quantitative segmentation tools allow computation of these parameters. Knowledge of the role of local biomechanical parameters in plaque development and stroke risk may support future improvements in risk prediction and will also enhance understanding of the role of biomechanical parameters in the pathophysiology of cardiovascular disease and its results may facilitate further study of the mechanisms of vulnerable plaque development and rupture.

References

1. Toussaint JF, LaMuraglia GM, Southern JF, Fuster V, Kantor HL. Magnetic resonance images lipid, fibrous, calcified, hemorrhagic, and thrombotic components of human atherosclerosis in vivo. Circulation. 1996;94(5):932-8.
2. Altaf N, Daniels L, Morgan PS, Auer D, MacSweeney ST, Moody AR, et al. Detection of intraplaque hemorrhage by magnetic resonance imaging in symptomatic patients with mild to moderate carotid stenosis predicts recurrent neurological events. J Vasc Surg. 2008;47(2):337-42.
3. Altaf N, MacSweeney ST, Gladman J, Auer DP. Carotid intraplaque hemorrhage predicts recurrent symptoms in patients with high-grade carotid stenosis. Stroke. 2007;38(5):1633-5.
4. Gao P, Chen ZQ, Bao YH, Jiao LQ, Ling F. Correlation between carotid intraplaque hemorrhage and clinical symptoms: systematic review of observational studies. Stroke. 2007;38(8):2382-90.
5. Singh N, Moody AR, Gladstone DJ, Leung G, Ravikumar R, Zhan J, et al. Moderate carotid artery stenosis: MR imaging-depicted intraplaque hemorrhage predicts risk of cerebrovascular ischemic events in asymptomatic men. Radiology. 2009;252(2):502-8.
6. Teng Z, He J, Degnan AJ, Chen S, Sadat U, Bahaei NS, et al. Critical mechanical conditions around neovessels in carotid atherosclerotic plaque may promote intraplaque hemorrhage. Atherosclerosis. 2012;223(2):321-6.
7. Saam T, Hetterich H, Hoffmann V, Yuan C, Dichgans M, Poppert H, et al. Meta-analysis and systematic review of the predictive value of carotid plaque hemorrhage on cerebrovascular events by magnetic resonance imaging. J Am Coll Cardiol. 2013;62(12):1081-91.
8. Takaya N, Yuan C, Chu B, Saam T, Underhill H, Cai J, et al. Association between carotid plaque characteristics and subsequent ischemic cerebrovascular events: a prospective assessment with MRI--initial results. Stroke. 2006;37(3):818-23.
9. Takaya N, Yuan C, Chu B, Saam T, Polissar NL, Jarvik GP, et al. Presence of intraplaque hemorrhage stimulates progression of carotid atherosclerotic plaques: a high-resolution magnetic resonance imaging study. Circulation. 2005;111(21):2768-75.
10. Bitar R, Moody AR, Leung G, Symons S, Crisp S, Butany J, et al. In vivo 3D high-spatial-resolution MR imaging of intraplaque hemorrhage. Radiology. 2008;249(1):259-67.
11. Cappendijk VC, Cleutjens KB, Kessels AG, Heeneman S, Schurink GW, Welten RJ, et al. Assessment of human atherosclerotic carotid plaque components with multisequence MR imaging: initial experience. Radiology. 2005;234(2):487-92.
12. Moody AR. Magnetic resonance direct thrombus imaging. J Thromb Haemost. 2003;1(7):1403-9.
13. Lee RT, Yamamoto C, Feng Y, Potter-Perigo S, Briggs WH, Landschulz KT, et al. Mechanical strain induces specific changes in the synthesis and organization of proteoglycans by vascular smooth muscle cells. J Biol Chem. 2001;276(17):13847-51.
14. Lehoux S, Esposito B, Merval R, Tedgui A. Differential regulation of vascular focal adhesion kinase by steady stretch and pulsatility. Circulation. 2005;111(5):643-9.
15. Shaw A, Xu Q. Biomechanical stress-induced signaling in smooth muscle cells: an update. Curr Vasc Pharmacol. 2003;1(1):41-58.

16. Wung BS, Cheng JJ, Hsieh HJ, Shyy YJ, Wang DL. Cyclic strain-induced monocyte chemotactic protein-1 gene expression in endothelial cells involves reactive oxygen species activation of activator protein 1. Circ Res. 1997;81(1):1-7.
17. Kolodgie FD, Narula J, Yuan C, Burke AP, Finn AV, Virmani R. Elimination of neoangiogenesis for plaque stabilization: is there a role for local drug therapy? J Am Coll Cardiol. 2007;49(21):2093-101.
18. O'Rourke MF, Hashimoto J. Mechanical factors in arterial aging: a clinical perspective. J Am Coll Cardiol. 2007;50(1):1-13.
19. Hashimoto J, Ito S. Some mechanical aspects of arterial aging: physiological overview based on pulse wave analysis. Ther Adv Cardiovasc Dis. 2009;3(5):367-78.
20. Ishikawa T, Hashimoto J, Morito RH, Hanazawa T, Aikawa T, Hara A, et al. Association of micro-albuminuria with brachial-ankle pulse wave velocity: the Ohasama study. Am J Hypertens. 2008;21(4):413-8.
21. Franklin SS, Khan SA, Wong ND, Larson MG, Levy D. Is pulse pressure useful in predicting risk for coronary heart Disease? The Framingham heart study. Circulation. 1999;100(4):354-60.
22. Mattace-Raso FU, van der Cammen TJ, Hofman A, van Popele NM, Bos ML, Schalekamp MA, et al. Arterial stiffness and risk of coronary heart disease and stroke: the Rotterdam Study. Circulation. 2006;113(5):657-63.
23. Dart AM, Kingwell BA. Pulse pressure--a review of mechanisms and clinical relevance. J Am Coll Cardiol. 2001;37(4):975-84.
24. Kopec G, Podolec P. Central pulse pressure: is it really an independent predictor of cardiovascular risk? Hypertension. 2008;52(1):e4; author reply e5.
25. Phan TG, Beare RJ, Jolley D, Das G, Ren M, Wong K, et al. Carotid artery anatomy and geometry as risk factors for carotid atherosclerotic disease. Stroke. 2012;43(6):1596-601.
26. Odink AE, van der Lugt A, Hofman A, Hunink MG, Breteler MM, Krestin GP, et al. Association between calcification in the coronary arteries, aortic arch and carotid arteries: the Rotterdam study. Atherosclerosis. 2007;193(2):408-13.
27. Herisson F, Heymann MF, Chetiveaux M, Charrier C, Battaglia S, Pilet P, et al. Carotid and femoral atherosclerotic plaques show different morphology. Atherosclerosis. 2011;216(2):348-54.
28. Virmani R, Burke AP, Kolodgie FD, Farb A. Pathology of the thin-cap fibroatheroma: a type of vulnerable plaque. J Interv Cardiol. 2003;16(3):267-72.
29. Schulz UG, Rothwell PM. Major variation in carotid bifurcation anatomy: a possible risk factor for plaque development? Stroke. 2001;32(11):2522-9.
30. Hedna VS, Bodhit AN, Ansari S, Falchook AD, Stead L, Heilman KM, et al. Hemispheric differences in ischemic stroke: is left-hemisphere stroke more common? J Clin Neurol. 2013;9(2):97-102.
31. Naess H, Waje-Andreassen U, Thomassen L, Myhr KM. High incidence of infarction in the left cerebral hemisphere among young adults. J Stroke Cerebrovasc Dis. 2006;15(6):241-4.
32. Foerch C, Misselwitz B, Sitzer M, Berger K, Steinmetz H, Neumann-Haefelin T, et al. Difference in recognition of right and left hemispheric stroke. Lancet. 2005;366(9483):392-3.
33. Fink JN. Underdiagnosis of right-brain stroke. Lancet. 2005;366(9483):349-51.

34. Chambless LE, Heiss G, Folsom AR, Rosamond W, Szklo M, Sharrett AR, et al. Association of coronary heart disease incidence with carotid arterial wall thickness and major risk factors: the Atherosclerosis Risk in Communities (ARIC) Study, 1987-1993. Am J Epidemiol. 1997;146(6):483-94.
35. Lorenz MW, Markus HS, Bots ML, Rosvall M, Sitzer M. Prediction of clinical cardiovascular events with carotid intima-media thickness: a systematic review and meta-analysis. Circulation. 2007;115(4):459-67.
36. Rothwell PM, Villagra R, Gibson R, Donders RC, Warlow CP. Evidence of a chronic systemic cause of instability of atherosclerotic plaques. Lancet. 2000;355(9197):19-24.
37. Elias-Smale SE, Wieberdink RG, Odink AE, Hofman A, Hunink MG, Koudstaal PJ, et al. Burden of atherosclerosis improves the prediction of coronary heart disease but not cerebrovascular events: the Rotterdam Study. Eur Heart J. 2011;32(16):2050-8.
38. Nambi V, Pedroza C, Kao LS. Carotid intima-media thickness and cardiovascular events. Lancet. 2012;379(9831):2028-30.
39. Yuan C, Mitsumori LM, Beach KW, Maravilla KR. Carotid atherosclerotic plaque: noninvasive MR characterization and identification of vulnerable lesions. Radiology. 2001;221(2):285-99.
40. Derksen WJ, Peeters W, Tersteeg C, de Vries JP, de Kleijn DP, Moll FL, et al. Age and coumarin-type anticoagulation are associated with the occurrence of intraplaque hemorrhage, while statins are associated less with intraplaque hemorrhage: A large histopathological study in carotid and femoral plaques. Atherosclerosis. 2010;214(1):139-43.
41. Vink A, Schoneveld AH, Richard W, de Kleijn DP, Falk E, Borst C, et al. Plaque burden, arterial remodeling and plaque vulnerability: determined by systemic factors? J Am Coll Cardiol. 2001;38(3):718-23.
42. Hellings WE, Peeters W, Moll FL, Piers SR, van Setten J, Van der Spek PJ, et al. Composition of carotid atherosclerotic plaque is associated with cardiovascular outcome: a prognostic study. Circulation. 2010;121(17):1941-50.
43. Kodama T, Narula N, Agozzino M, Arbustini E. Pathology of plaque haemorrhage and neovascularization of coronary artery. J Cardiovasc Med (Hagerstown). 2012;13(10):620-7.
44. Vrijenhoek JE, Den Ruijter HM, De Borst GJ, de Kleijn DP, De Vries JP, Bots ML, et al. Sex Is Associated With the Presence of Atherosclerotic Plaque Hemorrhage and Modifies the Relation Between Plaque Hemorrhage and Cardiovascular Outcome. Stroke. 2013;44(12):3318-23.
45. Rozie S, de Weert TT, de Monye C, Homburg PJ, Tanghe HL, Dippel DW, et al. Atherosclerotic plaque volume and composition in symptomatic carotid arteries assessed with multidetector CT angiography; relationship with severity of stenosis and cardiovascular risk factors. European radiology. 2009;19(9):2294-301.
46. de Labriolle A, Mohty D, Pacouret G, Giraudeau B, Fichet J, Fremont B, et al. Comparison of degree of stenosis and plaque volume for the assessment of carotid atherosclerosis using 2-D ultrasound. Ultrasound Med Biol. 2009;35(9):1436-42.
47. Hameeteman K, van 't Klooster R, Selwaness M, van der Lugt A, Witteman JC, Niessen WJ, et al. Carotid wall volume quantification from magnetic resonance images using deformable model fitting and learning-based correction of systematic errors. Physics in medicine and biology. 2013;58(5):1605-23.

48. Virmani R, Kolodgie FD, Burke AP, Finn AV, Gold HK, Tulenko TN, et al. Atherosclerotic plaque progression and vulnerability to rupture: angiogenesis as a source of intraplaque hemorrhage. Arterioscler Thromb Vasc Biol. 2005;25(10):2054-61.
49. Michel JB, Virmani R, Arbustini E, Pasterkamp G. Intraplaque haemorrhages as the trigger of plaque vulnerability. Eur Heart J. 2011.
50. Glagov S, Weisenberg E, Zarins CK, Stankunavicius R, Kolettis GJ. Compensatory enlargement of human atherosclerotic coronary arteries. N Engl J Med. 1987;316(22):1371-5.
51. Yuan C, Beach KW, Smith LH, Jr., Hatsukami TS. Measurement of atherosclerotic carotid plaque size in vivo using high resolution magnetic resonance imaging. Circulation. 1998;98(24):2666-71.
52. Strobl FF, Rominger A, Wolpers S, Rist C, Bamberg F, Thierfelder KM, et al. Impact of cardiovascular risk factors on vessel wall inflammation and calcified plaque burden differs across vascular beds: a PET-CT study. Int J Cardiovasc Imaging. 2013;29(8):1899-908.
53. Virani SS, Catellier DJ, Pompeii LA, Nambi V, Hoogeveen RC, Wasserman BA, et al. Relation of cholesterol and lipoprotein parameters with carotid artery plaque characteristics: the Atherosclerosis Risk in Communities (ARIC) carotid MRI study. Atherosclerosis. 2011;219(2):596-602.
54. Hofman A, Darwish Murad S, van Duijn CM, Franco OH, Goedegebure A, Ikram MA, et al. The Rotterdam Study: 2014 objectives and design update. Eur J Epidemiol. 2013;28(11):889-926.
55. Libby P, Theroux P. Pathophysiology of coronary artery disease. Circulation. 2005;111(25):3481-8.
56. Wasserman BA, Astor BC, Sharrett AR, Swingen C, Catellier D. MRI measurements of carotid plaque in the atherosclerosis risk in communities (ARIC) study: methods, reliability and descriptive statistics. J Magn Reson Imaging. 2010;31(2):406-15.
57. Wasserman BA, Sharrett AR, Lai S, Gomes AS, Cushman M, Folsom AR, et al. Risk factor associations with the presence of a lipid core in carotid plaque of asymptomatic individuals using high-resolution MRI: the multi-ethnic study of atherosclerosis (MESA). Stroke. 2008;39(2):329-35.
58. Fernandez-Ortiz A, Jimenez-Borreguero LJ, Penalvo JL, Ordovas JM, Mocoroa A, Fernandez-Friera L, et al. The Progression and Early detection of Subclinical Atherosclerosis (PESA) study: rationale and design. Am Heart J. 2013;166(6):990-8.
59. Bots ML, Hofman A, Grobbee DE. Increased common carotid intima-media thickness. Adaptive response or a reflection of atherosclerosis? Findings from the Rotterdam Study. Stroke. 1997;28(12):2442-7.
60. O'Leary DH, Polak JF, Kronmal RA, Manolio TA, Burke GL, Wolfson SK, Jr. Carotid-artery intima and media thickness as a risk factor for myocardial infarction and stroke in older adults. Cardiovascular Health Study Collaborative Research Group. N Engl J Med. 1999;340(1):14-22.
61. Corti R, Fuster V. Imaging of atherosclerosis: magnetic resonance imaging. Eur Heart J. 2011;32(14):1709-19.
62. Hatsukami TS, Ross R, Polissar NL, Yuan C. Visualization of fibrous cap thickness and rupture in human atherosclerotic carotid plaque in vivo with high-resolution magnetic resonance imaging. Circulation. 2000;102(9):959-64.
63. Gold GE, Pauly JM, Glover GH, Moretto JC, Macovski A, Herfkens RJ. Characterization of atherosclerosis with a 1.5-T imaging system. J Magn Reson Imaging. 1993;3(2):399-407.

64. Wasserman BA, Smith WI, Trout HH, 3rd, Cannon RO, 3rd, Balaban RS, Arai AE. Carotid artery atherosclerosis: in vivo morphologic characterization with gadolinium-enhanced double-oblique MR imaging initial results. Radiology. 2002;223(2):566-73.
65. Hatsukami TS, Ferguson MS, Beach KW, Gordon D, Detmer P, Burns D, et al. Carotid plaque morphology and clinical events. Stroke. 1997;28(1):95-100.
66. Erlichman M. Surface/specialty coil devices and gating techniques in magnetic resonance imaging. Health technology assessment reports. 1990(3):1-23.
67. Dong L, Kerwin WS, Ferguson MS, Li R, Wang J, Chen H, et al. Cardiovascular magnetic resonance in carotid atherosclerotic disease. J Cardiovasc Magn Reson. 2009;11:53.
68. van 't Klooster R, de Koning PJ, Dehnavi RA, Tamsma JT, de Roos A, Reiber JH, et al. Automatic lumen and outer wall segmentation of the carotid artery using deformable three-dimensional models in MR angiography and vessel wall images. J Magn Reson Imaging. 2012;35(1):156-65.
69. Landry A, Spence JD, Fenster A. Measurement of carotid plaque volume by 3-dimensional ultrasound. Stroke. 2004;35(4):864-9.
70. Wagenknecht L, Wasserman B, Chambless L, Coresh J, Folsom A, Mosley T, et al. Correlates of carotid plaque presence and composition as measured by MRI: the Atherosclerosis Risk in Communities Study. Circ Cardiovasc Imaging. 2009;2(4):314-22.
71. Wannarong T, Parraga G, Buchanan D, Fenster A, House AA, Hackam DG, et al. Progression of carotid plaque volume predicts cardiovascular events. Stroke. 2013;44(7):1859-65.
72. Malek AM, Alper SL, Izumo S. Hemodynamic shear stress and its role in atherosclerosis. JAMA. 1999;282(21):2035-42.
73. Chatzizisis YS, Jonas M, Coskun AU, Beigel R, Stone BV, Maynard C, et al. Prediction of the localization of high-risk coronary atherosclerotic plaques on the basis of low endothelial shear stress: an intravascular ultrasound and histopathology natural history study. Circulation. 2008;117(8):993-1002.
74. Lee RT, Schoen FJ, Loree HM, Lark MW, Libby P. Circumferential stress and matrix metalloproteinase 1 in human coronary atherosclerosis. Implications for plaque rupture. Arterioscler Thromb Vasc Biol. 1996;16(8):1070-3.
75. Xu D, Hippe DS, Underhill HR, Oikawa-Wakayama M, Dong L, Yamada K, et al. Prediction of High-Risk Plaque Development and Plaque Progression With the Carotid Atherosclerosis Score. JACC Cardiovasc Imaging. 2014.

Summary
Samenvatting

Summary

Chapter 1 introduces the background and the aim of the thesis. Atherosclerotic plaques located in the carotid arteries are the main cause of stroke. Current treatment strategies that target atherosclerosis are insufficient to early identify the individual who is at risk of stroke and the incidence of cerebrovascular events remains dramatically high. Recent advances in the prevention of stroke include discrimination of different plaque components and the recognition of the vulnerable atherosclerotic plaque, which could consist of an intraplaque haemorrhage. Intraplaque hemorrhage is assumed to be caused by rupture or leakage of plaque neovasculature, and, stimulates the progression and destabilization of the plaque. Magnetic resonance imaging (MRI) is able to discriminate between the different atherosclerotic plaque components and it can accurately detect intraplaque hemorrhage in atherosclerotic plaques of the carotid artery. Knowledge about factors that influence carotid atherosclerotic plaque composition may eventually contribute to stroke prevention. Therefore, the first objective was to identify biomechanical parameters for carotid atherosclerosis and more specifically for carotid intraplaque hemorrhage. Secondly, we aimed to increase understanding of the role of biomechanical parameters in the pathophysiology of cardiovascular disease. Thirdly, we aimed to develop automated segmentation methods in order to reliably quantify plaque burden and volume change of IPH. In order to do this, we scanned the carotid arteries on both sides in almost 2000 individuals from the Rotterdam Study; an ongoing prospective population-based cohort study.

Hypertension is a highly prevalent condition and a major contributor to atherosclerotic cardiovascular disease. In **Chapter 2.1** we investigated different blood pressure parameters more deeply and evaluated their relation to presence of carotid IPH. We showed that the pulsatile component of blood pressure, as indicated by pulse pressure, was the strongest determinant of IPH. Previous experimental studies support the association between cyclic hemodynamic factors and atherosclerosis progression and plaque instability. Pulsatile strain affects the endothelium, vascular smooth muscle cells, the production of elastin, collagen, glycosaminoglycans, and results in increased atherosclerotic plaque volume. Rupture of an atherosclerotic plaque may be expected when the stress acting on the vessel wall exceeds its strength. Accordingly one would expect a greater contribution of the systolic blood pressure than pulse pressure causing rupture of the neovessels. However, our findings suggest that the pulsatile mechanical load that acts on the arterial wall, irrespectively of the absolute value of blood pressure, is at least as important in the development of IPH.

An underlying pathophysiological mechanism linking pulse pressure to IPH could include the involvement of arterial stiffness. In an additional study (**Chapter 2.2**), we therefore investigated the relation of arterial stiffness to presence of atherosclerotic plaques and to IPH using a direct measurement of arterial stiffness, namely pulse wave velocity. In this study, we showed that arterial stiffness is associated with presence and composition of carotid atherosclerotic plaques in the general population. Furthermore, among individuals with a

plaque in the carotid arteries, arterial stiffness was an important determinant of IPH. Stiffening of the arterial tree may lead to early pulse wave reflection, and as consequence an increase in central systolic blood pressure, a decrease in diastolic blood pressure, and an increase in pulse pressure. Hence, the pulse wave velocity reflects the cumulative damage on the arterial wall. Although we also found that pulse wave velocity is associated with IPH independent of pulse pressure, we should note that there is a complex relation between pulse pressure and arterial stiffness and pulse pressure may be considered both a cause and consequence of arterial stiffness.

Ischemic strokes are more often diagnosed in the left hemisphere than in the right, therefore we hypothesized that asymmetry in carotid atherosclerosis may play a role in this observation. In **Chapter 3**, we assessed the prevalence, severity and composition of atherosclerotic carotid plaque and investigated whether these characteristics differed between the left and right carotid artery. Our findings demonstrated that plaque prevalence, severity and composition are not equally distributed among the left and right carotid arteries. Most individuals had bilateral carotid disease. Unilateral plaques were usually located on the left. Left-sided plaques were slightly thicker than the contralateral side. Whereas IPH and lipid were mostly observed in left-sided plaques, these plaques were predominantly composed of IPH and fibrous tissue. These findings suggest that atherosclerotic plaques on the left are more vulnerable than on the right. In contrast, right-sided plaques were predominantly composed of calcification, which is considered more stable and therefore less likely to result in thromboembolic complications. Differences in plaque thickness and composition between the left and right carotid arteries might be explained by hemodynamic or geometrical factors such as wall shear stress, bifurcation angle, or because of the direct connection of the left carotid artery to the aortic arch, leading to increased exposure in arterial pressures. We believe that understanding their contributions may explain the variation between left and right carotid atherosclerosis.

Chapter 4 Since atherosclerosis is a chronic inflammatory condition with various local and systemic manifestations, researchers have raised the hypothesis that plaque instability may also be a systemic condition, influenced by systemic risk factors. For this reason, the term vulnerable patient was introduced, indicating that changes found in one vessel bed may be predictive of risk of events in another vessel bed. We examined the association between carotid atherosclerotic plaque characteristics, including vulnerable components, and history of ischemic stroke and coronary heart disease. We found different atherosclerotic plaque characteristics related to coronary heart disease as compared to ischemic stroke. Whereas plaque thickness and stenosis were associated with a history of coronary heart disease and ischemic stroke, IPH was associated with ischemic stroke only. These associations were primarily present in men and less so in women. Whereas several reports previously suggested a relation between carotid IPH and CHD, we did not find any significant association between any of the carotid plaque components and history of CHD. A possible explanation for this discrepancy is that we focused on the independent risks of ischemic stroke and

coronary heart disease separately instead of restricting the study to one end organ or using composite end points. However, another explanation, and also the main limitation of this study, is that we used prevalent cardiovascular events as surrogate end point in order to explore the relation between carotid plaque composition and clinical event. As a consequence, fatal events, in which advanced atherosclerosis is expected, were not considered in the present study. This may have led to an underestimation of the association between vulnerable plaque characteristics and clinical events. Therefore, prospective studies that investigate the relation between carotid plaque characteristics and incident coronary heart disease and incident ischemic stroke in the general population are required.

Direct non-invasive measurements of the burden and composition of preclinical atherosclerosis have been proposed as a way to improve cardiovascular disease prevention and management. It has been suggested that plaque burden may provide more information on the extent of atherosclerosis beyond luminal stenosis. In **Chapter 5.1**, we describe a novel method for volumetric assessment of carotid plaque burden and lumen volumes. The method combines lumen and outer wall segmentation based on deformable model fitting with a learning-based segmentation correction step. We found that the automatic method performs comparably to the manual annotations in terms of wall volume and normalized wall index measurements and can therefore be used to replace the manual measurements.

Using this automated method, we evaluated age and sex distributions of plaque burden and lumen volume in the general population and investigated relations of cardiovascular risk factors. **Chapter 5.2** describes the sex-related differences in plaque burden and lumen volumes. We found that women have a larger plaque burden and smaller lumen volume than men. Also in women, age, HDL-levels and systolic blood pressure were independently associated with plaque burden and lumen volume. In men, cholesterol levels and statin use were significantly associated with plaque burden and lumen volume, whilst smoking and diabetes related only to lumen volume. Hence, the control of modifiable risk factors can prove beneficial in lowering plaque burden. Prospective longitudinal studies should investigate whether these cardiovascular risk factors are also associated with plaque progression. In this study, we also showed that IPH was found to be an additional risk factor for plaque burden and that it also strongly affects lumen narrowing independent of plaque size. This finding is supported by a previous study that found that lesions with IPH at baseline had a greater increase in wall volume and reduction in lumen volume compared with arteries without IPH.

Manual quantification of IPH volume is a laborious procedure and may easily result in segmentation errors when measuring inter- and intra-observer variability. Therefore, there is a large interest in automated procedures for IPH volume measurement. In **Chapter 6.1** we presented a semi-automatic IPH segmentation and quantification method that does neither require manual annotation of the inner or outer vessel wall nor preprocessing to correct for intensity inhomogeneity's. The method segments the IPH using a piecewise

smooth regional level set initialized by a set of manually clicked seed points. The inter-scan reproducibility experiments showed that the segmented volumes of the semi-automatic method have a much higher reproducibility than those of the observers. In this study we demonstrated that the manual annotation of IPH is subject to large observer variability. Therefore the semi-automatic results can at best also have a moderate agreement with the manual reference standard. However, the robustness and inter-scan reproducibility of the semi-automatic method is better than the manual observations.

In **Chapter 6.2** we aimed to evaluate the visual and quantitative change of IPH after one year follow up in asymptomatic subjects and to identify risk factors of IPH growth. In a nested-case-control study, we used automated segmentation to assess IPH volumes as detected on MRI. Serial imaging of IPH after one year follow up revealed in the majority of cases (96%) persistence of high signal on T1w-sequence. This finding is consistent with a previous study conducted in symptomatic individuals and 18 months follow up. In all individuals, IPH at baseline was found to be present at follow up. In the present study, we also assessed IPH change both qualitatively and quantitatively. We found that the largest proportion of IPH exhibited no visual change in size. However, we also report the novel finding that IPH may also regress or disappear.

In **chapter 7**, the general discussion, the main findings are reviewed in the context of current knowledge. Also, methodological considerations with regard to the studies in this thesis are described; this includes aspects of population-based imaging, cross-sectional study design, MRI imaging and post-processing techniques with automated segmentation. Finally, future research directions and clinical implications are discussed, such as the use of intraplaque hemorrhage as an imaging marker for screening and the role of biomechanical markers in the etiology of carotid atherosclerosis.

Samenvatting

Hoofdstuk 1 introduceert de achtergrond en de doel van het proefschrift. Atherosclerotische plaques in de carotiden zijn de hoofdoorzaak van herseninfarcten. De huidige behandelingen die gericht zijn op atherosclerose zijn onvoldoende om personen vroegtijdig te identificeren die een verhoogd risico hebben op het krijgen van een herseninfarct, waardoor de incidentie van herseninfarcten dramatisch hoog blijft. De huidige ontwikkelingen die gericht zijn op het voorkomen van herseninfarcten zijn onder andere het onderscheiden van verschillende plaque componenten en het herkennen van vulnerabele atherosclerotische plaques. Laatstgenoemde kunnen gekenmerkt worden door bijvoorbeeld de aanwezigheid van plaquebloedingen. Er wordt aan-genomen dat plaquebloedingen veroorzaakt worden door een scheur of lekkage in de vaatnieuwvormingen in een plaque, welke vervolgens tot progressie en instabiliteit van de plaque kunnen leiden. Magnetic resonance imaging (MRI) is geschikt om de verschillende plaquecomponenten te onderscheiden en het kan plaquebloedingen in de carotiden nauwkeurig opsporen. Kennis over de factoren die de atherosclerotische plaque samenstelling beïnvloeden kan bijdragen aan het voorkomen van herseninfarcten. Daarom, het eerste doel was het identificeren van biomechanische parameters voor atherosclerose in de carotiden en in het bijzonder plaquebloedingen in de carotiden. Ten tweede, we streefden ernaar om de rol van de biomechanische parameters bij de pathofysiologie van hart- en vaat ziekten beter te begrijpen. Ten derde, we streefden ernaar om geautomatiseerde segmentatie methoden te ontwikkelen om plaqueomvang en plaquebloedingen betrouwbaar te kunnen meten. Om deze onderzoeksvragen te beantwoorden hebben wij beiderzijds de carotiden van bijna 2000 deelnemers uit de Rotterdam Studie gescand. De Rotterdam Studie is een lopend groot prospectief cohort onderzoek in de algemene bevolking.

Hoge bloeddruk, oftewel hypertensie, is een veelvoorkomende aandoening en draagt aanzienlijk bij aan atherosclerose gerelateerde hart- en vaatziekten. In **hoofdstuk 2.1** heb-ben wij verschillende bloeddruk parameters nauwkeuriger onderzocht en hebben wij hun relatie tot plaquebloedingen in de carotiden geëvalueerd. Wij toonden aan dat het pulsatiele onderdeel van de bloeddruk, uitgedrukt in polsdruk, de sterkste voorspeller was voor plaquebloedingen. Voorgaande experimentele onderzoeken ondersteunen de associatie tussen periodieke hemodynamische factoren en atherosclerose progressie en plaque instabiliteit. Pulsatiele spanning beïnvloedt het endotheel, de gladde spiercellen in de vaatwand, de aanmaak van elastine, collageen, glycosaminoglycans, en leidt tot toename van het atherosclerotische plaquevolume. Een scheur in de atherosclerotische plaque wordt geacht te ontstaan als de krachten die zich op de vaatwand uitoefenen toenemen. Op dezelfde manier zou men een grotere bijdrage verwachten van de systolische bloeddruk dan van de pulsatiele bloeddruk die leidt tot het scheuren van de vaatnieuwvormingen. Echter, onze bevindingen suggereren dat de pulsatiele druk, een mechanische kracht is die inspeelt op de vaatwand van de slagader, ongeacht van de ab-

solute hoogte van de bloeddruk, en die op z'n minst even belangrijk is bij de ontwikkeling van plaquebloedingen.Het onderliggende mechanisme dat de relatie vormt tussen polsdruk en plaquebloedingen kan mogelijk te maken hebben met de vaatstijfheid. In een aanvullend hoofdstuk (**hoofdstuk 2.2**) hebben wij de relatie onderzocht tussen vaatstijfheid en de aanwezigheid van atherosclerotische plaques en plaquebloedingen met behulp van een directe meting van vaatstijfheid, namelijk polsgolfsnelheid. In dit onderzoek hebben wij aangetoond dat de vaatstijfheid geassocieerd is met de aanwezigheid en de samenstelling van atherosclerotische plaques in de carotiden bij mensen uit de algemene bevolking. Bovendien was vaatstijfheid een belangrijke determinant voor plaquebloedingen bij mensen die een plaque in de carotiden hadden. Een toegenomen vaatstijfheid kan leiden tot een vroege uitgekaatste drukgolf met als gevolg een toename in centrale systolische bloeddruk, een afname in diastolische bloeddruk en een toename in polsdruk. Daarom weerspiegelt de polsdrukgolf de cumulatieve schade aan de vaatwand. Ondanks onze bevinding dat de polsdrukgolf geassocieerd was met plaquebloedingen onafhankelijk van de polsdruk, is het toch vermeldenswaardig dat er een gecompliceerde relatie bestaat tussen polsdruk en vaatstijfheid. Polsdruk kan beschouwd worden als zowel de oorzaak als het gevolg van vaatstijfheid.

Ischemische herseninfarcten worden vaker gediagnosticeerd in de linker hersenhelft dan in de rechter, daarom hadden wij de hypothese dat asymmetrie van atherosclerose in de carotiden hierbij mogelijk een rol kon spelen hierbij. In **hoofdstuk 3** hebben wij de prevalentie, ernst en compositie van atherosclerotische plaques bepaald en hebben wij onderzocht of er verschillen zijn tussen de linker- en rechtercarotis. Onze bevindingen toonden aan dat de plaque prevalentie, ernst en compositie niet gelijk verdeeld zijn over de linker- en rechtercarotis. De meerderheid van de deelnemers had beiderzijds atherosclerose in de carotiden. Enkelzijdige plaques waren voornamelijk links gelokaliseerd. Linkszijdige plaques waren enigszins dikker dan de plaques aan de contralaterale zijde. Terwijl aanwezigheid van plaquebloedingen en vetophoping met name geobserveerd werd aan de linkerzijde, bestonden de linkszijdige plaques hoofdzakelijk uit plaquebloedingen en fibreus weefsel. Deze bevindingen suggereren dat linkszijdige atherosclerotische plaques meer vulnerabel zijn dan de rechtszijdige plaques. In tegenstelling tot rechtszijdige plaques, welke hoofdzakelijk bestaan uit calcificaties, hetgeen beschouwd wordt als meer stabiel en een groter thromboembolisch complicatie risico vormt. De verschillen in plaquedikte en compositie tussen de linker- en de rechtercarotis kunnen verklaard worden door de hemodynamische of geometrische factoren, zoals de wrijvingskracht, bifurcatiehoek of door het feit dat de linkercarotis in directe verbinding staat met de aortaboog waardoor de arteriële druk daar hoger is. Beter inzicht in de individuele bijdrages van deze factoren kan mogelijk de variabiliteit tussen de linker- en rechtercarotis beter verklaren.

Hoofdstuk 4 Atherosclerose is een chronisch inflammatoire aandoening is met diverse lokale en systemische manifestaties. Daarom hebben onderzoekers de hypothese opgesteld dat plaque instabiliteit ook een systemische aandoening kan zijn, welke beïnvloed wordt door systemische risicofactoren.

Dit leidde tot de introductie van de term "vulnerabele pa-tiënt', hetgeen suggereert dat veranderingen die in het ene vaatbed gevonden worden mogelijk voorspellend konden zijn voor events die vanuit een ander vaatbed ontstaan. In dit hoofdstuk hebben wij de associatie tussen atherosclerotische plaque eigenschappen, inclusief de vulnerabele plaquecomponenten, en een voorgeschiedenis van ischemische herseninfarct of coronair vaatlijden onderzocht. Wij vonden dat atherosclerotische plaque eigenschappen verschillend gerelateerd waren aan coronair vaatlijden in vergelijking tot ischemische herseninfarcten. Terwijl plaque dikte en stenose het sterkst geassocieerd waren met een voorgeschiedenis van coronair vaatlijden en ischemische herseninfarcten, waren plaquebloedingen alleen geassocieerd met ischemische herseninfarcten. Deze associaties waren voornamelijk aanwezig in mannen en minder in vrouwen. Terwijl voorgaande onderzoeken een relatie suggereerden tussen plaquebloedingen in de carotis en coronair vaatlijden, hebben wij geen enkele associatie gevonden tussen de plaquecomponenten en een voorgeschiedenis van coronair vaatlijden. Een mogelijke verklaring voor deze discrepantie is dat wij ons binnen dit onderzoek geconcentreerd hebben op de onafhankelijke risico's op ischemische herseninfarcten en coronair vaatlijden, terwijl de andere onderzoeken soms zich tot één eindorgaan beperkten of juist de risico's op beide aandoeningen combineerden. Echter, een andere verklaring, en ook een beperking van deze studie, is dat wij gebruik maakten van doorgemaakte cardiovasculaire events ter benadering van toekomstige events bij het vergelijken van de onderlinge risico's op deze aandoeningen. Als gevolg daarvan zijn de fatale events, waarbij vergevorderde atherosclerose verwacht wordt, niet in overweging genomen in het huidige onderzoek. Dit zou mogelijk tot een onderschatting kunnen hebben geleid van de associatie tussen vulnerabele plaque eigenschappen en klinische events. Daarom zijn meer prospectieve onderzoeken naar de relatie tussen plaque eigenschappen in de carotis en de incidentie van coronair vaatlijden en ischemische herseninfarcten in de algemene bevolking vereist.

Directe non-invasieve metingen van de belasting en compositie van preklinische atherosclerose kunnen mogelijk de preventie en behandeling van hart- en vaatziekten verbeteren. Voorheen werd gesuggereerd dat plaquebelasting mogelijk meer informatie bevat over atherosclerose dan dat luminale stenose kan bieden. In **hoofdstuk 5.1** beschrijven wij een nieuwe methode om de plaquevolume en lumenvolumes te bepalen. Deze methode combineert contouren van het lumen en van de buitenwand op basis van een deformabel fitting model met een learning-based segmentatie correctie. Wij hebben gevonden dat deze geautmatiseerde methode vergelijkbare resultaten produceert als de handmatige benadering wanneer het gaat om de plaquevolumes en de genormaliseerde wandindex. Deze methode kan daarom de handmatige metingen vervangen.

Met behulp van deze geautomatiseerde methode hebben wij de leeftijd- en geslachts- verdelingen van plaquebelasting en lumenvolume in de algemene bevolking geëvalueerd en de relaties met cardiovasculaire risicofactoren onderzocht. **Hoofdstuk 5.2** beschrijft de geslachtsspecifieke verschillen in plaquebelasting en lumenvolumes.

Wij vonden dat in vrouwen, leeftijd, HDL-niveau en systolische bloeddruk onafhankelijk geassocieerd waren met plaquebelasting en lumenvolume. In mannen waren cholesterol niveau en statine gebruik significant geassocieerd met plaquebelasting en lumenvolume, terwijl roken en suikerziekte slechts gerelateerd waren aan lumenvolume. Het beter controleren van de be-invloedbare risicofactoren kan daarom bevorderlijk zijn voor het verlagen van de plaque-belasting. Prospectieve longitudinale onderzoeken zouden ook moeten uitmaken of deze cardiovasculaire risicofactoren ook geassocieerd zijn aan plaqueprogressie. In dit onderzoek hebben wij ook aangetoond dat plaque bloedingen een aanvullende risicofactor vormen voor plaquebelasting en dat het lumenvernauwing sterk kan beïnvloeden onafhankelijk van plaqueomvang. Deze bevinding is in lijn met een voorgaande studie die vond dat carotiden die een plaquebloeding bevatten tot een grotere toename in wandvolume en afname in lumenvolume zorgden in vergelijking met carotiden zonder plaquebloedingen. Het handmatig meten van de volumes van de plaquebloedingen is een tijdrovende proce-dure en is gevoelig voor segmentatievariatie tussen dezelfde en verschillende onderzoekers. Daarom is er een grote behoefte naar geautomatiseerde procedures om plaquebloedingen beter te kunnen meten. **In hoofdstuk 6.1** presenteren wij een (semi)geautomatiseerde segmentatie en kwantificatie methode voor plaquebloedingen. Deze methode vereist geen handmatige contouren van de binnen- en buitenwand en ook geen voorbewerking om te corrigeren voor de heterogeniteit in intensiteit. Deze methode segmenteert plaquebloedingen middels een stapsgewijze smooth-regional-niveau methode welke bepaald wordt door een aantal handmatig geplaatste markeringspunten. Het reproduceer-baarheidsonderzoek toonde aan dat de geautomatiseerde contouren beter reproduceerbaar waren dan de handmatige. In dit onderzoek hebben wij aangetoond dat handmatige metingen van plaquebloedingen gevoelig zijn voor variatie. Daarom is de kwaliteit van de geautomatiseerde contouren vergelijkbaar met de handmatige contouren die hierbij als referentie gelden. Echter, de robuustheid en de inter-scan reproduceerbaarheid van de geautomatiseerde methode zijn beter dan de handmatige benadering.

In **hoofdstuk 6.2** was het doel om de visuele en kwantitatieve veranderingen in plaquebloedingen te meten na ruim één jaar follow up in asymptomatische personen en om risicofactoren voor groei van plaquebloedingen te identificeren. In een ingesteld case-control onderzoek hebben wij geautomatiseerde contouren gebruikt om de volumes van plaquebloedingen te bepalen zoals deze zichtbaar zijn op MRI. Herhaaldelijke beeldvorming van plaquebloedingen na één jaar follow up toonde aan dat de meerderheid van de gevallen (96%) een persisterend hoog signaal had op de T1-gewogen beelden. Deze bevinding komt overeen met een voorgaand onderzoek dat uitgevoerd was in symptomatische personen en 18 maanden durende follow up had. Alle plaquebloedingen die op de eerste scan aanwezig waren bleven zichtbaar na 18 maanden follow up.

In het huidige onderzoek hebben wij tevens de verandering in plaquebloeding middels een kwalitatieve en een kwantitatieve methode vastgesteld. Wij vonden dat het grootste deel van de plaquebloedingen visueel niet leek te veranderen. Echter, wij hebben wel de nieuwe observatie gerapporteerd dat plaquebloedingen kunnen afnemen in omvang en zelfs ook verdwijnen.

Hoofdstuk 7 is een algemene discussie waarin de hoofdbevindingen besproken worden binnen het kader van de huidige kennis. Ook methodologische overwegingen met betrek-king tot de onderzoeken die verricht zijn binnen dit proefschrift worden beschreven; hierbij worden besproken: de beeldvorming binnen de algemene bevolking, dwarsdoorsnedeonder-zoek, MRI beeldvorming alsmede beeldverwerkingstechnieken middels geautomatiseerde segmentatie. Tot slot worden toekomstige onderzoeksrichtingen en klinische toepassin-gen besproken, zoals het gebruik van plaquebloedingen als een beeldvormingsmarker bij screeningsdoeleinden en de rol van biomechanische markers bij de etiologie van athero-sclerose in de carotiden.

Publication list
Journal papers

Selwaness M, Van den Bouwhuijsen Q, Verwoert GC, Mattace-Raso FUS, Hofman A, Franco OH, Van der Lugt A, Witteman JCM, Wentzel JJ. *Blood pressure parameters and carotid intraplaque haemorrhage as measured by magnetic resonance imaging: The Rotterdam Study.* Hypertension, 2013 Jan;61(1):76-81.

Selwaness M, Van den Bouwhuijsen Q, Mattace-Raso FUS, Verwoert GC, Hofman A, Franco OH, Van der Lugt A, Vernooi M, Witteman JCM, Wentzel JJ. *Arterial stiffness is associated with carotid intraplaque haemorrhage in the general population: The Rotterdam Study.* Arterioscler Thromb Vasc Biol, 2014 Apr;34(4):927-32.

Selwaness M, Van den Bouwhuijsen Q, Van Onkelen R, Hofman A, Franco OH, Van der Lugt A, Witteman JCM, Wentzel JJ, Vernooi M. *Atherosclerotic plaque in the left carotid artery is more vulnerable than on the right.* [Stroke 2014. Epub ahead of print]

Selwaness M, Van den Bouwhuijsen Q, Portegies M, Hofman A, Franco OH, Van der Lugt A, Wentzel JJ, Vernooij M. *History of ischemic Stroke and coronary heart diease and carotid plaque composition.* [Paper submitted to Eur. Heart J.]

Selwaness M, Hameeteman K, Van den Bouwhuijsen Q, Hofman A, Franco OH, Vernooij M, Wentzel JJ, Van der Lugt A. *Automated segmentation of atherosclerotic plaque burden in the general population.* [Paper submitted to Atherosclerosis.]

Tang H, **Selwaness M**, Hameeteman R, Dijk A, Van der Lugt A, Witteman JC, Niessen WJ, Van Vliet LJ, Van Walsum T. *Semi-automatic segmentation and volume quantification of intraplaque hemorrhage in T1w-MRI.* Int J Comput Assist Radiol Surg. 2014 May 12

Hameeteman K, Van 't Klooster R, **Selwaness M**, Van der Lugt A, Witteman JC, Niessen WJ, Klein S. *Carotid wall volume quantification from magnetic resonance images using deformable model fittin and learning-based correction of systemic errors.* Phys Med Biol. 2013 Mar 7;58(5):1605-23.

Selwaness M, Van den Bouwhuijsen Q, Tang H, Van Dijk AC, Hameeteman R, Van Walsum T, Niessen WJ, Hofman A, Franco OH, Van der Lugt A, Vernooij MW. *Change of carotid intraplaque hemorrhage in the general population: a 1-year follow up study.* Paper to be submitted.

Hameeteman K, Van 't Klooster R, **Selwaness M**, Van der Lugt A, Witteman JC, Niessen WJ, Klein S. *Carotid wall volume quantification from magnetic resonance images using deformable model fittin and learning-based correction of systemic errors.* Phys Med Biol. 2013 Mar 7;58(5):1605-23.

Carvalho DDB, Klein S, Akkus Z, Van Dijk AC, Tang H, **Selwaness M**, Schinkel AFL, Bosch JG, Van der Lugt A, Niessen WJ. *Joint intensity-and-point based registration of free-hand B-mode Ultrasound and MRI of the Carotid Artery*. Med Phys. 2014 May;41(5):052904. doi: 10.1118/1.4870383.

Acknowledgements
Dankwoord

Een PhD is als een reis, die gaat naar een bestemming die nieuw voor je is. Op sommige momenten word je uitgedaagd en je geduld, doorzettingsvermogen, karakter en creativiteit worden getest. Hoe zwaar het ook moge zijn, al deze momenten bieden de gelegenheid om te groeien. Hierbij wordt je persoonlijkheid gevormd en je koffer met persoonlijke ervaringen gevuld. Aan het begin van de de reis weet je nog niet wat je te wachten staat en op welke manier je de eindbestemming gaat halen. Gelukkig is de gedachte dat je nooit helemaal alleen zal zijn een geruststelling.

Tijdens elk station van de reis leer je andere mensen kennen. Elke ontmoeting heeft een reden. Je realiseert je dat de mensen die je onderweg ontmoet en voor wie je deze weg aflegt de reis tot eenprachtige ervaring maken! Vandaag mag ik zeggen dat ik mijn bestemming heb gehaald en daarom wil ik graag bedanken eenieder die mij bij deze reis heeft gesteund, die ik heb leren kennen onderweg en met wie ik mooie herinneringen heb opgebouwd.

Ik wil al mijn collega's van de afdelingen Epidemiologie, Cardiologie, Radiologie en BIGR bedanken en uiteraard al mijn familieleden en vrienden. In het bijzonder wil ik mijn promo-toren bedanken Prof. dr. Aad van der Lugt en Prof. dr. Oscar H. Franco en mijn copromotoren dr. Jolanda J. Wentzel en dr. Meike W. Vernooij.

Lieve Aad, je praktische houding en nuchtere blik zijn ontzettend leerzaam geweest. Op de moeilijkste momenten stond jij voor mij klaar en had je al een oplossing paraat. Ik waardeer ook je oprechte zorg om alle niet-PhD gerelateerde zaken. Ik ben erg blij dat ik met je heb mogen samenwerken en kijk uit naar nog meer samenwerkingen in de toekomst.

Dear Oscar, I really appreciate your support during the last stage of my PhD. Your door has always been open for me to walk-in at any time, even to discuss non-scientific issues. Thanks for providing me the opportunity to become the president of social affairs. You are a great supervisor and I wish we will continue working together in the future.

Lieve Jolanda, met oprechte zorg, liefde en geduld heb jij mij de afgelopen jaren begeleid. Je was mijn mentor, coach en vriendin, en ik waardeer alle tijd en moeite die je geïnvesteerd hebt in onze wekelijkse meetings. Ik respecteer enorm de manier waarop jij de BME groep tot een familie hebt gemaakt. Het is een eer dat ik je PhD studente mocht zijn en bij de BME familie mocht horen. Bedankt.

Lieve Meike, ik ben je zo ontzettend dankbaar dat jij het laatste jaar je met mijn PhD wilde bemoeien. In dat ene jaar heb ik ontzettend veel van je geleerd en je betrokkenheid heeft de kwaliteit van het onderzoek en artikelen een enorme boost gegeven. Ik weet dat ik niet zo ver had kunnen komen zonder jou! Ook buiten het werk om bleek je een geweldige vriendin te zijn en wist je met je heldere en gestructureerde gesprekken mij telkens moed in te blazen om door te gaan. Ik zou nog even door kunnen gaan over hoe dankbaar ik ben, maar woorden zullen nooit genoeg zijn. Meike, het was in ieder geval een groot plezier om je beter te mogen leren kennen!

Een speciale dank gaat uit naar de eerste persoon die ik ontmoet heb bij mijn sollicitatie in het Erasmus MC, Prof. dr. Jacqueline C.M. Witteman. Jacqueline, vanaf het begin af aan toonde je vertrouwen in mij en ik heb ontzettend veel van je geleerd tijdens mijn PhD. Bedankt dat je er was op de momenten dat ik je nodig had en ik wens je het allerbeste toe in je leven.

Abbas, if it was not for you, I would not have been here. Thank you for your sincere advise to accept this position, I have never regretted working here. In fact, I enjoyed it every day! Thanks for your continuous support. I really appreciate it.

Ik heb de afgelopen jaren het geluk gehad om mijn kamer te delen met verschillende ontzettend lieve collega's. Germaine en Quirijn, ook al was het een korte tijd dat we samen waren, het was altijd gezellig met jullie. Ik ben trots op alles wat jullie beiden bereikt hebben vandaag de dag en wens jullie het allerbeste toe in je carrière en persoonlijke leven. Bouwe, de meest vriendelijke collega die ik gekend heb de afgelopen jaren, en ook degene met wie ik het langst een kamer gedeeld heb. Ik heb genoten van je aanwezigheid en met plezier kijk ik terug op alle onze gesprekken en thee momenten.

Ook heb ik het geluk gehad om een kamer te delen met Janine, Edith, Anna, Ayesha, Adriana, Lisanne en Charlotte. Jullie hebben de afgelopen jaren voor heel veel gezel-ligheid gezorgd, ik heb enorm veel goede herinneringen hieraan overgehouden. Bedankt.

Lieve Janine, ook al was je een beetje twijfelend aan het begin of je wel een kamer met mij wilde delen, ik ben blij dat je het toch gedaan hebt, want het is het begin geworden van een mooie vriendschap. Ik heb enorm genoten van je betrokkenheid in mijn leven en wens je het allerbeste in je carrière.

Lieve Edith, mijn ex-Blijdorp-maatje, met jou heb ik toch zoveel gelachen! Bedankt dat je mij wekelijks trouw een bericht stuurde voor onze lunch date, ik waardeerde dat enorm. We moeten nog een etentje bij mij thuis doen als ik weer terug ben in NL.

Lieve Ayesha, Munich was so much fun together, thanks for allowing me to take part in many special moments in your life, you are a wonderful friend and I wish you a happy life with Midas and the baby.

Natuurlijk kan ik niet vergeten mijn hele lieve vriendinnen van de spelletjes avond Epic-groep, Annemarie, Lisette, Rachel, Henriet, Nikkie, Maartje, Heidi en Nese'e. Ieder van jullie heeft een speciale betekenis gehad in mijn leven en ik ben zo dankbaar dat jullie er altijd voor mij waren. Ik kijk met plezier terug op de spelletjes avonden, het koken, de gezellige gesprekken en de skype meetings! Ik hoop dat onze Epic-groep nog lang blijft bestaan!! Veel succes verder bij de rest van jullie carrières waar in de wereld dat ook moge zijn!

Grote dank aan twee hele lieve vrienden die ik beschouw als zus en broer, Ling en Edwin. Vanaf het begin af aan klikte het meteen en mocht ik op jullie bruiloft komen. Jullie zijn een prachtpaar en ik waardeer het enorm dat jullie er altijd voor mij waren. Ling, wat heb ik toch genoten van onze theemomenten en wat waren de ECR en RSNA toch erg gezellig met jullie beiden! Ik kijk uit naar meer contactmomenten als ik weer terug ben in Rotterdam en, Ling, succes met je promotie bij de Interne Geneeskunde!

Graag wil ik al mijn collega's van de Epidemiologie en Erasmus Age bedanken. Allereerst Prof. dr. Albert Hofman voor het mogelijk maken van de Rotterdam Studie. Bedankt Bert dat je mij regelmatig benaderde om te vragen hoe het met me ging. Met plezier denk ik terug aan onze gesprekken over het onderzoek in Nederland en daarbuiten. Ook wil ik bedanken alle collega's uit Ommoord, in het bijzonder Anneke, de dames van de echo Ingrid, Toos, Saskia en mijn lieve collega die enorm veel tijd en moeite gestoken heeft bij het maken van alle MRI scans: Charlotte, je inzet is absoluut niet ongemerkt gebleven! Dankjewel voor alles! Ook wil ik verder bedanken van de afdeling Epidemiologie Miriam Hunnink, Arfan, Henning, Jan, Maryam Kavousi, Jessica, Jolande Verkroost, Nano, Frank, Renee, Maarten, Raha, Marieke, Sanaz, Paul, Symon, Daan, Lies, Raymond, Virginie, Gabrielle, Ben, Daniel, Vincent K, Vincent V, Reneé, Eline, Marielle, Elizabeth, Renske, Lot, Hazel, Liz, Saloua, Marileen.

Ik heb enorm veel geluk gehad dat ik op verschillende afdelingen mocht werken, waaronder de Biomedical Engineering afdeling onder leiding van Prof. dr. Ton van der Steen. Ik wil graag bedanken Frank, Hans, Kim, Kimmetje, Lambert, Ali, Leah, Merih, Jelle, Harm, Zaid, Dyon, Bibi en Bahar. Ik kan over ieder van jullie wel een pagina vullen met al onze mooie herinneringen, zoals de lunches, de koffiemomenten, het lab-uitje, de libdub, het skaten, het poolen, de picknick, het zeilen, de dansjes van Kimmetje en met de meiden (Powergirls haha) alle etentjes! (Dat moeten we snel weer eens plannen trouwens!) Jullie zijn geweldige mensen en ik heb enorm veel plezier beleefd wanneer we samen waren!! Lambert en Kim, ik wil jullie nog speciaal bedanken dat jullie als broer en zus altijd voor mij klaar stonden, ook in avonden en weekenden, en met humor en vele wijze woorden mij door verschil-lende stress-momenten wisten te slepen! Nog gefeliciteerd met de bruiloft, jullie zijn een prachtkoppel en ik wens jullie een gelukkig en lang leven samen!

I would like to thank my dear collegues from the BIGR department. It was a great pleasure to work with you Reinhard, Stefan, Hui Tang, Theo, Arna, Andres, Marleen and Diego.

Ik heb de kans gehad om te mogen werken op de afdeling Radiologie en heb een aantal ontzettend lieve meiden leren kennen, Anouk, Rebecca en Carolina, de ECR en RSNA waren erg gezellig met jullie! Ook wil ik graag bedanken Jolanda Meijer en Diana voor hun steun de afgelopen jaren en Ton Everaars voor zijn steun bij het maken van dit proefschrift. Ook wil ik graag bedanken Prof. dr. Krestin en dr. Winnifred van Lankeren dat ze mij de kans hebben geboden om in opleiding te komen bij de Radiologie in het Erasmus MC.

Furthermore, I would like to thank my committee members Prof. dr. Peter Koudstaal, Prof. dr. Eric Boersma, Prof. dr. Michiel Bots, Prof. dr. Wiro Niessen en Prof. dr. David Bluemke. I really appreciate your presence. David, I would also like to thank you for granting me the opportunity to work with you at the National Institute of Health and for flying all over to the Netherlands to attend my PhD defense.

Graag wil ik bedanken twee hele belangrijke mensen in mijn leven, die beiden toegestemd hebben om naast mij te staan op de dag van mijn verdediging, mijn paranimfen Annemarie en Rosalie.

Lieve Annemarie, je nuchtere kijk op het leven en je spontaniteit hebben tot een verrijking geleid van mijn PhD periode. Met veel plezier denk ik terug aan onze Parijs-reis, de treinen in Holland Casino (je weet wat ik bedoel), mijn logeermomenten bij jou en de gezellige gesprekken in de oude haven of via skype. Dankjewel voor alles en heel veel succes in Manchester!

Lieve Rosalie, ik weet dat ik het jou ontzettend moeilijk heb gemaakt de afgelopen jaren en vaak er niet voor je was omdat werk al mijn tijd opeiste, het spijt mij, maar gelukkig kon jij begrip opbrengen voor de situatie. Jouw gezelligheid, humor, wijsheid, gelach, doorzett-ingsvermogen en ambitie zijn dingen waar ik geen genoeg van kan krijgen en, ook al ben je de jongste, ik kijk erg naar je op. Bedankt dat je niet alleen tijdens mijn PhD, maar je hele leven naast me heb willen staan.

Ook wil ik mijn vrienden bedanken uit de Koptisch Orthodoxe kerk. De lijst van mensen die wekelijks naar mij vroegen en erop toe keken dat alles op werk of tijdens mijn verblijf in Rotterdam of in Amerika goed ging is enorm lang. Ik wil graag noemen Anba Arseny, alle priesters en al mijn lieve zussen en broers uit de kerk en mijn mede zondagschooldienaren. Dankjewel!

I also would like to thank all my friends in the USA during the final stage of my PhD. Thanks for the warm welcome when I moved to the USA. You have all been so supportive for me and I am so grateful for having you in my life now!

Ik weet zeker dat ik nog velen niet genoemd heb, maar ik heb zoveel prachtige mensen ontmoet met wie ik ontzettend leuke en inspirerende gesprekken gehad heb. Bedankt allemaal, jullie hebben mijn PhD periode tot een fantastische ervaring gemaakt.

Papa, mama, Rosalie en Amir, bedankt dat jullie er altijd voor mij waren. Woorden zullen niet genoeg zijn om te beschrijven hoeveel jullie mij hebben gesteund de afgelopen jaren. Jullie zijn het allerbelangrijkste in mijn leven, mijn inspiratie, mijn geluk, en ik ben God elke dag dankbaar dat hij mij jullie geschonken heeft. Ik hou van jullie!

How great is Your Generosity, O God, which You prepared for those who fear You! How sweet is Your Grace and Love for those who love You! I thank You, my Lord, Who cares for me. (Prayer after Communion).

Mariana Selwaness, Rotterdam, October 2014

PhD portfolio - Summary of PhD training and teaching activities

Name	Mariana Selwaness
PhD period	2010 - 2014
Erasmus MC Departments	Radiology, Epidemiology, Cardiology
Research School	NIHES and COEUR
Promotors	Prof. dr. Aad van der Lugt
	Prof. dr. Oscar H. Franco
Copromotors	dr. Jolanda J. Wentzel
	dr. Meike W. Vernooij.

Research Skills

2010-2013 MSc in Clinical Epidemiology, Netherlands Institute for Health Sciences, Erasmus University Rotterdam, the Netherlands

General Academic Skills

2013 Biomedical English Writing and Communication, Erasmus MC, Rotterdam, the Netherlands

In-depth courses

2010 Methodologie van Patientgebonden onderzoek en voorbereiding van subsidieaanvragen
2010 Study design
2010 Classical methods for Data-analysis
2010 Courses for the quantitative researcher
2011 Pharmaco-epidemiology and Drug safety
2011 Principals in research in Medicine
2011 Clinical decision analysis
2011 Methods of public health research
2011 Markers and prognostic health research
2011 The practice of epidemiologic analysis
2011 Methodologic Topics in Epidemiologic Research
2011 Pharmaco-epidemiology and Drug Safety
2011 Biostatistical Methods II: Popular Regression Models
2012 Repeated Measurements
2012 Missing Values in Clinical Research
2012 Case-control studies
2012 Clinical Epidemiology
2012 History of epidemiologic ideas
2012 Advances in Epidemiologic Analysis
2013 Planning and Evaluation of Screening
2013 Introduction to global public health

National and international conferences

Presentations at (inter)national conferences

2011 Trends in Medical Technology: Cardiovascular Imaging
2011 Biomechanics in Vascular Biology and cardiovascular disease
2012 European Society of Radiology
2012 Werkgroep Epidemiologisch Onderzoek Nederland
2012 European Society of Cardiology
2012 Radiologendagen
2013 European Society of Radiology
2013 Radiological Society of North America

Seminars organized by COEUR Research school

2010 Imaging of Atherosclerosis
2011 Detection of early atherosclerosis
2011 Healthy aging
2013 Imaging Carotid Arteries: structure and function

Teaching activities

Supervising Master students in writing their thesis:

2012 Jasper van der Scheer – Thesis title: Progression of Intraplaque Hemorrhage after one year of follow up
2013 Laura Pletsch Borba – Thesis title: Change in carotid plaque composition over time: a 4 year follow up study using serial magnetic resonance imaging
2014 Annelies Tuenter – Thesis title: Wall shear stress as determinant for carotid plaque composition
2014 Milan Stojkovic – Thesis title: Epicardial fat as determinant of coronary heart disease: The Rotterdam Study

ISBN: 978-94-6259-332-9